**Title**
INTRINSIC AND EXTRINSIC NON-STOICHIOMETRY IN THE LEAD ZIRCONATE-TITANATE SYSTEM



**Author**
Holman, Robert L.

**Publication Date**
1972-07-01

LBL-880

# INTRINSIC AND EXTRINSIC NON-STOICHIOMETRY IN THE LEAD ZIRCONATE-TITANATE SYSTEM

Robert L. Holman
(Ph. D. Thesis)

July 1972

AEC Contract No. W-7405-eng-48




LBL-880

## DISCLAIMER

INTRINSIC AND EXTRINSIC NON-STOICHIOMETRY
IN THE LEAD ZIRCONATE-TITANATE SYSTEM

Contents

# INTRINSIC AND EXTRINSIC NON-STOICHIOMETRY IN THE LEAD ZIRCONATE-TITANATE SYSTEM

Robert L. Holman

Inorganic Materials Research Division, Lawrence Berkeley Laboratory
and Department of Materials Science and Engineering,
College of Engineering; University of California,
Berkeley, California 94720

## ABSTRACT

An investigation of the range of intrinsic and the nature of extrinsic non-stoichiometry in lead zirconate-titanate (PZT) has been conducted. Methods were developed to obtain precise and reproducible control of the defect structure. The intrinsic defect structure was established by continuously weighing a PZT sample during its vapor phase equilibration with a controlled PbO atmosphere provided by constant activity multi-phase (CAMP) PZT crucibles. Similar data was obtained by performing a modified Knudsen effusion experiment. The extrinsic defect structure associated with ionic substitutions into the PZT perovskite lattice as well as the kinetics of solution were determined by a modified vapor phase equilibration equipment.

The two different gravimetric experiments led to similar values for the $Pb_{1-x}\square_x(Ti_yZr_{1-y})O_{3-x}\emptyset_x$ single-phase region width at 1100°C ($x_{max}$ = 0.10 at y = 1.0, $x_{min}$ = 0.016 at y = 0.40). First, the development of the high and low CAMP crucibles made possible the gravimetric vapor phase equilibration of a PZT sample and a PbO atmosphere. Weight changes produced in obtaining equilibrium indicated the extent of the stoichiometric variations. Second, the modified Knudsen effusion experiment yielded the same width of the PZT single-phase region, as well as the relative location of the stoichiometric compound within the region,

and complete thermodynamic vapor pressure data.

By modifying the vapor phase equilibration technique, gravimetric analysis was used to study the kinetics of solution of Bi, Nb, La, and Sc ions in PZT. Results indicated a lead vacancy defect structure created by the substitution of Bi, Nb, and La in the PZT lattice. An oxygen vacancy defect structure was found for Sc. All cases studied obeyed electroneutrality rules and followed simple predictions of crystal chemistry ($Bi^{3+}$ and $La^{3+}$ substitution for $Pb^{2+}$; $Nb^{5+}$ and $Sc^{3+}$ substitution for $(Ti,Zr)^{4+}$).

The production of multi-phase crucibles, in addition to allowing gravimetric experiments, afforded atmosphere control and a simple processing technique. Thus, it is possible to fabricate PZT materials with precise, reproducible, and homogeneous intrinsic or extrinsic stoichiometry.

# I. GENERAL INTRODUCTION

Polycrystalline lead zirconate-titanate (PZT) ceramics are of commercial interest because of their high dielectric constants, pronounced ferroelectric, piezoelectric, and electro-optic behavior, coupled with low cost of processing and manufacture. Levitt[1] and Webster et al.[2] have shown that very significant changes in physical properties can result from only slight compositional changes created during processing due to the evaporation of lead oxide (PbO) at temperatures above 1000°C. This causes difficulties in the manufacturing of reproducable PZT materials of controlled composition.

The nature of the compositional changes has been investigated by several approaches. Northrop[3] used gravimetric techniques to study the evaporation of PbO from sintered PZT discs. Extensive phase equilibria studies ($PbO-TiO_2-ZrO_2$) have been conducted by Moon,[4] Fushimi and Ikeda[5] and Ikeda et al.[6] Fushimi's results indicated a range of PZT non-stoichiometry. This has been supported by the recent sintering studies of Atkin and Fulrath.[7]

Several attempts have been made to control the compositional changes due to PbO evaporation. Jaffe et al.[8] (1955) sought to inhibit the undesirable evaporation of PbO by sintering PZT samples in the presence of the PbO atmosphere provided by lead oxide enriched lead zirconate discs. This technique has been recently modified by Snow[9] who has been able to sinter La doped PZT to optical transparency. Dungan et al.[10] (1962) used a burial powder of the exact composition of the sample to produce the necessary local lead oxide environment. Atkin and Fulrath[7] continued this approach with improved sintering although stoichiometry

variations were still observed.

To achieve the high densities required in practical devices, second phase impurities are commonly used to enhance sintering. However, Weston et al.[11] and Hardtl and Hennings[12] have developed methods that suggest that as the impurities react with PZT, in addition to enhancing sintering, defect structures and stoichiometric variations are likely. The extent to which the impurities react with PZT, as well as the degree of simultaneous PbO evaporation, can markedly effect the sample composition and its useful properties (particularly optical[13-17] and electrical[18-26] behavior).

Improved methods are required to obtain precise and reproducible processing of both pure and impure homogeneous lead zirconate-titanate compositions.

To this end, the present work establishes the extent of both intrinsic and extrinsic non-stoichiometry possible in lead zirconate-titanate. Techniques are presented to measure the width of any PZT single-phase region. A procedure is established that allows reproducible and homogeneous processing of any PZT composition to a precise and known stoichiometry.

One experimental technique is modified to allow the determination of the valence of any ionic addition in the PZT system and the lattice site where it substitutes, while also providing a continuous monitoring of the solubility kinetics. This method also characterizes the extent of non-stoichiometry created by ionic substitution as a function of time at temperature.

## II. INTRINSIC NON-STOICHIOMETRY

### A. Vapor Phase Equilibration Method

#### 1. Introduction

To date, phase equilibria investigations in the lead zirconate-titanate system have not clearly established the width of non-stoichiometric single-phase region. Some extension of the $Pb(Ti,Zr)O_3$ phase field was suggested by the X-ray studies of Fushimi and Ikeda,[5] and Ikeda et al.[6] Atkin and Fulrath[7] observed that small variations from the stoichiometric compound, $PbTi_{.5}Zr_{.5}O_3$, significantly affect the sinterability of the material. From this and reaction weight changes they have suggested the existence of a rather wide single-phase region.

It is well known that lead zirconate-titanate compositions lose lead oxide readily by evaporation at temperatures above 1000°C, and that this tendency to decompose may be inhibited by several schemes. Dungan et al.[10] in 1962, approximated an equilibrium environment for PZT samples, by burying his samples in a protective powder of the same composition. Thus, the sample and the powder were in local atmospheric equilibrium, while the outer layers of the burial powder evaporated lead oxide.

However, it is now apparent that the diffusion rate of PbO in solid PZT is comparable to the evaporation rate[27] from the surface in air. Therefore, if the composition of the atmosphere powder near the sample changes with time, non-reproducible and unpredictable deviations in the sample's stoichiometry can occur.

Dungan's technique can be improved by modifying the composition of the atmosphere material. Instead of creating a transient "equilibrium" with approximately stoichiometric single-phase PZT powder, multi-phase PZT mixtures of (PZT+PbO) or (PZT+Z+T) may be substituted as the packing powder for the sample. The principal advantage obtained is that for as long as the phases are in equilibrium, a constant lead oxide activity is maintained. The evaporation of lead oxide from this atmosphere material can alter the relative amounts of the phases, but as long as the phases are present, the PbO vapor pressure will remain constant and predictable at a given temperature.

Weston et al.[11] have shown that weight-change analysis is a successful way of studying the impurity induced extrinsic defect structure in PZT. This approach may also be adapted to characterize the extent of the intrinsic defect structure.

Thermogravimetry, in conjunction with equilibrium atmosphere control, affords a simple method for the determination of the width of a $PbTi_xZr_{1-x}O_3$ single-phase region. Thermodynamically, when a single-phase PZT sample has a different lead oxide activity than that provided by its environment, transport will occur, via the vapor phase, until the PbO activities of the sample and the environment are equal. This means that a small sample will either gain or lose PbO until an equilibrium activity balance is attained. The composition of the sample will then remain fixed for as long as the environment provides the constant lead oxide activity.

Lead zirconate-titanate constant activity multi-phase (CAMP) atmosphere crucibles have been developed that allow both gravimetric studies and reproducible and predictable processing of homogeneous PZT materials.

2. Experimental

a. Technique. A single-phase, high purity and porous $Pb(Ti_xZr_{1-x})O_3$ sample is alternately equilibrated with the PbO vapor pressure established by constant activity multi-phase (CAMP) crucibles fabricated from compositions that provide a constant lead oxide vapor pressure within them.

The proposed $PbO-TiO_2$ phase diagram[4] is shown in Fig. 1a. A deviation from perfect lead titanate stoichiometry is assumed. The general form of the PbO activity-composition diagram at constant temperature (1100°C) may be drawn[28] (Fig. 1b). It is assumed that this type of diagram is applicable to the analysis of all $PbO-(Ti_xZr_{1-x})O_2$ "quasi-binaries." Composition A, high PbO CAMP, refers to a two-phase mixture of PZT with excess PbO. Composition B, low PbO CAMP, refers to a multi-phase mixture of PZT with excess titania and/or zirconia. Composition C designates the initial stoichiometry of a single-phase sample. The exact location of C is dependent upon the material's processing history.

The sample, activity C, is first equilibrated with the atmosphere provided by a high CAMP crucible of composition A. The activity difference between the sample and the crucible, assisted by the high vapor

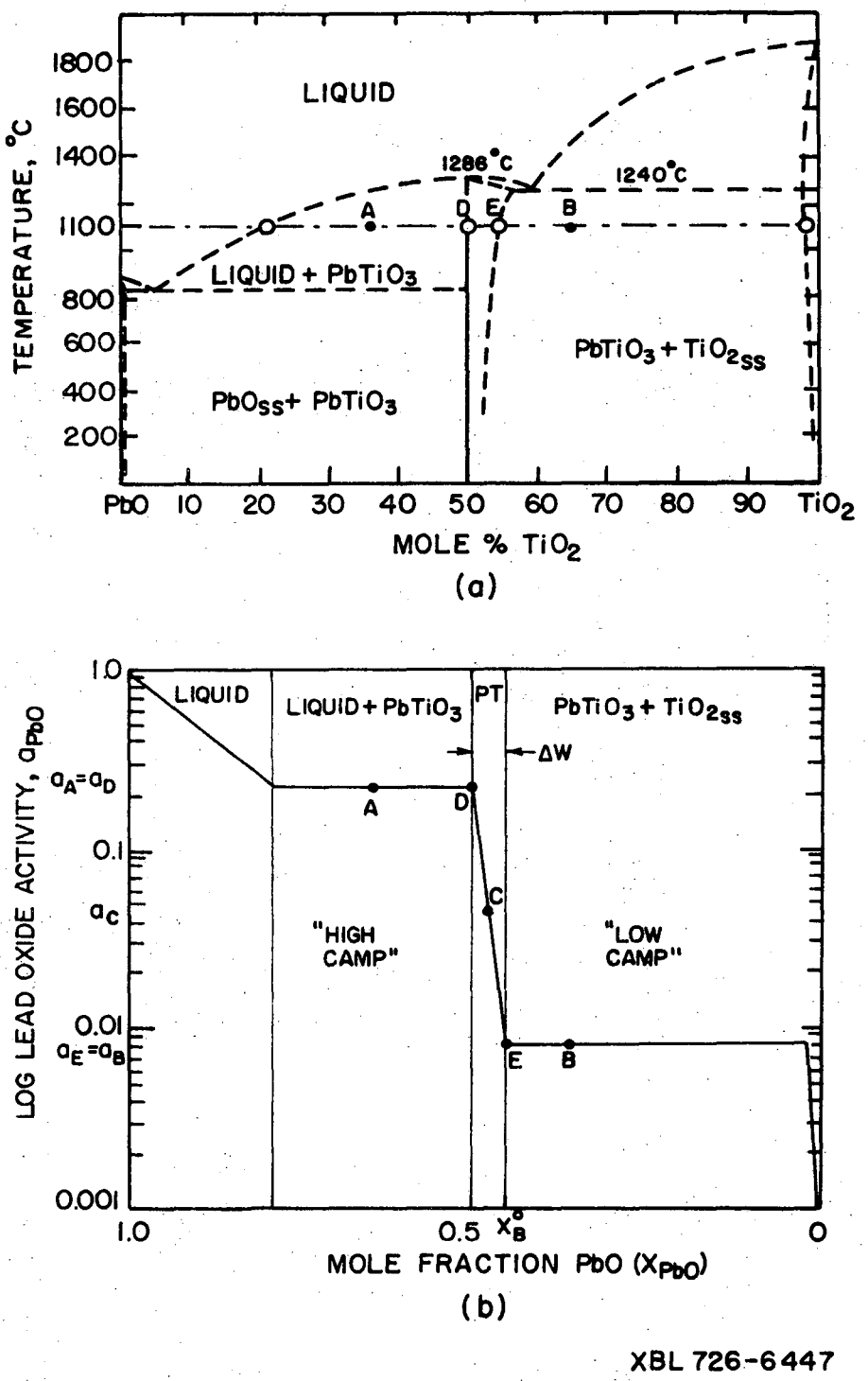


Fig. 1. (a) Proposed PbO-$TiO_2$ phase diagram after Moon,[4] and assuming a lead titanate region of non-stoichiometry.
(b) Activity of PbO vs. mole fraction PbO at constant temperature (1100°C) for the lead titanate binary.
Points A and B designate the constant PbO atmospheres provided by the CAMP crucibles of these compositions; point C locates the composition and activity of the nearly stoichiometric single-phase compound, whereas D and E indicate the single-phase boundaries.

pressure of PbO at temperature,* causes the sample to gain weight (PbO) until its activity is raised to equal that within the crucible of PbO activity A. This is shown in Fig. 2a. Weight gain will stop at composition point D, fixing one side of the single-phase region. The sample will continue to maintain this weight for as long as the atmosphere within the crucible remains at a constant PbO activity.

Next, this sample, now with PbO activity D, is equilibrated with a low CAMP crucible of composition and PbO activity B. This new PbO activity difference causes the sample to lose weight to the atmosphere, until as in Fig. 2b, point E is attained. This point defines the low PbO activity side of the single-phase region. Hence, the weight change (loss), D to E, should exactly correspond to the molar width of the single-phase region.

By replacing the sample at activity E, in the first crucible of high activity A, reversibility may be demonstrated by a weight gain exactly corresponding to the previous weight loss.

b. PZT (CAMP) Crucible Fabrication. The desired crucible composition was obtained by homogeneously mixing correct proportions of the reagent grade oxides of lead, titanium, and hafnium-free zirconium. Approximately 300 grams of the selected composition was isostatically pressed (30,000 psi) about a tapered stainless steel plug (1-3/4 in. x 7/8 in. dia.). Carefully sawing the top of the resultant shape allowed the removal of the steel plug, leaving a formed crucible and cap.

---

*The vapor pressure of PbO above $Pb(Ti_{.5}Zr_{.5})O_3$ + zirconia is approximately $5 \times 10^{-4}$ atm. at 1100°C.[29]

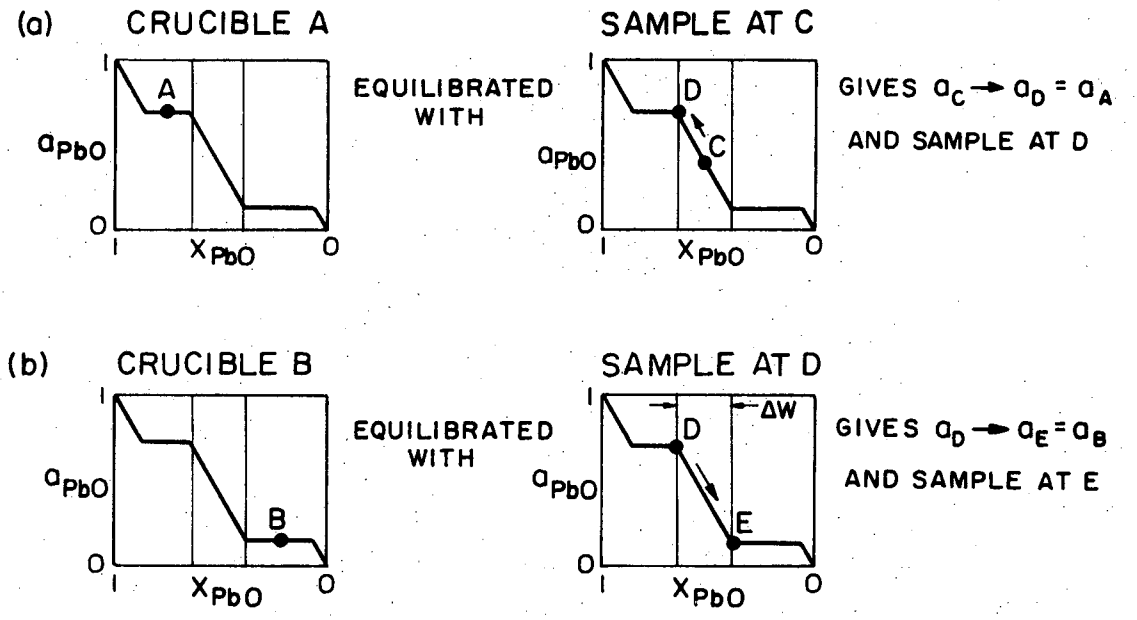


Fig. 2. Activity-composition diagrams illustrating two-step experiment to determine the width of $Pb(Ti_xZr_{1-x})O_3$ single-phase regions.

High CAMP crucibles containing excess PbO required further treatment since a liquid phase developed at firing temperatures. This liquid phase aided sintering and resulted in densification such that PbO vapor transport was restricted. The addition of about 20 vol % of finely crushed napthalene crystals provided ample controlled porosity after sintering. The napthalene was slowly burned out at 250°C.

All crucibles were calcined in air for 30 hours at 850°C in clean, covered platinum crucibles. X-ray diffractometer analysis of the calcined crucibles revealed traces of the major lines of PbO or $ZrO_2$ or $TiO_2$ originally added in excess at 2 mole % to give the multi-phase compositions.

After this step, the crucibles were soft enough to "finish." The tops and bottoms of both the crucible and cap were ground flat by hand. A 1/8 in. diameter hole was then drilled through the center of the cap, allowing access to the cavity for the platinum wire from a micro-balance.

Some experimental difficulties were encountered with compositions that yield either pure $PbTiO_3$ or $PbZrO_3$. The calcination of these crucible compositions produces a large volume expansion (associated with the compound formation) which causes severe cracking to occur. The resultant crucibles are too fragile to handle. If crucibles are formed from calcined multi-phase powder mixtures, little advantage is realized as cracking can occur due to rapid heating or cooling through the crystallographic phase transition that occurs at the Curie temperature.

c. Sample Fabrication. The homogeneously mixed oxides were combined with 30-40 vol % napthalene crystals (to provide controlled porosity), and the mixture was isostatically pressed (30,000 psi) around a clean

platinum coil (shown in Fig. 3). The napthalene was evaporated slowly (1C°/min to 250°C, 12 h soak) in air. The pressed sample was then placed in a clean covered platinum crucible and calcined for 30 hours at 850°C in air. (See Fig. 4.)

d. The Weight-Change Cell and Apparatus. The positioning of the sample in the crucible is diagrammed in Fig. 3. Samples to be used for future analysis could be placed within enclosed cavities in the cap as shown and removed at temperature without interrupting the gravimetric experiment. The TGA assembly, shown in Fig. 5, involved a vertically movable Kanthal wound furnace and a continuously recording microbalance. The sample was hung from the microbalance by an 8 mil dia. platinum wire with a short 16 mil dia. section in the hot zone of the furnace.

The sample was always weighed, before and after each experiment on a separate balance. The TGA platinum sample wire was weighed to determine the amount of PbO that condensed on it.

Spectrographic analysis showed that processing had not caused any observable contamination. The major impurities were 0.03% Bi, 0.03% Al, 0.02% Si, 0.01% Fe, and 0.06% Nb (all as oxide weight percents).

3. Results and Discussion

a. Error Reduction and Experimental Control. The use of a PZT CAMP crucible as a controlled and constant source of PbO vapor, is subject to several apparent errors that must be either minimized or proved negligible.

First, the sample could lose PbO by diffusion out the hole provided in the crucible cap. This problem was shown to be insignificant if the

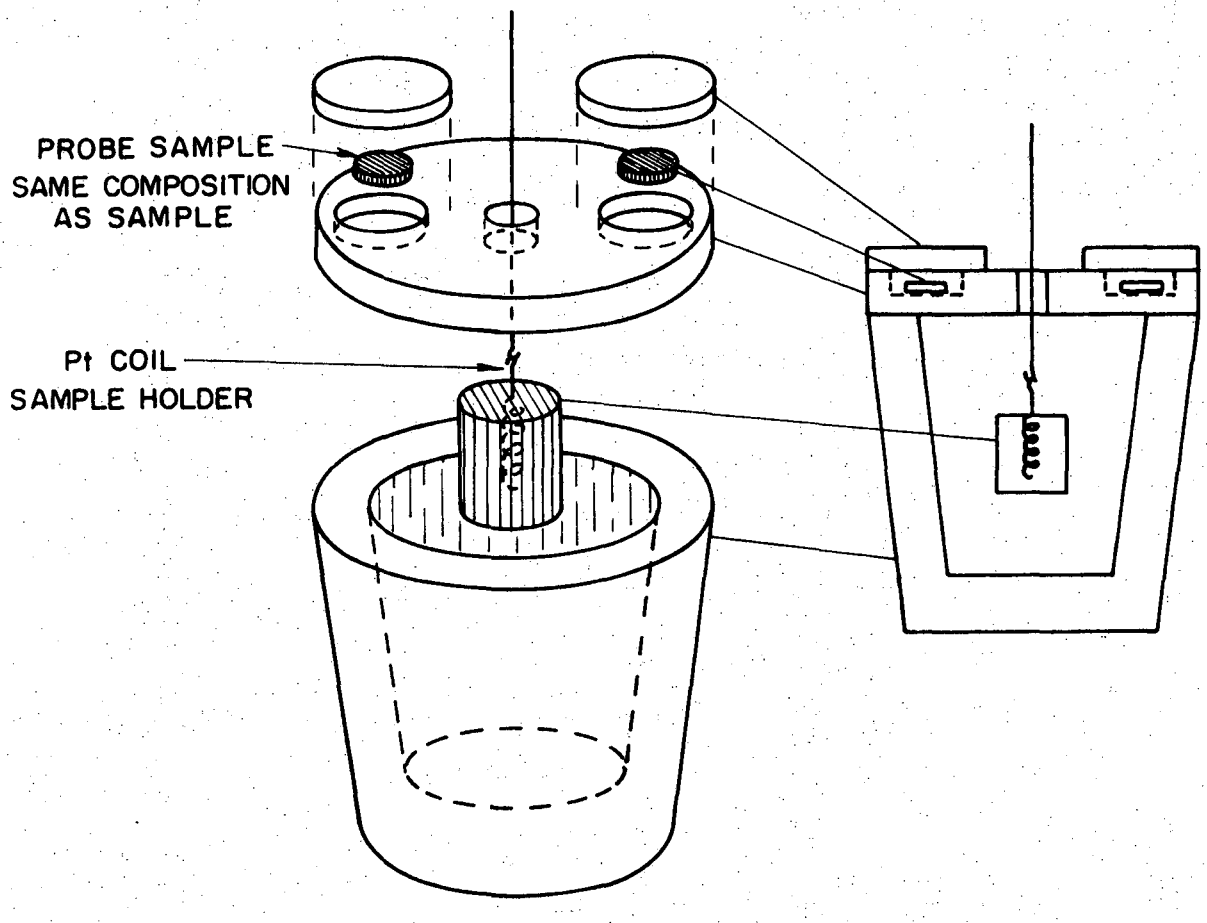


Fig. 3. Weight-change (CAMP) crucible for thermogravimetry.

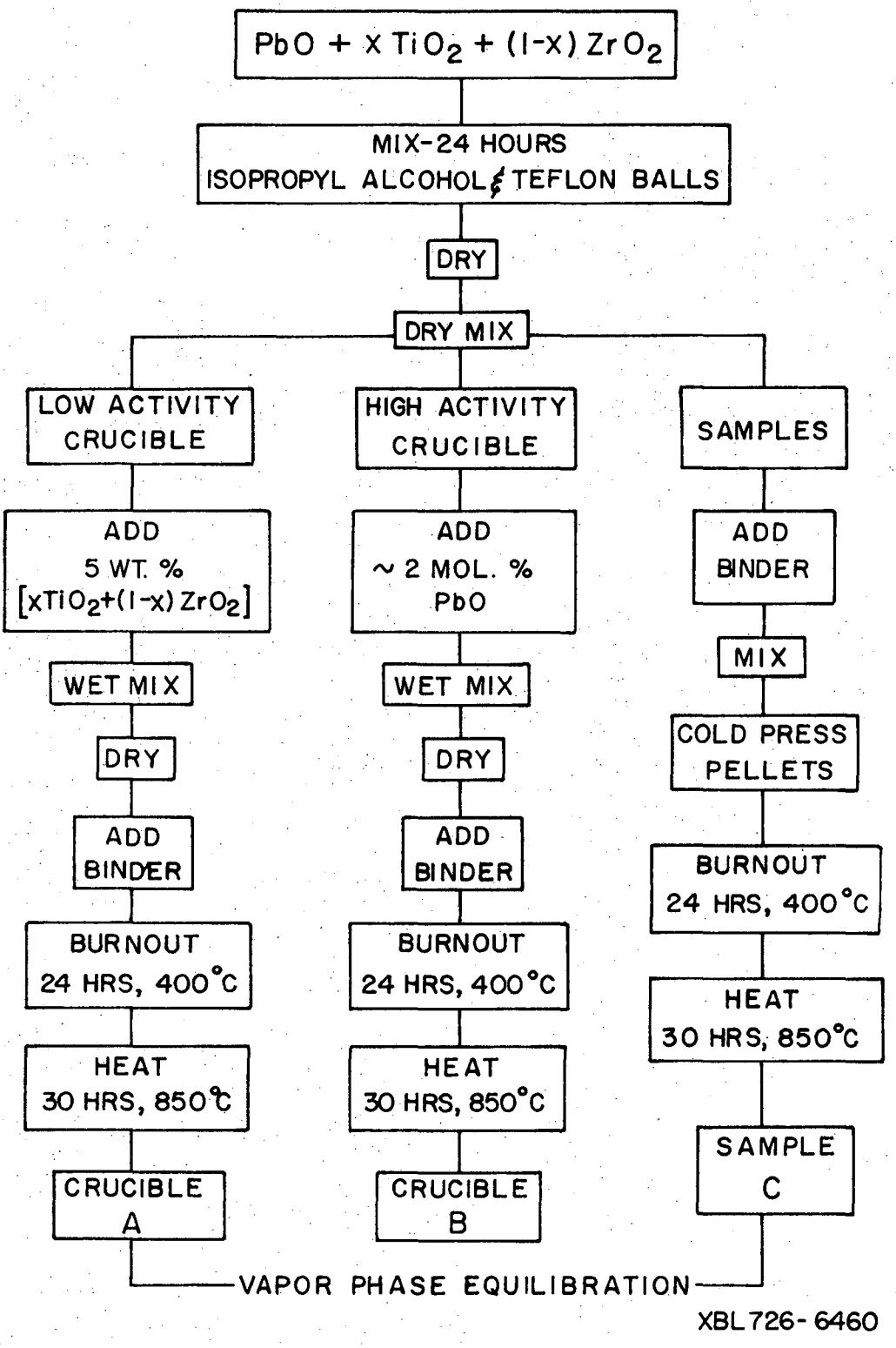


Fig. 4. Sample and crucible processing diagram-for the vapor phase equilibration experiment.

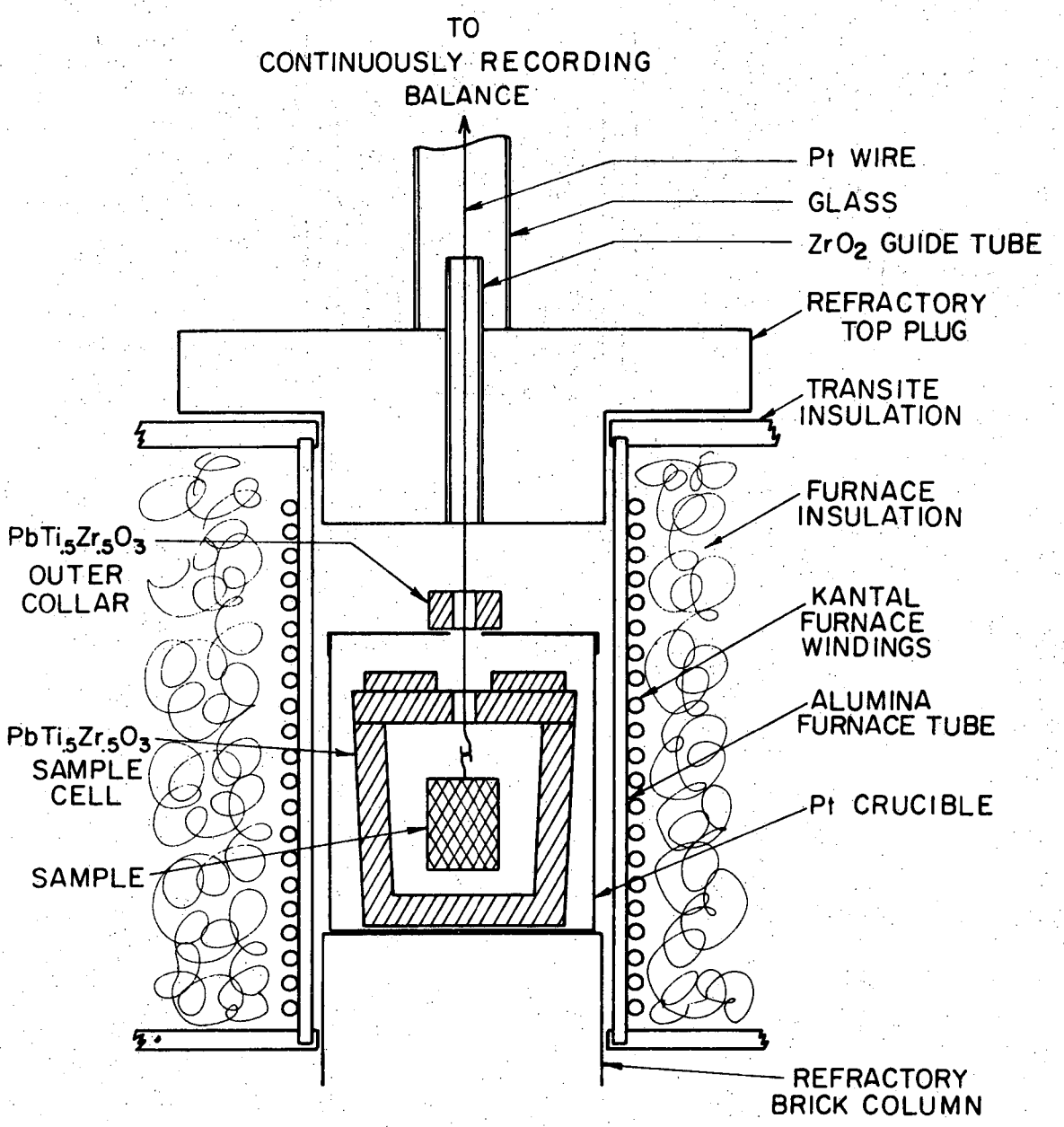


EXPERIMENTAL ARRANGEMENT

XBL 7010-6819

Fig. 5. The experimental arrangement for the vapor phase equilibration experiments.

sample was placed deep enough within the crucible. A check was made by comparing the weight changes produced by heating control samples equilibrated in both sealed and normal (1/8 in. dia. hole) crucibles. Identical results were obtained, indicating the rate of loss of PbO to be much slower than its volatilization from the crucible material.

Also, at operating temperatures the PbO evaporation from the PZT material of the crucible will condense on any surface with a temperature below that of the furnace hot zone. The platinum suspending wire, a good conductor of heat allowed PbO vapor to condense on it, indicating an erroneous weight gain. The magnitude of this gain was measured for a platinum wire hanging into a typical PZT crucible. The error could be reduced to only 5 mg/experiment by minimizing PbO escape (furnace chimney effect) and using a thin platinum wire that had previously become saturated with PbO.

A final problem was encountered with the high PbO CAMP crucible compositions. These cells were required to provide large amounts of PbO to the sample (typically 300 mg). When this PbO vaporized from the crucible wall to the sample, it left behind a transient PbO-depleted layer to be replenished by PbO diffusion from the bulk of the wall. However, the presence of the liquid phase enhanced densification of the crucible wall, thereby retarding the PbO diffusivity in the wall. Then the PbO evaporation rate from the surface of the wall can exceed its rate of replenishment by diffusion. When this occurs, the PbO activity in the cell is controlled by the lead-depleted surface layer, resulting in a corresponding weight loss of the equilibrated sample that increases

with time. This error could not be completely eliminated, but was minimized by increasing the porosity of the CAMP crucible wall, to create shorter diffusion paths.

Low density (high surface area) CAMP crucibles were made, first by a napthalene addition during fabrication, and then by painting a mixture of PZT and PbO (suspended in isopropyl alcohol) on the inner walls, prior to the experiment. Sample sizes were made small enough so that weight gains of no more than 150 mg would be expected. Under these conditions, the maximum usable length of a single run at 1100°C was found to be 15 hours with the cell maintaining "equilibrium" for 12 hours, before a slow sample weight loss (3 mg/hr) could be detected.

By comparison, the low CAMP crucibles showed no degradation after more than 1000 hours at a temperature of 1100°C.

To provide a final check on the validity of this equilibration method, the solid state substitutions of bismuth and niobium ions in $Pb(Ti_{.5}Zr_{.5})O_3$ were compared with results obtained by a discontinuous weight-change method (see Appendix A). These experiments agreed with the previous results and provided additional data from which previously unresolvable initial reaction kinetics could be interpreted.

b. The Single-Phase Region - $Pb(Ti_xZr_{1-x})O_3$. Experiments conducted to study the widths of the single-phase region of $Pb(Ti_xZr_{1-x})O_3$ are summarized in Table I for 1100°C. A width of 2.5 mole % PbO loss was indicated for $Pb(Ti_{.5}Zr_{.5})O_3$ at 1100°C. This would imply a total weight change of about 150 mg for a 10 gram sample. Several typical weight change cycles are shown in Fig. 6 (11.5 gram sample) illustrating the reversibility, and reproducibility of these experiments. Equilibration

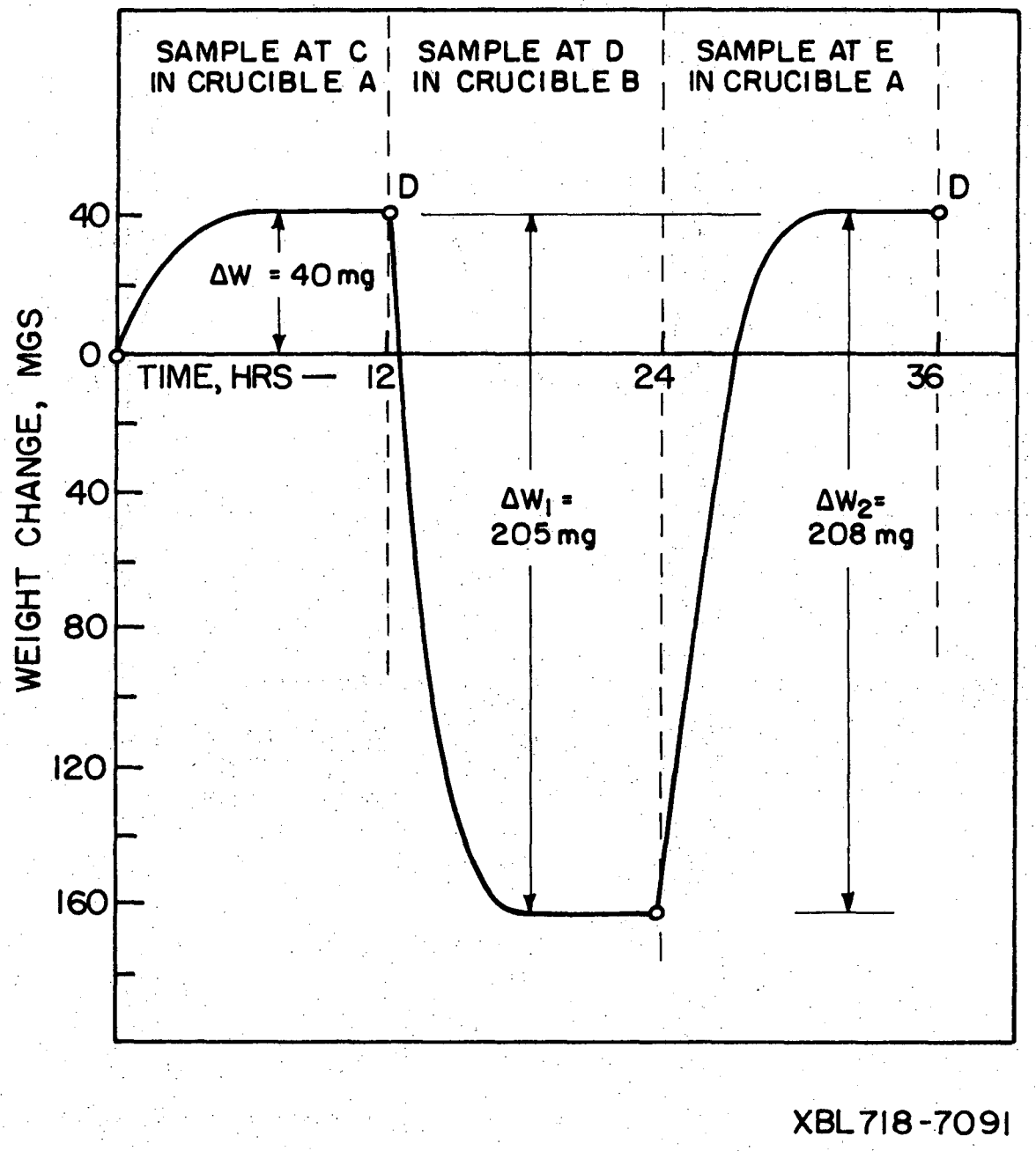


Fig. 6. Weight-change vs. time at constant temperature (1100°C). These three experimental curves illustrate the determination of the $PbTi_{.5}Zr_{.5}O_3$ single-phase width (ΔW) and the reproducibility of the experiment. The sample weight was 11.5 grams.

Table I. Summary of the vapor phase equilibration experiments based upon the sample weight changes (T = 1100°C)

$$[Pb_{1-x}\square_x(Ti_yZr_{1-y})O_{3-x}\emptyset_x]$$

| y | wt % PbO lost | mole % PbO lost | x |
|---|---|---|---|
| 0.9 | 4.01 | 5.5 | 0.055 |
| 0.8 | 3.1 | 4.2 | 0.042 |
| 0.65 | 1.89 | 2.7 | 0.027 |
| 0.50 | 1.72 | 2.5 | 0.025 |
| 0.40 | 1.08 | 1.6 | 0.016 |
| 0.20 | 1.98 | 3.0 | 0.030 |

□ indicates a lead ion vacancy

∅ indicates an oxygen ion vacancy

was somewhat more rapid in the low CAMP crucibles than in the high CAMP crucibles, probably due to the form of the activity variation with composition in the single-phase region. Both equilibration times were reasonable provided the sample retained adequate porosity.

Only a minor temperature dependence of the overall width of the single phase region could be detected (for $Pb(Ti_{.5}Zr_{.5})O_3$). When the temperature was raised to 1150°C, the zone widened about 0.08 mole % PbO loss. At 1200°C a similar increase was found. Incremental temperature lowering narrowed the region. No change in the width was detected when temperatures fell below 870°C, probably because the lowered PbO vapor pressure reduced mass transport to an immeasurable rate.

c. X-ray Diffractometry

X-ray diffraction techniques were used to identify the low temperature PZT phases as a function of non-stoichiometry. Gerson[20] has reported the low temperature phases for essentially stoichiometric PZT compositions. The results do not appear to be constant across the single-phase region. Stoichiometric $Pb(Ti_{.5}Zr_{.5})O_3$ is a tetragonally distorted perovskite, while the non-stoichiometric material produces diffraction lines corresponding to a mixture of rhombohedral and tetragonal phases. This probably indicates that the non-stoichiometric material is located on the phase boundary. A sketch, based on the analysis of several other compositions, is provided in Fig. 7. No attempt has been made to characterize the Curie temperature variation across the single-phase regions.

## B. Knudsen Effusion Experiment

### 1. Introduction

The "vapor phase equilibration," V.P.E., experiment, as described in the previous section, measures the width of most lead zirconate-titanate single-phase regions while affording a unique method of fixing the stoichiometry during processing. However, the technique could not be applied easily to the solid solution compositions at or quite near pure lead titanate or lead zirconate because of the difficulties encountered in fabricating the atmosphere crucibles and samples. Hence, another approach was taken.

A variation of the standard Knudsen effusion cell allows for an extended interpretation of the vapor pressure data. In fact, a single experiment may be designed to yield the width of any PZT single-phase

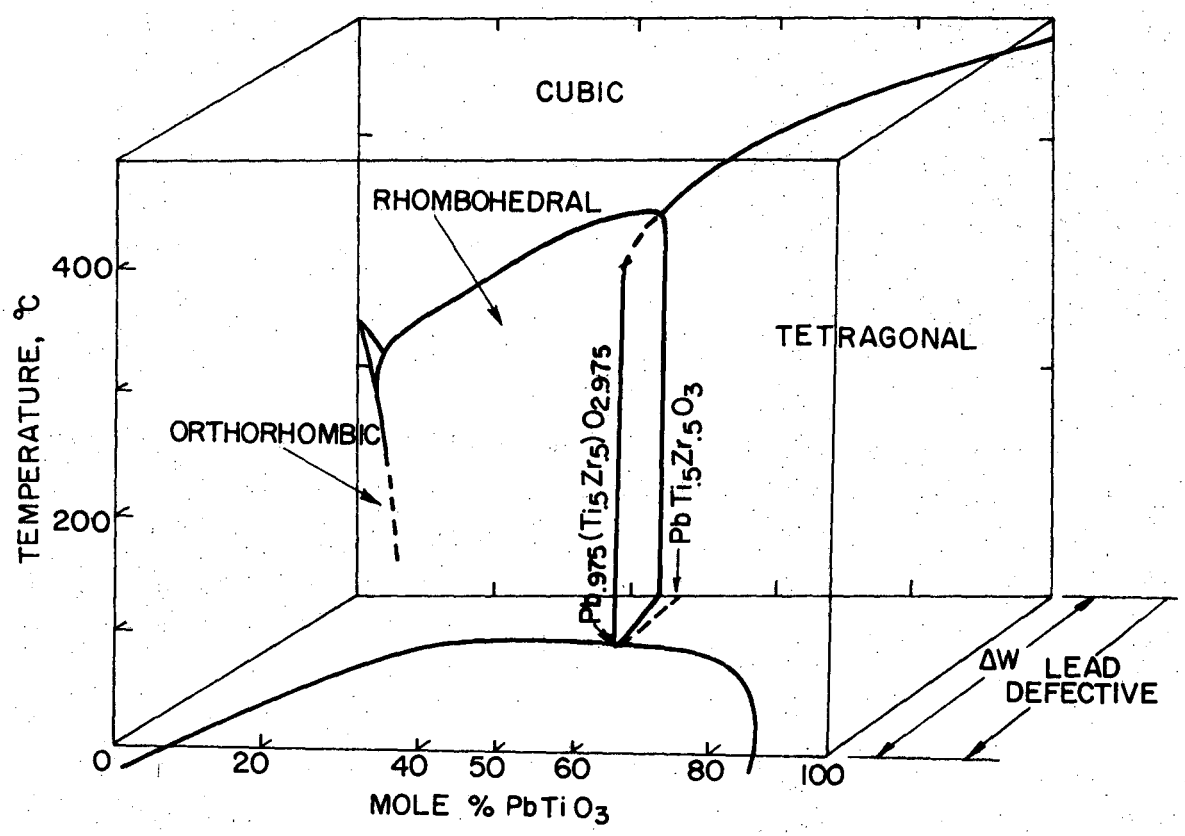


XBL726-6439

Fig. 7. Low temperature phase system of $Pb(Ti_xTr_{1-x})O_3$ modified to include the effect of non-stoichiometry. Tetragonal $Pb(Ti_{.5}Zr_{.5})O_3$ becomes tetragonal + rhombohedral $Pb_{.975}(Ti_{.5}Zr_{.5})O_{2.975}$; tetragonal $Pb(Ti_{.65}Zr_{.35})O_3$ becomes tetragonal $Pb_{.973}(Ti_{.65}Zr_{.35})O_{2.973}$.

region, the equilibrium lead oxide vapor pressure data as a function of temperature and composition, and the exact location of the stoichiometric composition, $Pb(Ti_xZr_{1-x})O_3$, within the single-phase region. This is possible because only a single component,[30,31] PbO, evaporates, so that the composition of the remaining condensed phase changes uniformly, and can be so constrained to cross the desired phase boundaries at a constant temperature.

In a typical Knudsen experiment,[28,32-34] the sample is sealed within a non-reacting cell with a small cylindrical orifice. Ideally, the equilibrium vapor pressure builds up within the Knudsen cell at a constant temperature. The orifice area acts as the effective area from which the vapor molecules will escape at the equilibrium rate. This equilibrium escape rate is inferred from the weight-change of the cell, by means of the Knudsen equation[32] (1):

$$p = (dw/dt)[2\ kT/m]^{1/2}/A_oW$$

where

$(dw/dt)$ = the weight-loss-rate (milligrams/hr) of the cell

$T$ = the orifice temperature in degrees Kelvin

$m$ = the mass of the effusing specie--taken as only the PbO molecule

$A_o$ = the orifice area

$W$ = the Clausing correction factor for the cylindrical orifice

$k$ = Boltzman's constant

In the usual Knudsen effusion method, the vapor pressure is measured above a material of fixed composition. However, because the samples in this study lose PbO by incongruent vaporization, PbO effusion causes the

sample composition to change with time. This allows the simultaneous collection of phase equilibria information.

The experimental variation instituted in this study, therefore, consisted of initially preparing a well characterized lead zirconate-titanate plus lead oxide sample, continuing the Knudsen effusion experiment until all the lead oxide is exhausted from the cell, and then recording the weight and analyzing the oxide residue. This technique is applicable to any $Pb(Ti_xZr_{1-x})O_3$ composition.

2. Experimental

a. Sample Preparation. The desired lead zirconate-titanate composition was prepared by carefully mixing the pure oxides in the manner that was previously described (see Fig. 8). The oxides were mixed with the concentration of lead oxide exceeding that of titania and zirconia by a known amount (4-16 wt %), to establish the overall sample composition at a known point within the (PZT+PbO) phase field. This powder was calcined in a [PZT+PbO] crucible to allow a brief high temperature soak (3 hrs., 1100°C) followed by a longer moderate temperature soak (20 hrs., 850°C). The powder was lightly re-mixed in a plastic mortar and pestle, and screened to remove the particles of less than 400 mesh.

Alternatively, the oxides were combined first in their stoichiometric proportions and calcined at a low temperature in air (840°C, 30 hrs.) to form the $Pb(Ti_xZr_{1-x})O_3$ compound. Then a precise amount of lead oxide (4-16 wt %) was added and homogeneously mixed with the PZT.

The overall composition in either case is located, for example, on the lead titanate phase diagram[4] shown in Fig. 9.

The powder was poured into the Knudsen cell to yield a low bulk density, which would inhibit sintering.

b. The Effusion Cell. The Knudsen effusion cells were fabricated from platinum, chosen for its low reactivity with lead oxide under the experimental conditions. Cylindrical cells were machined from 0.5 in. diameter rod, creating a cavity approximately 0.4 in. by 1.0 in. The cap was machined to the form shown in Fig. 10 and was drilled with a thin orifice, .013 in. in diameter, 0.15 in. thick. Appropriate corrections were made for the thermal expansion at a mean experimental

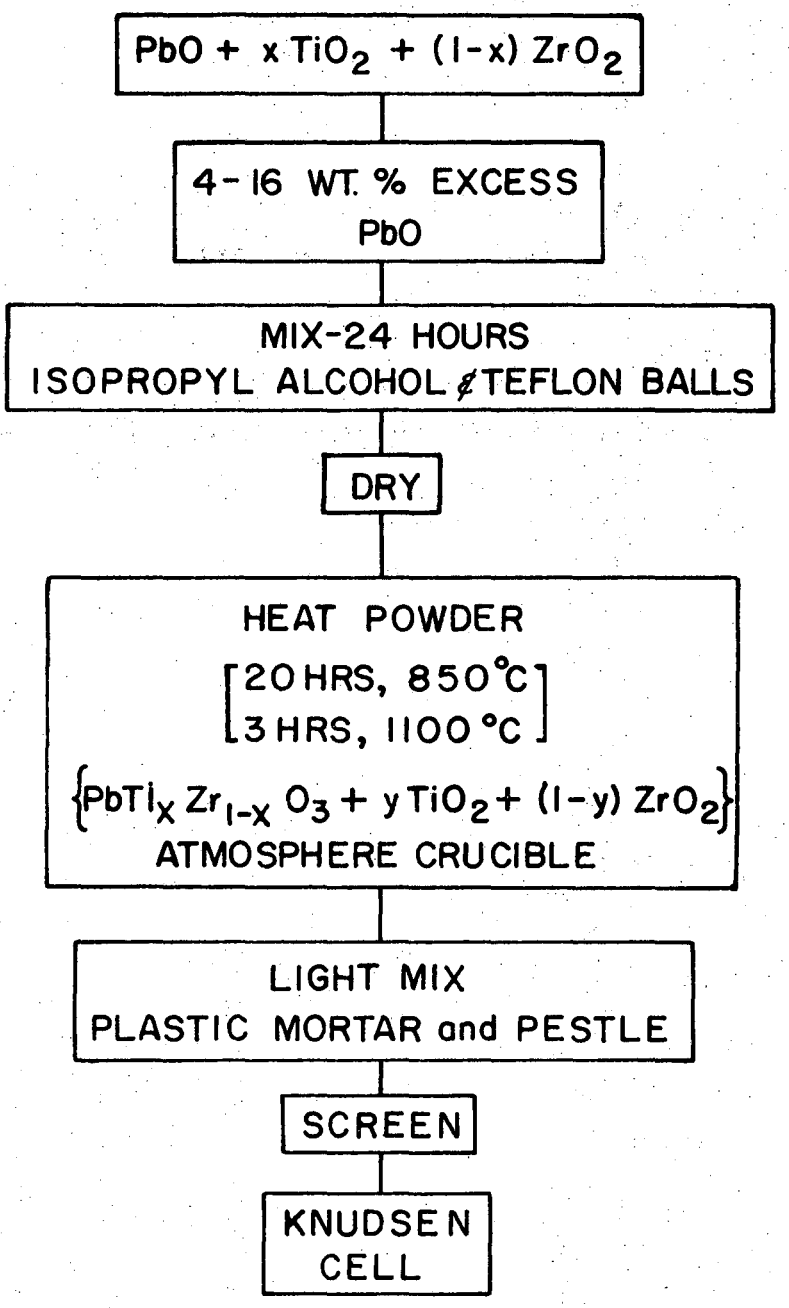


Fig. 8. Processing diagram for the Knudsen sample.

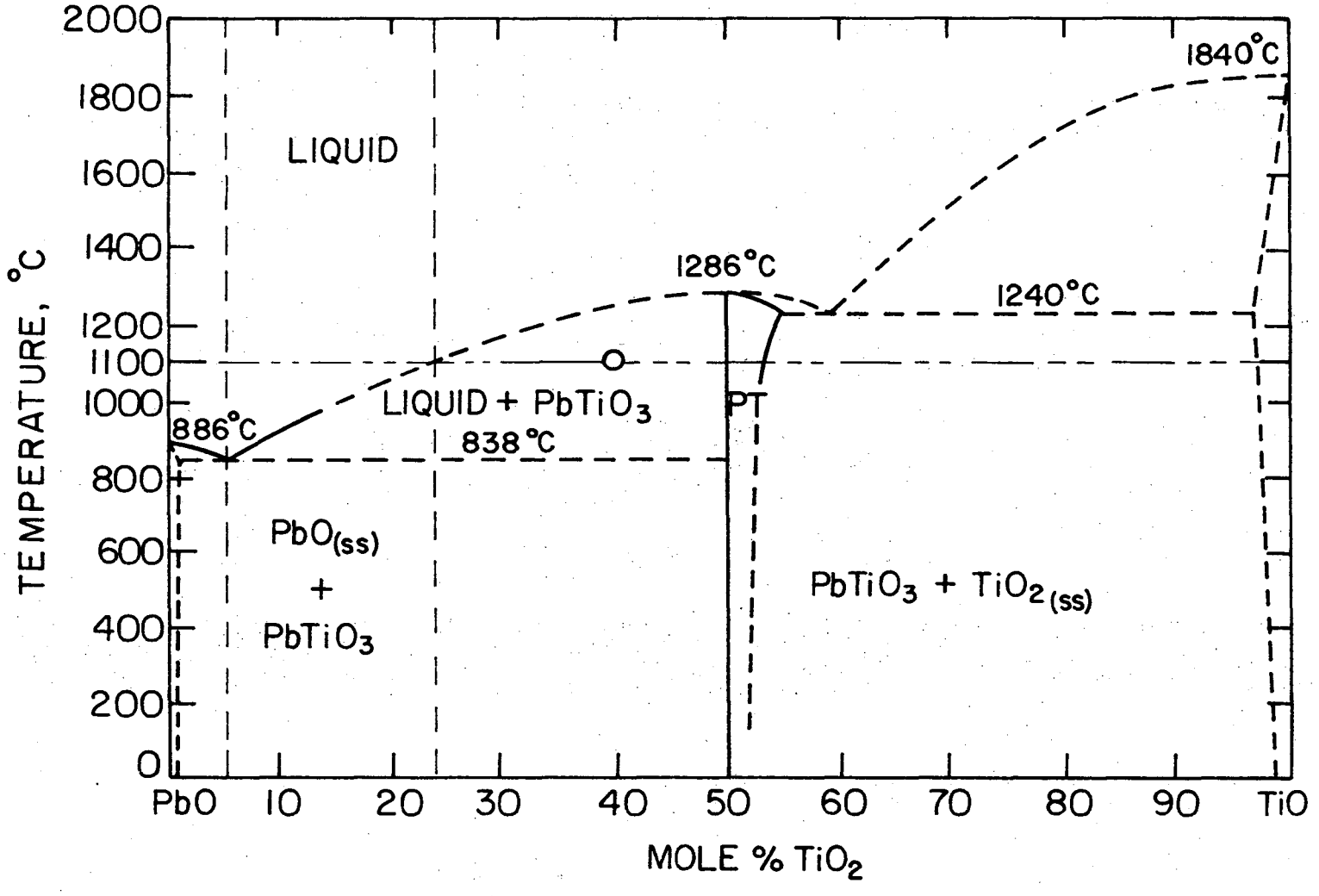


XBL726-6452

Fig. 9. Proposed $PbO-TiO_2$ phase diagram after Moon and including the experimentally measured lead titanate non-stoichiometry at 1100°C.

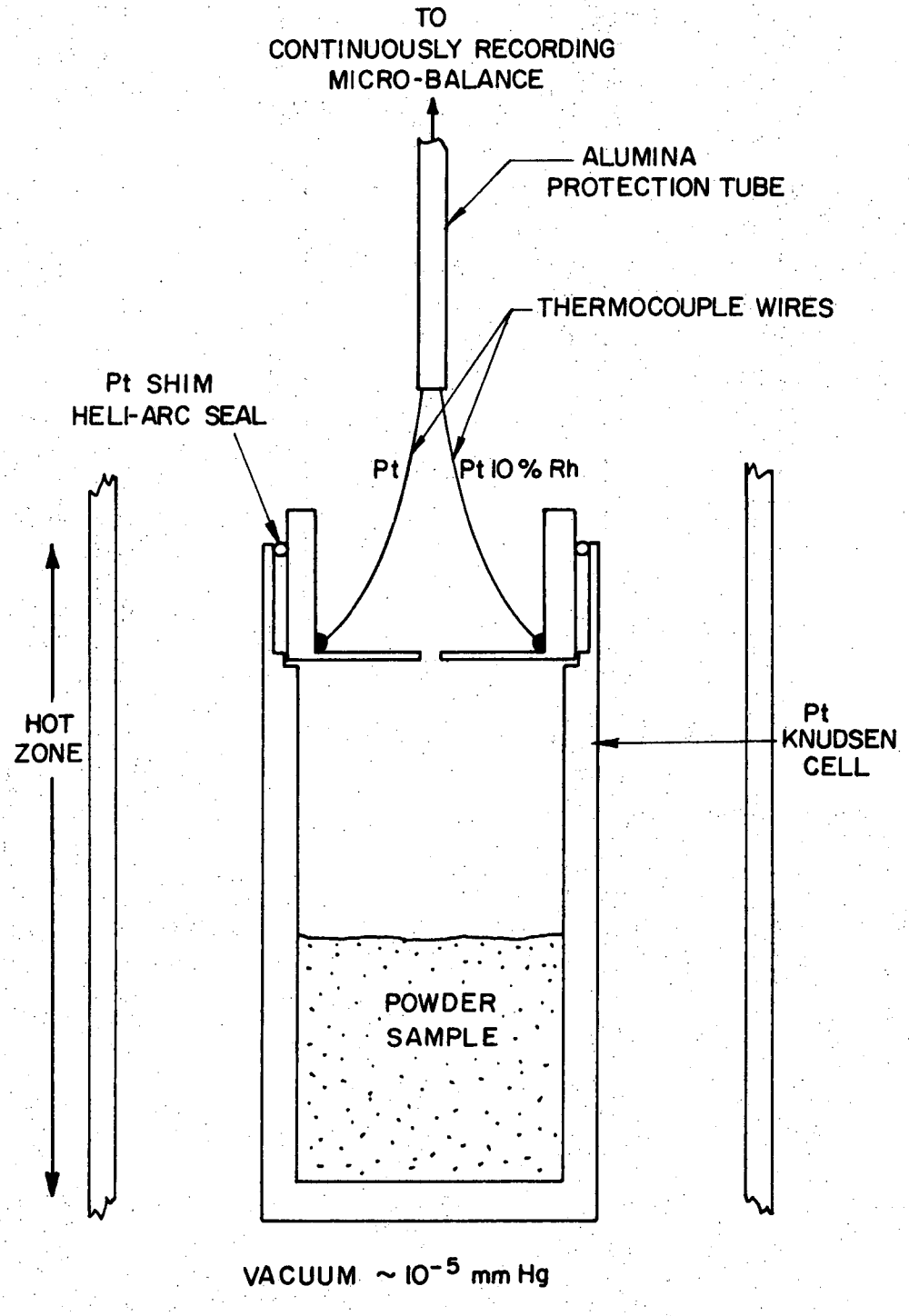


Fig. 10. Sectioned view of the Knudsen Effusion cell. Platinum shims are employed to allow sufficient heli-arc welding for a seal. The cell is suspended by a $Pt/Pt_{.9}Rh_{.1}$ thermodouple, with the temperature measuring junction created by the $Pt_{.9}Rh_{.1}//Pt$ cell junction.

temperature (1100°C) and the Clausing correction for the cylindrical orifice geometry chosen (0.485).

Temperature measurements were made by means of a Pt/Pt.$_9$Rh.$_1$ thermocouple, spot welded to the cap, in the manner illustrated in Fig. 10. A calibration experiment, with two thermocouples, one welded to the lid, and another welded to the bottom of the cell, indicated the temperature gradient was less than 0.5C° for all temperatures of interest.

The cap and the cell were sealed by heli=arc welding, utilizing a platinum shim. The cap design allowed alternate opening and re-sealing the crucible for a number of experiments.

c. The Thermogravimetric Apparatus. The experimental apparatus is diagrammed in Fig. 11. The balance used was an Ainsworth Recording Balance type RZA-AU-1, which records continuously the cell's weight loss in milligrams as a function of time. The system was evacuated by means of an oil diffusion pump to pressures in the $10^{-5}$ to $10^{-4}$ mm Hg range, where the lower limit was determined mainly by the outgassing of the extensive amounts of alumina bubble insulation material which was used so that the system could also be used for oxygen atmospheres.

The furnace was an alumina tube with resistance-wound Pt.$_8$Rh.$_2$ element, constructed such that the hot zone had a thermal gradient (vertical) of less than 1C° over a 3" zone. A permanently placed thermocouple was calibrated against the sample temperatures as determined by the spot-welded thermocouples as shown in Fig. 11.

The cell was suspended by a single thermocouple that was insulated by a thin, high-purity, dense alumina tube. Fine copper coils were employed to mechanically isolate the suspension system while allowing

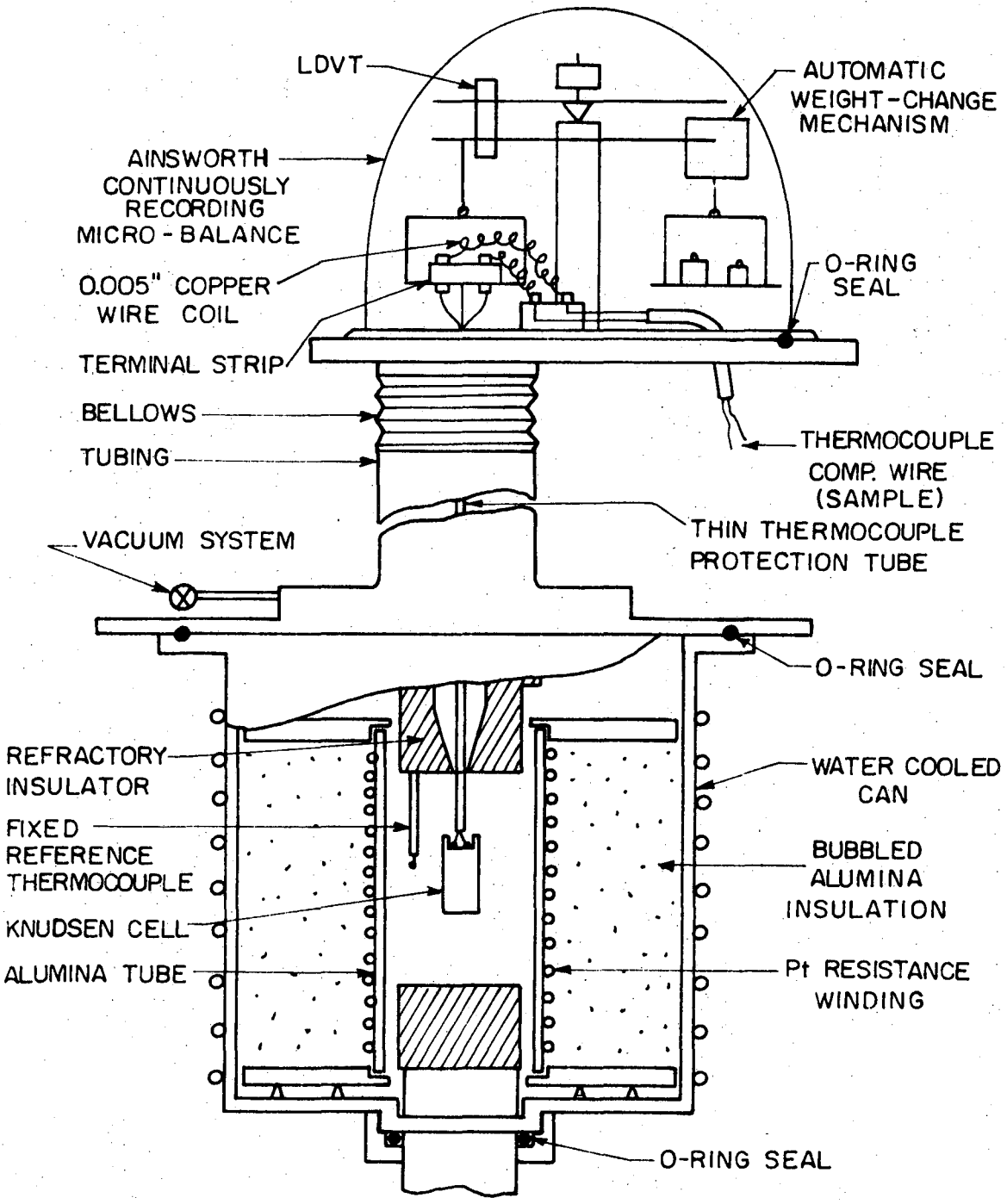


Fig. 11. The experimental apparatus used in the Knudsen Effusion Experiments. The continuously recording microbalance with automatic weight-change mechanism is an Ainsworth type RZA-AU-1. Thin copper coils from the sample suspension thermocouple to a terminal strip that may be reached by a vacuum feedthrough, serve to create mechanical isolation while providing electrical conduction.

potential measurements of the thermocouple, as shown in Fig. 11.

In these experiments, the thermocouple on the sample cell was used as the controlling thermocouple so that the cell would equilibrate to temperature changes rapidly. Provision was made so that this thermocouple could be connected to a potentiometer, when desired, to obtain accurate temperature measurements.

In some experiments a simpler arrangement was used. The cell was merely suspended by a 0.020 in. diameter $Pt._9Rh._1$ wire, and the temperature was calculated from that of the permanently placed thermocouple.

d. Experimental Procedure. The sample powder was first characterized by precise weighing, X-ray diffraction and chemical analysis for Pb, Ti and Zr content. The Knudsen cell was loosely filled with the powder (approximately 2 grams PZT, 0.40 grams excess PbO), sealed, dried, weighed, fitted with a thermocouple, and installed in the system. This was followed by a bakeout at 600°C for at least 24 hours to achieve a stable background pressure in the $10^{-5}$ to $10^{-4}$ mm Hg range. The cell was equilibrated and held successively at several different temperatures (i.e. 750°C, 800°C, 850°C, 900°C) for times long enough to obtain accurate, constant weight-loss rates which indicated the equilibrium lead oxide vapor pressures or activities. At the lower temperatures, where quite slow weight-loss rates were observed (less than 5 mg/hr), a discontinuous recording technique was required to conserve chart recorder paper and make the data analysis easier. The weight loss was marked at several long time intervals (1-10 hrs/interval).

Only a small portion of the excess lead oxide in the cell was exhausted by these preliminary weight losses. The sample, still possessing

two phases, was then equilibrated at the experimental temperature, 1100°C, while continuously recording the weight loss.

After some time, the loss of PbO significantly altered the sample compositions resulting in the formation of first, single-phase PZT, and then the multi-phase mixture of PZT with titania and/or zirconia. This is illustrated along the 1100°C isotherm drawn on the lead titanate and lead zirconate phase diagrams[5] shown in Figs. 9 and 12, and in the $PbO-TiO_2-ZrO_2$ isothermal ternary phase diagram[5,35] reproduced in Fig. 13. When two or more phases are in equilibrium, a constant weight-loss rate is to be expected. Again, the cell was equilibrated at several other temperatures (i.e. 1000°C, 1150°C, 1200°C, 1250°C, etc.), and the constant weight-loss rates that are proportional to the PbO vapor pressures above the multi-phase compositions were recorded.

Finally, the cell was held at 1200°C where a moderate and constant weight loss was expected until the end of the experiment when all PbO had been exhausted from the cell and no further weight loss was observed.

The cell was returned to room temperature, weighed, opened, and the contents weighed, collected, and analyzed. The total observed experimental weight loss should correspond to the amount of lead oxide initially in the cell.

This experiment can be repeated for any composition within the lead titanate-lead zirconate solid solution system.

3. Results and Discussion

The Knudsen effusion experimental data consisted of the effusion generated weight loss of lead oxide from the cell as a function of time at a constant temperature. The Knudsen equation applicable to this

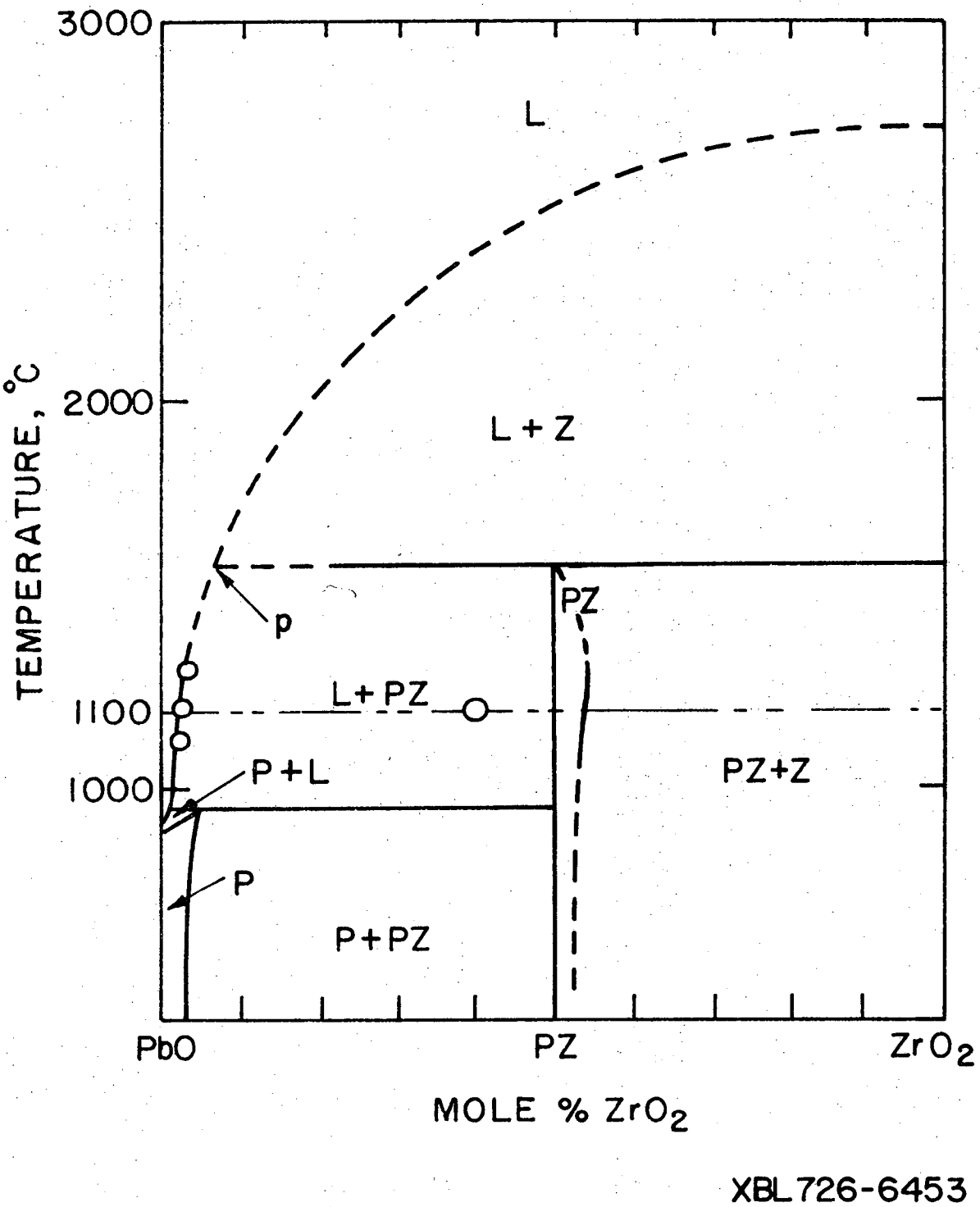


Fig. 12. The PbO - $ZrO_2$ phase diagram after Fushimi and including the experimentally measured lead zirconate non-stoichiometry at 1100°C.

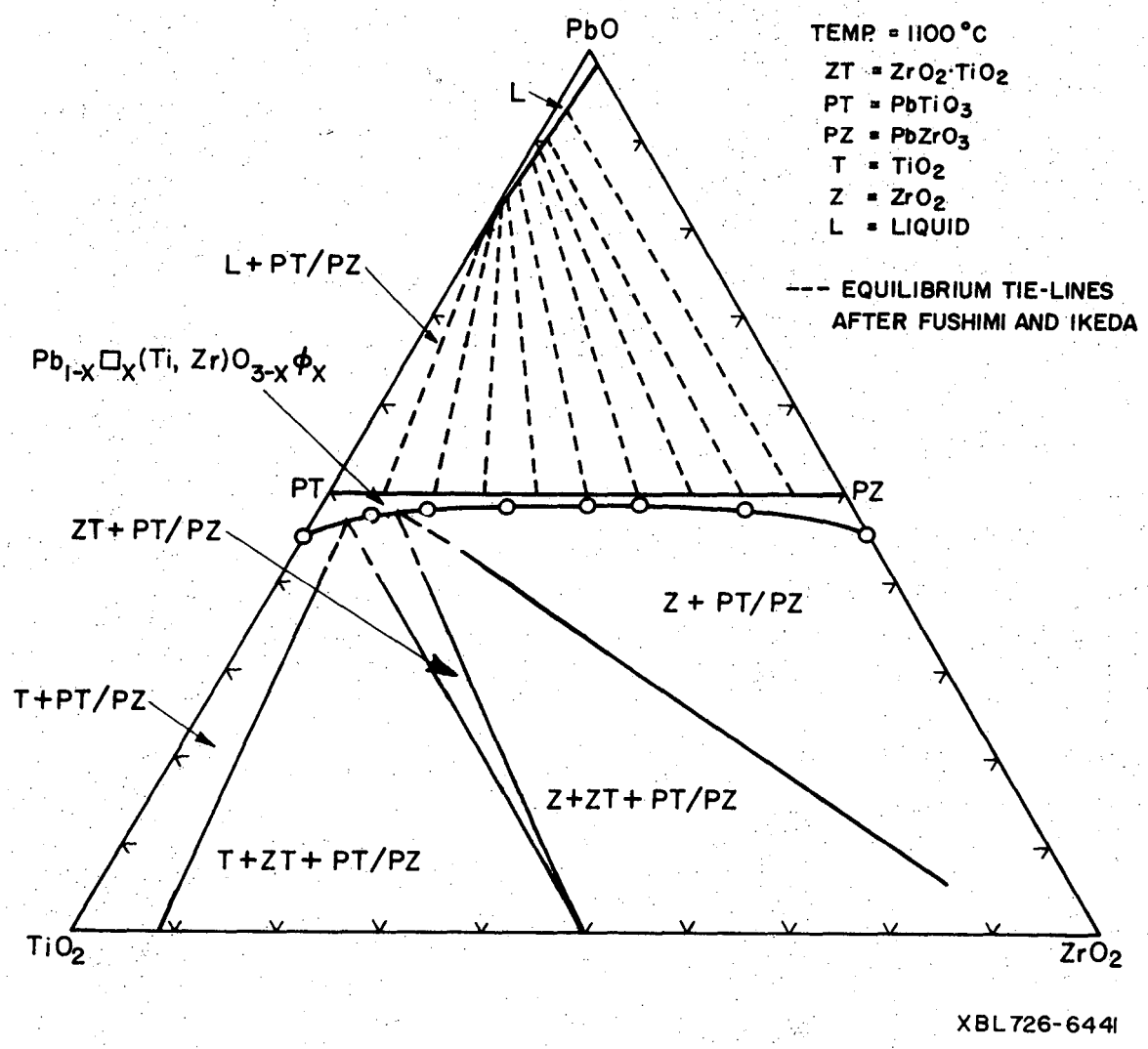


Fig. 13. The PbO - $TiO_2$ - $ZrO_2$ isothermal ternary phase diagram at 1100°C. The tie-lines in the PZT + LIQUID region were determined by Fushimi and Ikeda.[5,6] The phases present in the lower portion of the diagram were determined by Webster et al.[35] The variation in the width of the $PbTi_xZr_{1-x}O_3$ single phase region is drawn to scale.

system is

$$p(atm) = 4.675 \times 10^{-7} (dw/dt)[T]^{1/2}/W \qquad W = .485$$

W = the Clausing correction for a cylindrical orifice.[36,37]

No dependence upon the orifice area was found when an orifice diameter of 18 mils (doubling the orifice area) was used for PbO and $PbTiO_3$ experiments.

If the observed rate of weight loss of the cell is constant, so is the PbO equilibrium vapor pressure, and the composition of the sample lies in a two-phase region. On the other hand, when the rate of weight loss is not constant, the equilibrium PbO vapor pressure is changing with time. This is the case for the compositions within the single-phase region. When in a two-phase region, the overall sample composition is changing, but the vapor pressure of PbO is not.

When during the course of the experiment the lead oxide effusion causes the sample composition to cross into the PZT single phase region, the weight-loss rate observed became non-linear and slower, reflecting the reduced lead oxide activity in the sample as it becomes more deficient with respect to lead. When the continuous effusion of lead oxide caused the appearance of a new second phase (i.e. titania as in Fig. 9) the weight-loss rate, and therefore the vapor pressure, will become constant once again. Thus, the amount of lead oxide lost during the non-linear portion of the weight-loss data will correspond to the exact width of the PZT single-phase region with respect to PbO at that temperature, or the degree of non-stoichiometry of the compound, as is illustrated in general in Fig. 14.

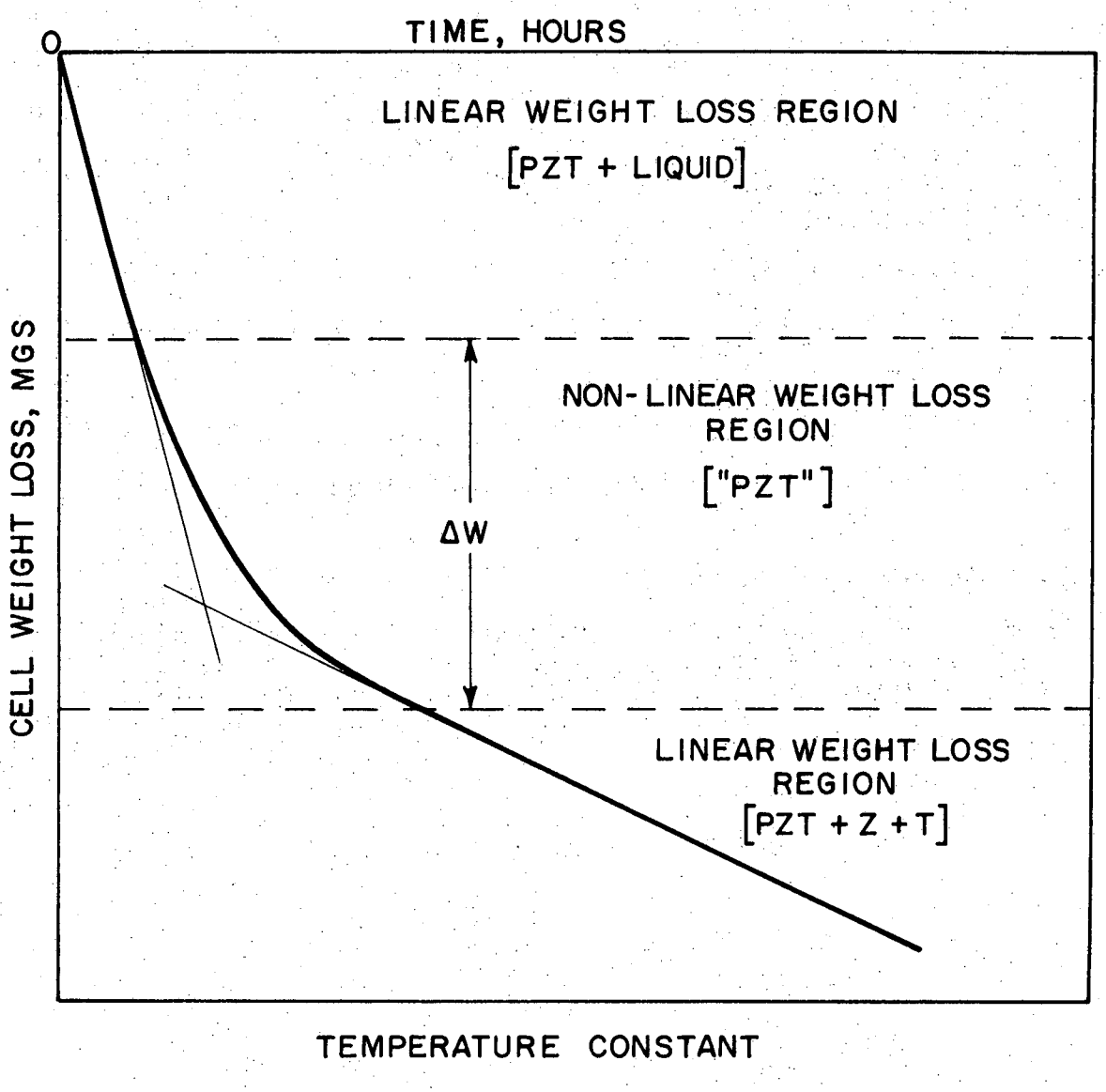


Fig. 14. General form of the Knudsen effusion data at a constant temperature when the Knudsen sample alters its composition through the $PbTi_xZr_{1-x}O_3$ single-phase region. This corresponds to the non-linear portion of the weight-loss vs time curve.

This non-linear region is measurable for all lead zirconate-titanate compositions, is quite reproducible, and is independent of the amount and particle size distribution of the sample powder. However, screening techniques were always used to remove the smallest particles from the distribution.

Figure 15 summarizes the entire form of the data. The actual results are summarized in Table II where "mol. and wt. %" refers to the percent lost. They agree closely with the data obtained in the "vapor phase equilibration" experiment, see Part II-A. The variation found in the width of the PZT single-phase regions is illustrated graphically in Fig. 16 in mole % PbO lost from the sample, mole % lead vacancies in the sample, and in mole fraction of PbO. This relation is drawn to scale on the ternary phase diagram in Fig. 13, the $PbTiO_3$ phase diagram in Fig. 9, and the lead zirconate phase diagram in Fig. 12. It is seen that both the terminal compositions, lead titanate and lead zirconate, possess the widest ranges of non-stoichiometry in the system.

Assuming the rate of weight loss to be proportional to the vapor pressure of PbO within the cell at all times, tangents constructed to the weight-loss curve allow calculation of the lead oxide vapor pressure or activity as a function of composition. The non-linear portion of one experiment is expanded in Fig. 17.

These data, tabulated in Appendix B, allows the graphical integration of the Gibbs-Duhem equation,[38-40] which yields the corresponding activity of titania or zirconia and consequently the free energy of mixing as a function of composition through the PZT single-phase region. This calculated free energy of mixing is found to have a minimum within

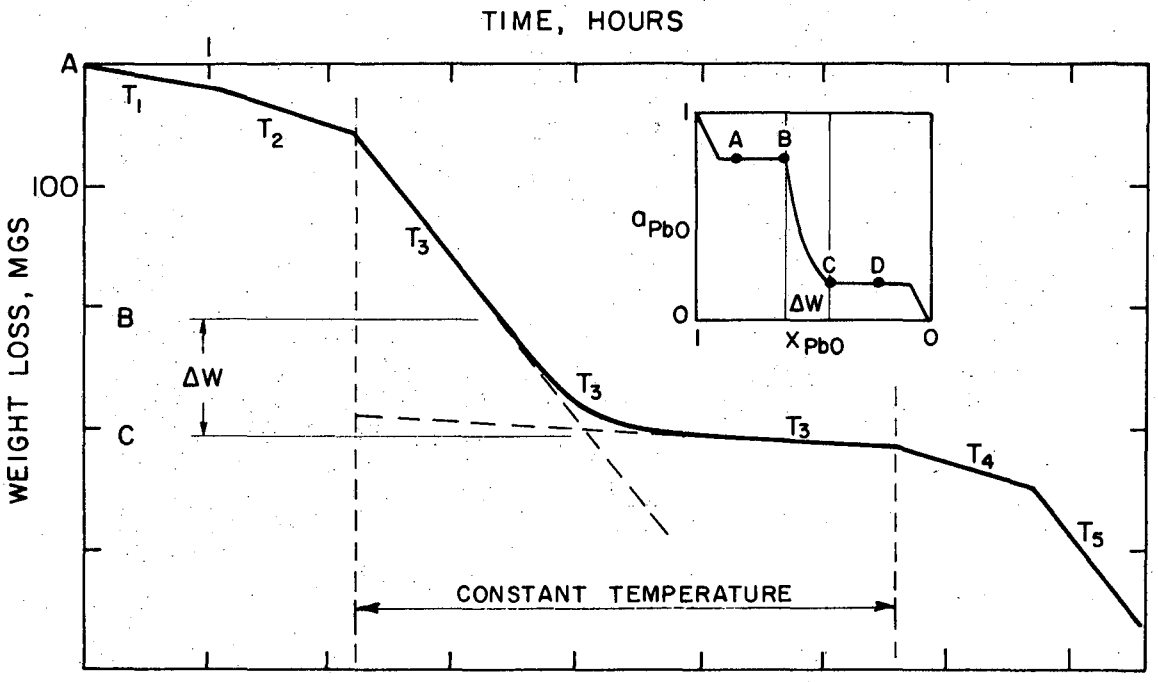


TYPICAL WEIGHT LOSS DATA FROM KNUDSEN EFFUSION EXPERIMENT ON $(Pb(Ti_xZr_{1-x})O_3 + \delta PbO)$

XBL 723-6075A

Fig. 15. Knudsen cell weight loss vs time during a typical experiment. Equilibration at successive temperatures on both sides of the single-phase region allows efficient collection of vapor pressure data. ΔW, corresponding to the weight-loss from B to C on the activity diagram, measures the width of the PZT single phase region.

Table II. Tabulated results of the "Vapor phase equilibration (VPE)" experiment and the Knudsen Effusion (KE) experiment defining the extent of non-stoichiometry or width of the PZT single-phase region.

$$Pb_{1-x}\square_x(Ti_yZr_{1-y})O_{3-x}\phi_x$$

| | ΔW SINGLE-PHASE WIDTH | | | SAMPLE COMPOSITION (BOUNDARY) | | | | | EXPERIMENTAL METHOD | |
|---|---|---|---|---|---|---|---|---|---|---|
| y | WT. % | "MOL. % PbO" | x | MOL. % PbO | MOL. % □, φ | MOL. % $TiO_2$ | MOL. % $ZrO_2$ | MOL. FRACTION PbO | V.P.E. | K.E. |
| 1.0 | 7.36 | 10.0±1.0 | 0.100 | 45.0 | 5.0 | 50.0 | 0 | 0.474 | | X |
| 0.9 | 4.01 | 5.5±0.5 | 0.055 | 47.25 | 2.75 | 45.0 | 5.0 | 0.486 | X | X |
| 0.8 | 3.1 | 4.2±0.5 | 0.042 | 47.9 | 2.1 | 40.0 | 10 | 0.490 | X | X |
| 0.65 | 1.89 | 2.7±0.3 | 0.027 | 48.65 | 1.35 | 32.5 | 17.5 | 0.493 | X | X |
| 0.5 | 1.72 | 2.48±0.3 | 0.025 | 48.75 | 1.25 | 25.0 | 25.0 | 0.494 | X | X |
| 0.4 | 1.08 | 1.6±0.2 | 0.016 | 49.2 | 0.8 | 20.0 | 30.0 | 0.495 | X | X |
| 0.2 | 1.98 | 3.0±0.5 | 0.030 | 48.5 | 1.5 | 10.0 | 40.0 | 0.4925 | X | X |
| 0 | 6.1 | 9.5±1.0 | 0.095 | 45.475 | 4.525 | 0 | 50.0 | 0.475 | | X |

## FORMULAE USED

*(1) $$\text{"MOL. \% PbO"} \equiv \frac{\text{NO. MOLES PbO LOST}}{\text{NO. MOLES PbO IN SAMPLE}}(100) = \frac{(\delta W)(MW\text{-}PZT)}{223.19\,(W_s)}(100)$$

*(2) $$\text{"WT. \% PbO"} \equiv \frac{(\text{GRAMS PbO LOST})}{(\text{GRAMS PbO IN SAMPLE})}(100) = \frac{(\delta W)(100)}{[(W_s)/(MW\text{-}PZT)](223.19)}$$

$$\text{"WT. \% PbO"} = \text{"MOL. \% PbO"}$$

(3) $$\text{WT. \%} \equiv \frac{\text{GRAMS LOST}}{\text{SAMPLE WT.}} \times 100 = \frac{\delta W}{W_s} \times 100$$

(4) $$\text{MOL. \% PbO} = \frac{(1-X)}{2}(100) \qquad \text{MOL. \% } TiO_2 = \frac{y}{2}(100)$$

$$\text{MOL. \% } \square, \phi = \frac{X}{2}(100) \qquad \text{MOL. \% ZrO} = \frac{(1-y)}{2}(100)$$

(5) $$\text{MOLE FRACTION PbO} = \frac{1-X}{(1-X)+1} = \frac{1-X}{2-X}$$

$\delta W$ = SAMPLE WT. LOSS

$W_s$ = INITIAL SAMPLE WT.

MW-PZT = MOLECULAR WT.

XBL726-6457

* "Mol. or wt. % PbO" refers to the percent lost from sample during experiment.

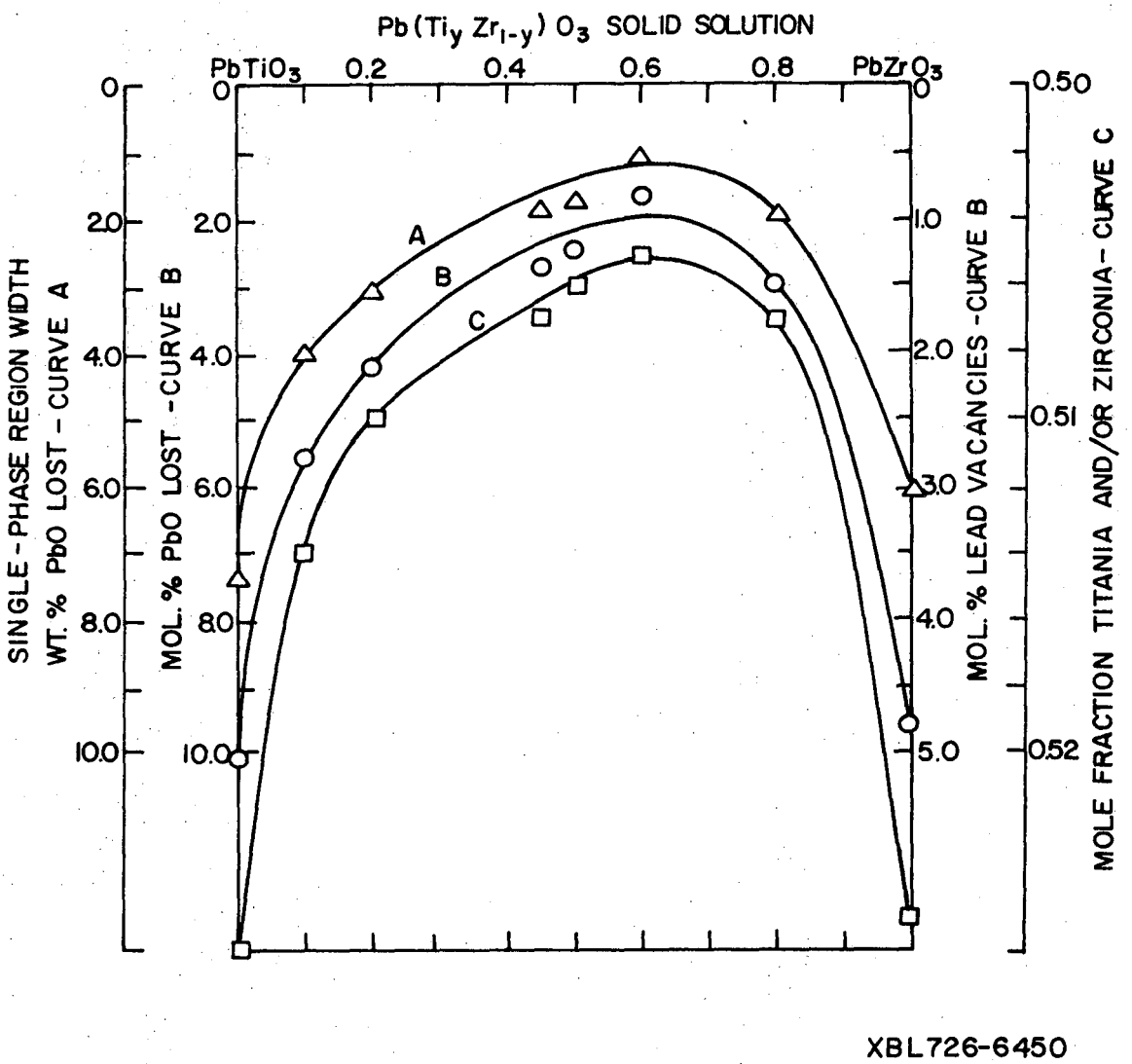


Fig. 16. Variation of non-stoichiometry in the lead titanate-lead zirconate solid solution system.

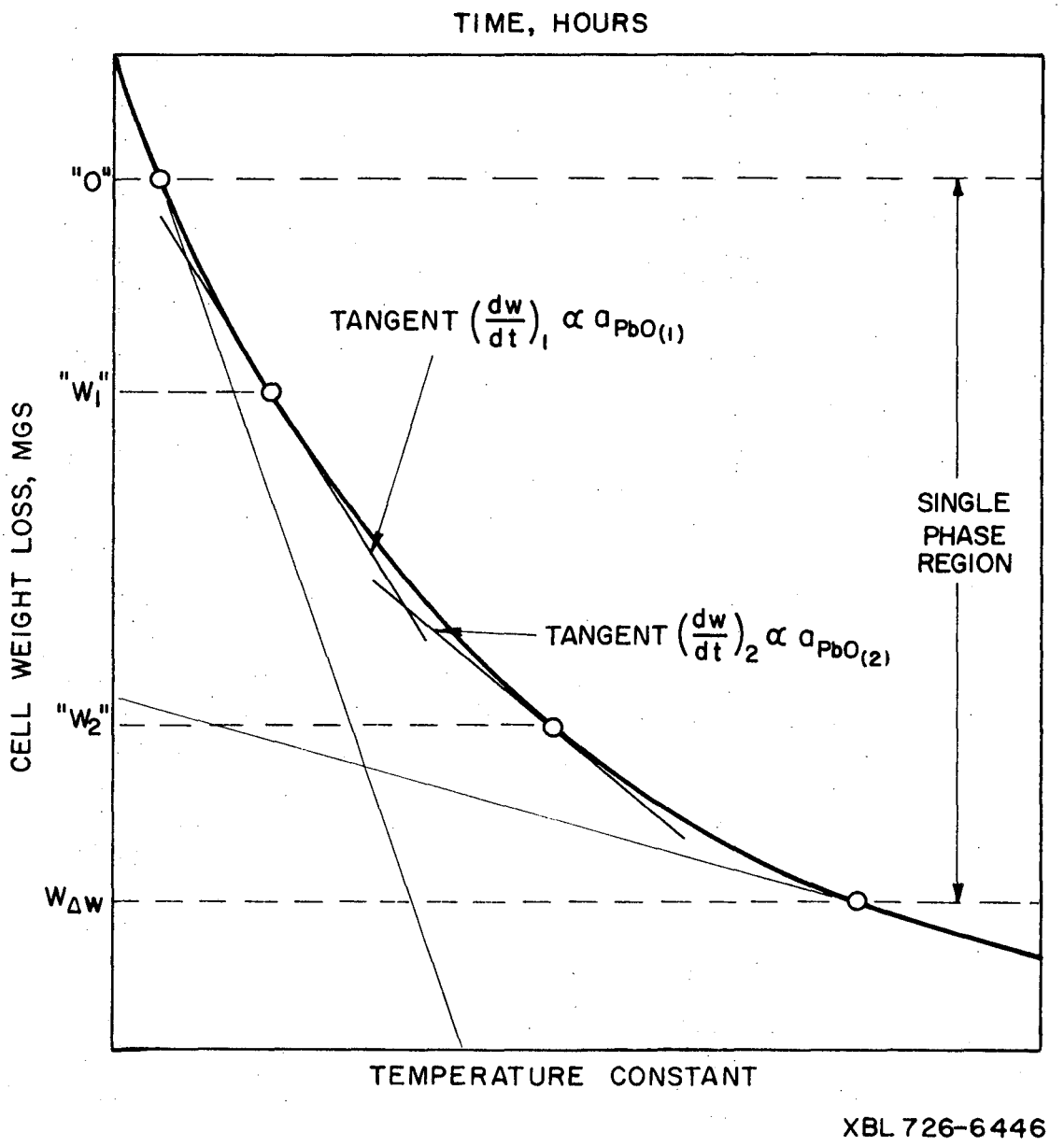


Fig. 17. Expanded non-linear portion of the Knudsen cell weight loss vs time data (single-phase region) allowing calculation of the lead oxide activity variation with composition through the single-phase region.

the single-phase region implying that the stoichiometric composition is not the most stable perovskite. The details of the analysis and the computer assisted calculation are presented in Appendix B. This analysis was applied to both lead titanate and lead zirconate. The reduced experimental results for activity as a function of composition are shown in Fig. 18 for $PbTiO_3$ and in Fig. 19 for $PbZrO_3$. The results of the free energy of mixings dependence on composition is offered for both materials in Fig. 20.

In addition, each experiment generates lead oxide vapor pressure data for the multi-phase regions that bound the non-stoichiometric compound. The results that are obtained compare favorably with those reported by Hardtl and Rau[29] for the (PZT+Z) phase field.

Pure lead oxide was used as a calibrating material since it has been extensively studied and is the only vapor species of consequence in the system.[30,31] However, some minor experimental difficulties were encountered that were associated with the formation of the lead oxide liquid at the temperatures of interest (850°C-1200°C). To determine if it was condensation and re-evaporation of lead oxide that was creating the difficulty, the hot stage of a scanning electron microscope was employed. A small model Knudsen cell was fabricated containing the same orifice geometry as the actual experimental cells, and pure PbO powder was placed in it.

The scanning microscope revealed that as the temperature was increased towards the melting point of PbO, some of the loosely packed powder expanded towards the orifice, and upon melting, wetted the orifice and outside of the cap. However, these effects could be virtually

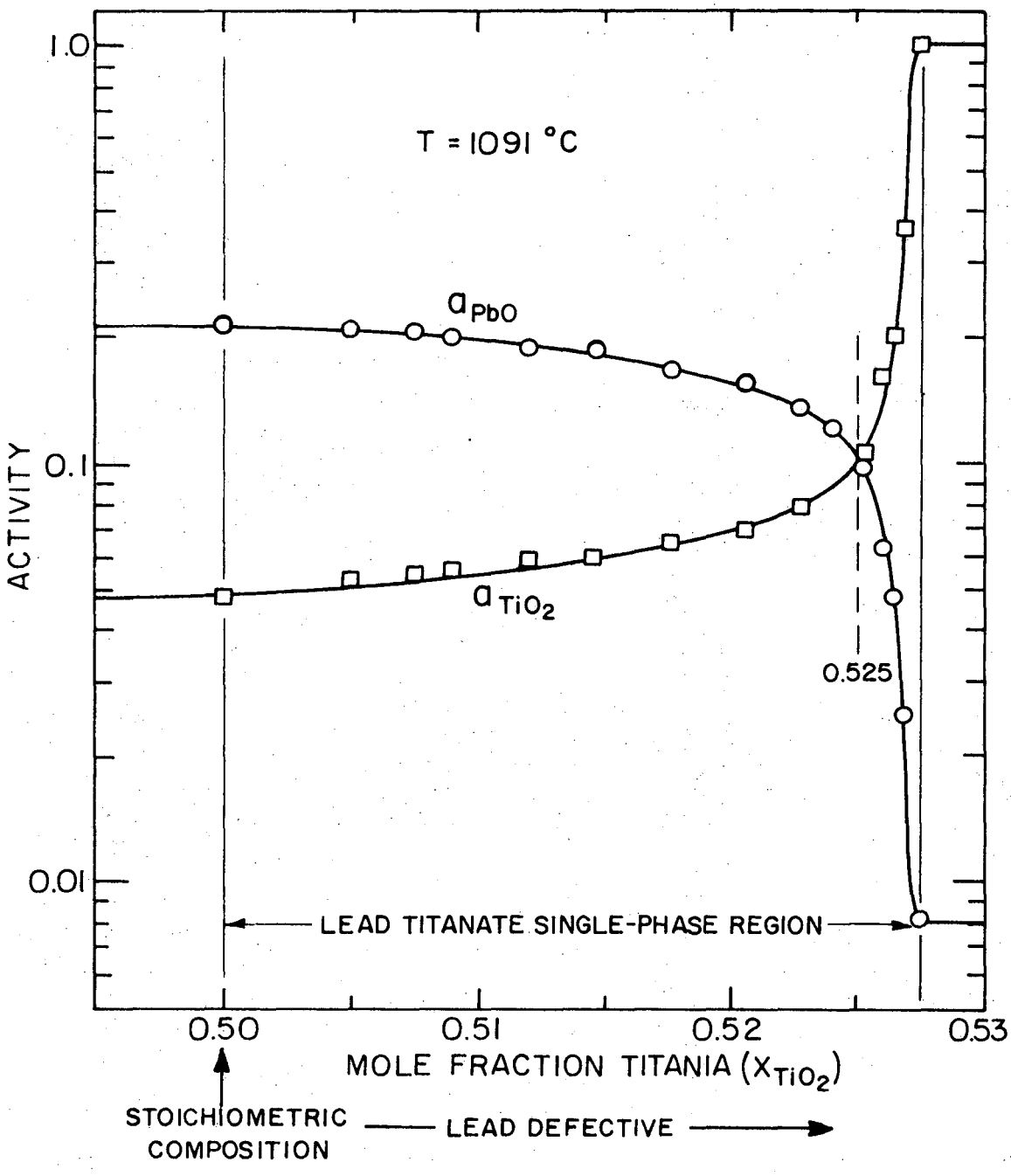


Fig. 18. Lead oxide and titania activity as a function of composition in the lead titanate single-phase region as determined from analysis of the Knudsen effusion data and a graphical integration of the Gibbs-Duhem equation (see Appendix B).

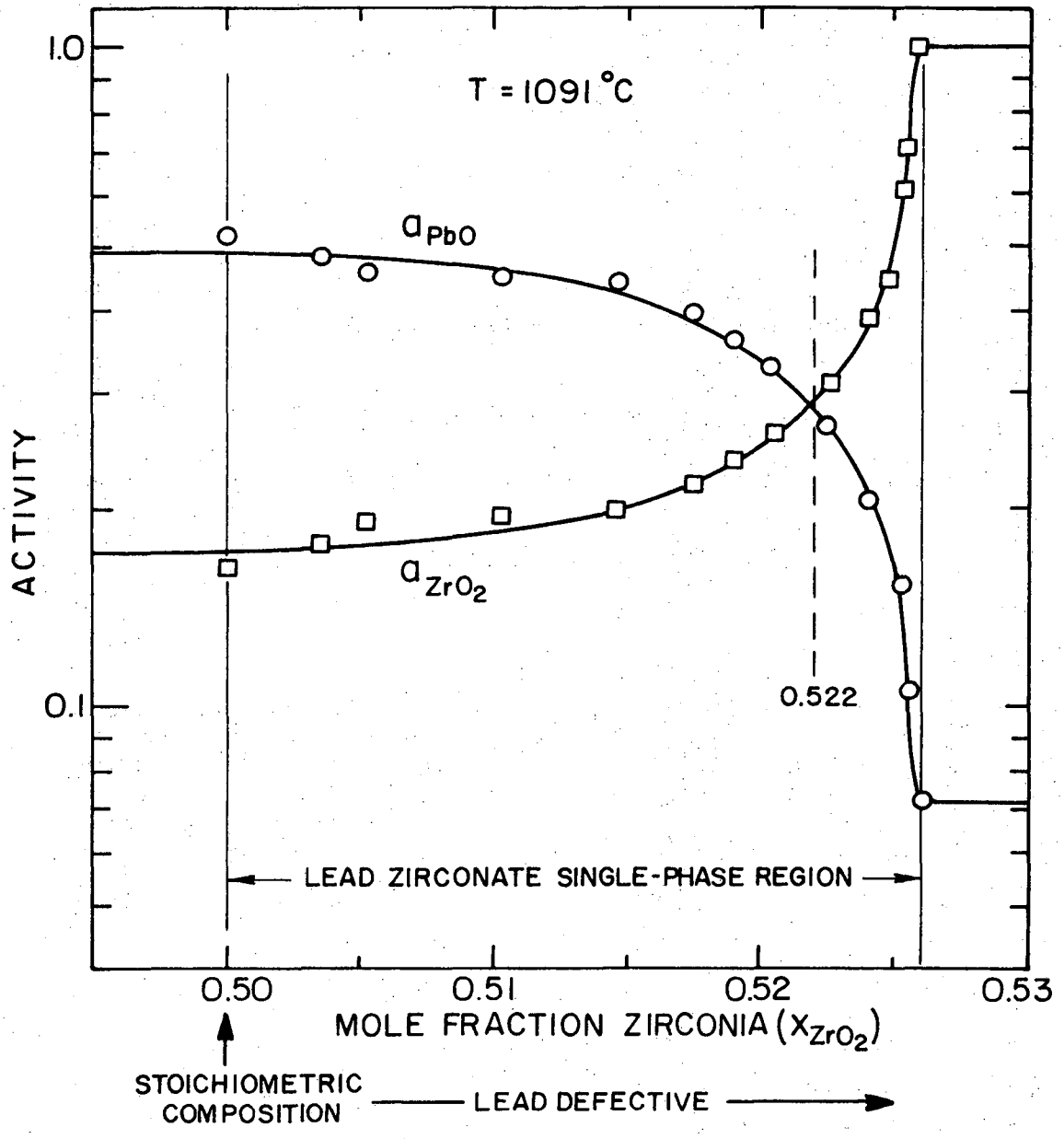


Fig. 19. Lead oxide and zirconia activity as a function of composition in the lead zirconate single-phase region as determined from analysis of the Knudsen effusion experimental data and a graphical integration of the Gibbs-Duhem equation (see Appendix B).

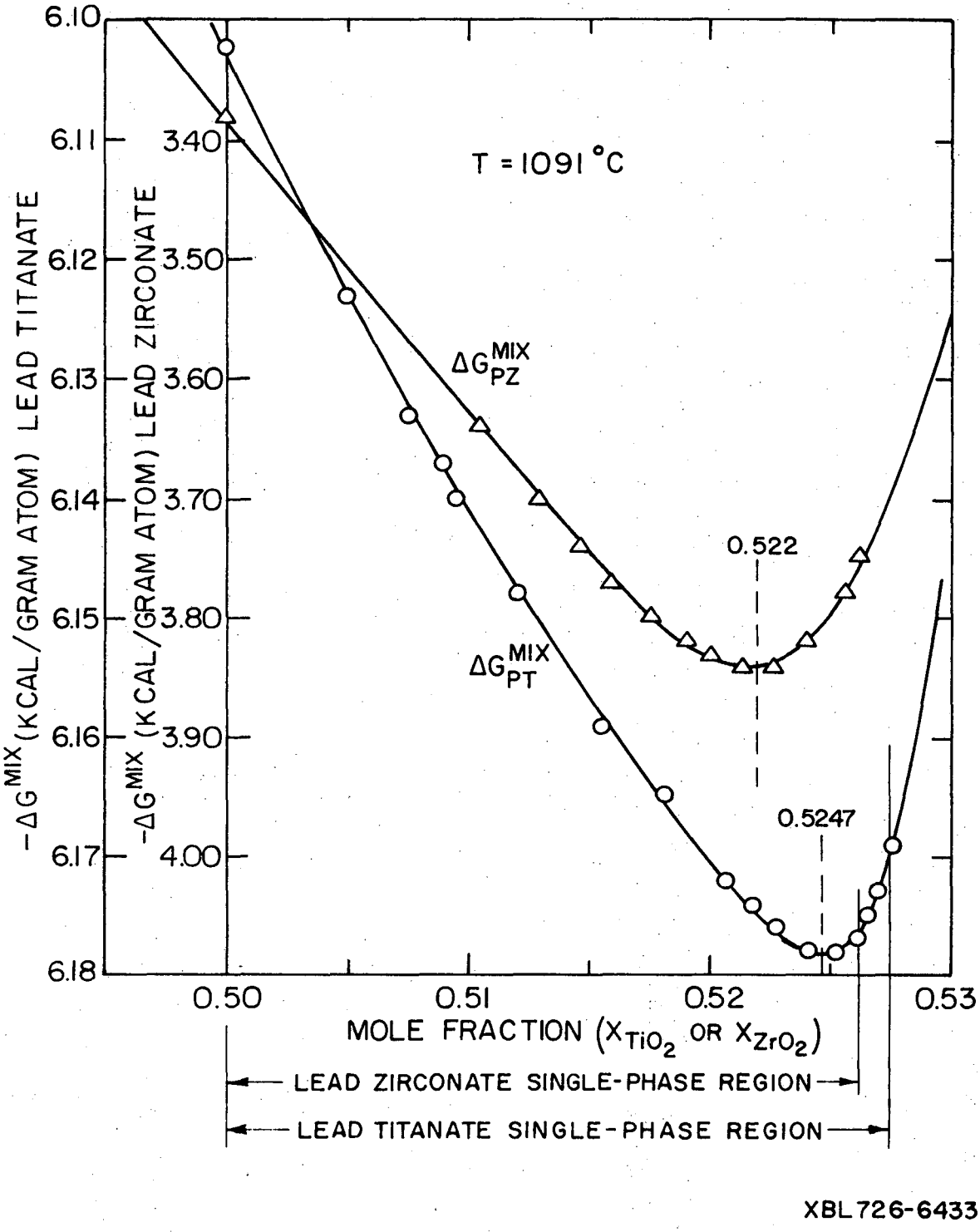


Fig. 20. The free energy of mixing PbO and either $TiO_2$ or $ZrO_2$ as a function of composition in either the lead titanate or the lead zirconate single-phase region.

eliminated by pre-melting the PbO powder in the unsealed Knudsen cell. Using this approach, there appeared to be only a transient plugging of the orifice, that readily disappears upon temperature equilibration. This is shown in Fig. 21(a) and (b). When the experimental technique, found to eliminate significant PbO liquid loss, was applied to the actual Knudsen experiment, vapor pressure data were obtained for pure lead oxide that are in excellent agreement with the thermochemical data as tabulated by Kubaschewski et al.[41] and JANF tables,[42] and in fair agreement with the lead oxide standard used by Hardtl and Rau.[29] The results are graphically compared in Fig. 22. The raw data is summarized in Appendix C.

The lead oxide vapor pressures obtained for the PZT composition in equilibrium with either the lead rich liquid phase or the oxide solid phase, are presented in Figs. 23 and 24. The analytical vapor pressure expressions, the enthalpy, entropy, and the standard deviations are reported in Table III. (The data points were least squares fitted to the linear form, $\ln p = A(1/T)+B$.)

Because PbO is the only significant vapor species in the $PbO-TiO_2-ZrO_2$ system, it is expected that a second law analysis of the Knudsen effusion vapor pressure data should yield equivalent values for the entropies of vaporization. This is observed (Table III) for PbO, $PbTiO_3+TiO_2$, and $PbZrO_3+ZrO_2$.

Entropy and enthalpy are defined assuming a composition that is invarient with temperature. Entropy correlation cannot be expected for $PbTiO_3$+liquid or $PbZrO_3$+liquid, as the lead rich liquid compositions change appreciably with temperature (see Figs. 9 and 12). Consequently,

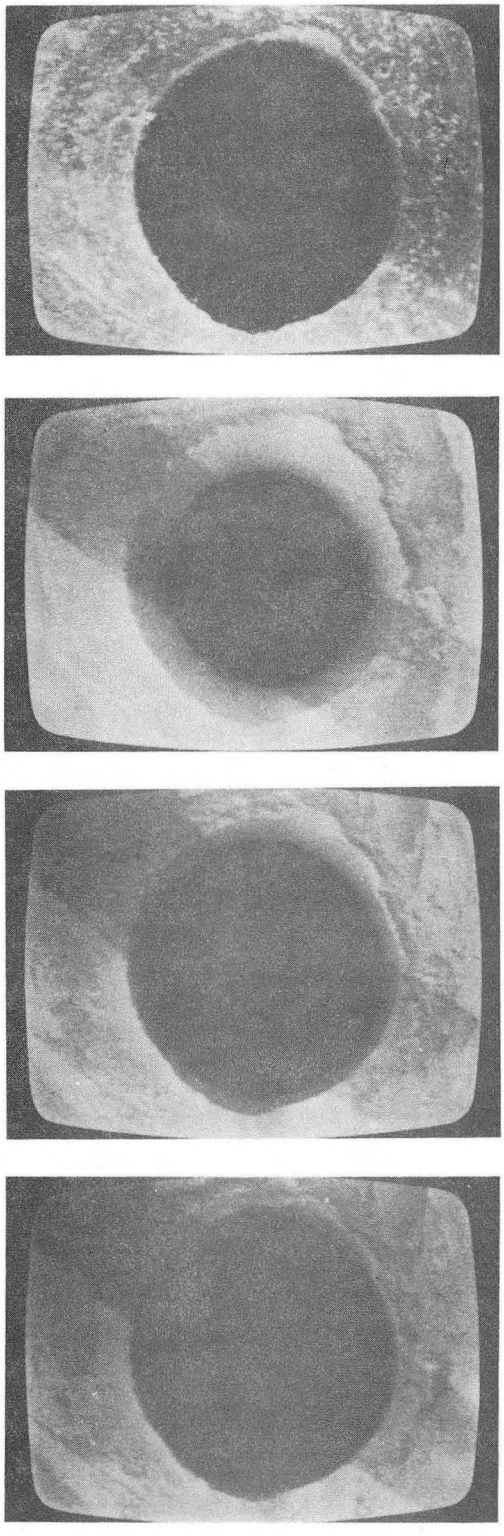


XBB 726-3502

Fig. 21. Scanning Electron Microscope (SEM) photographs of a Knudsen cell containing pure PbO in a hot stage [0.013 in. orifice diameter].

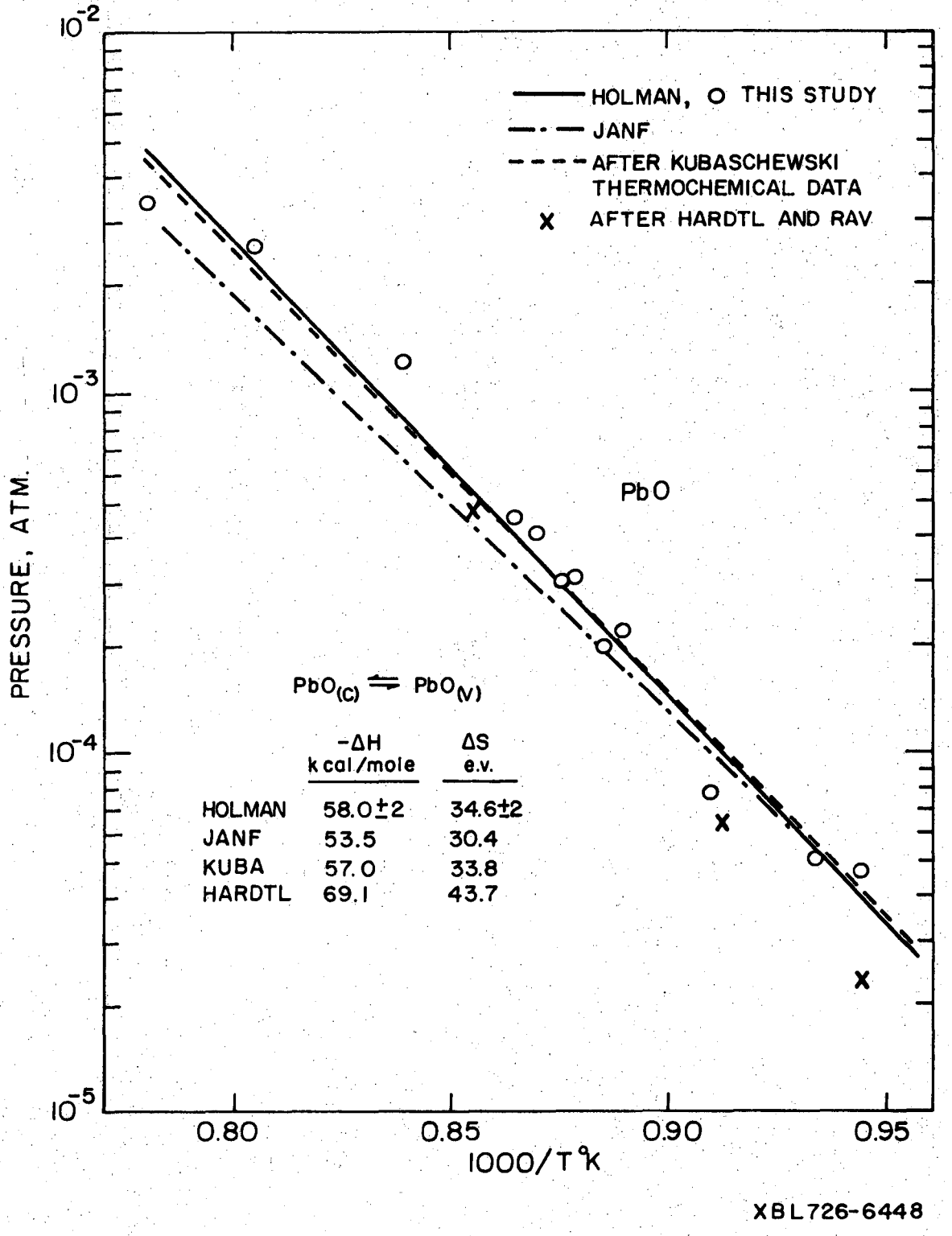


Fig. 22. Natural log of vapor pressure (PbO) vs. 1000/T°K as determined by the Knudsen Effusion experiments. (This data is least squares fitted to a linear form and is compared to the thermochemical data and the results of another Knudsen experiment).

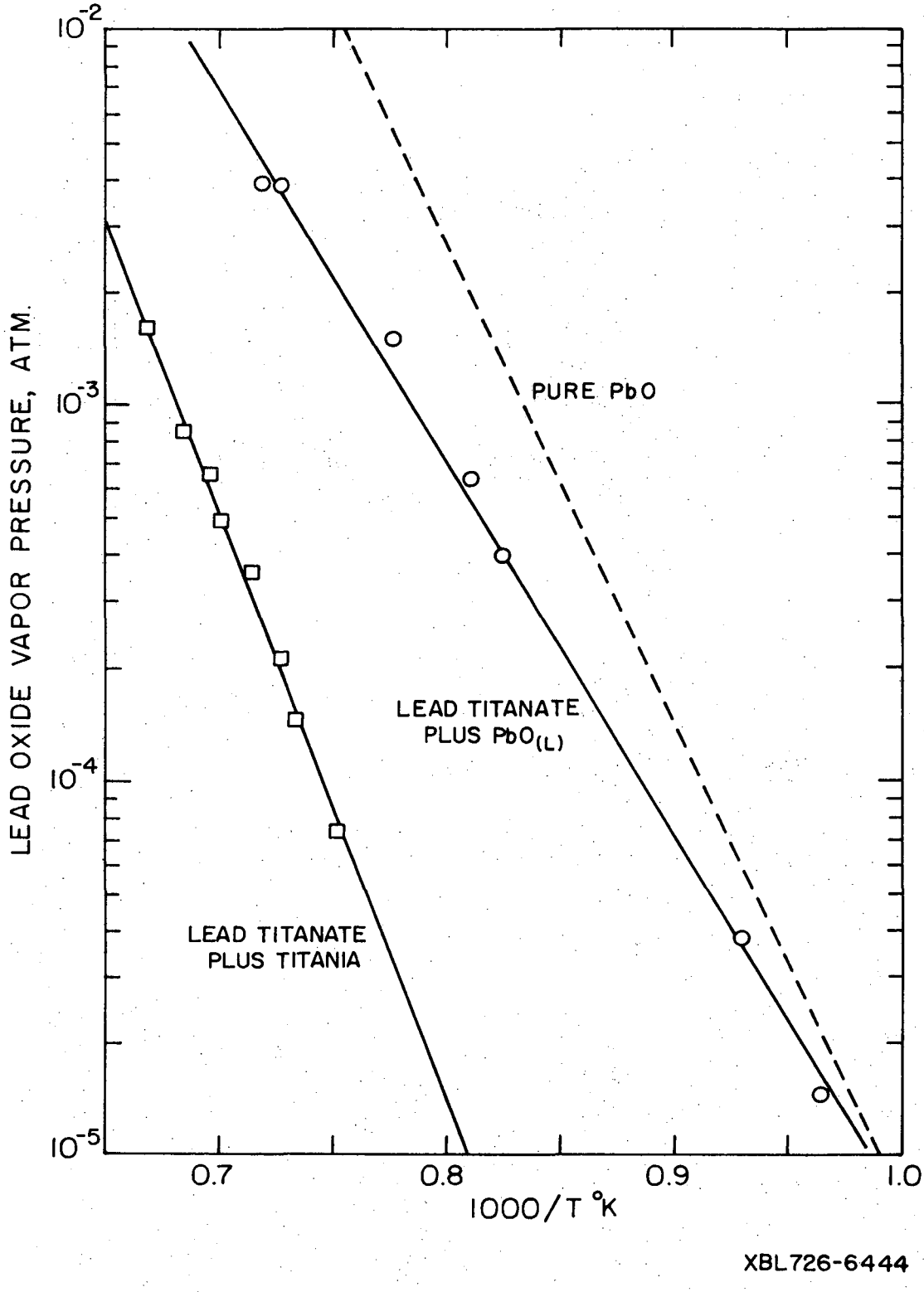


Fig. 23. $\text{Log}_e$(lead oxide vapor pressure) vs. 1000/T°K for lead titanate in equilibrium with a lead rich liquid and with titania. The results are compared to those for pure lead oxide.

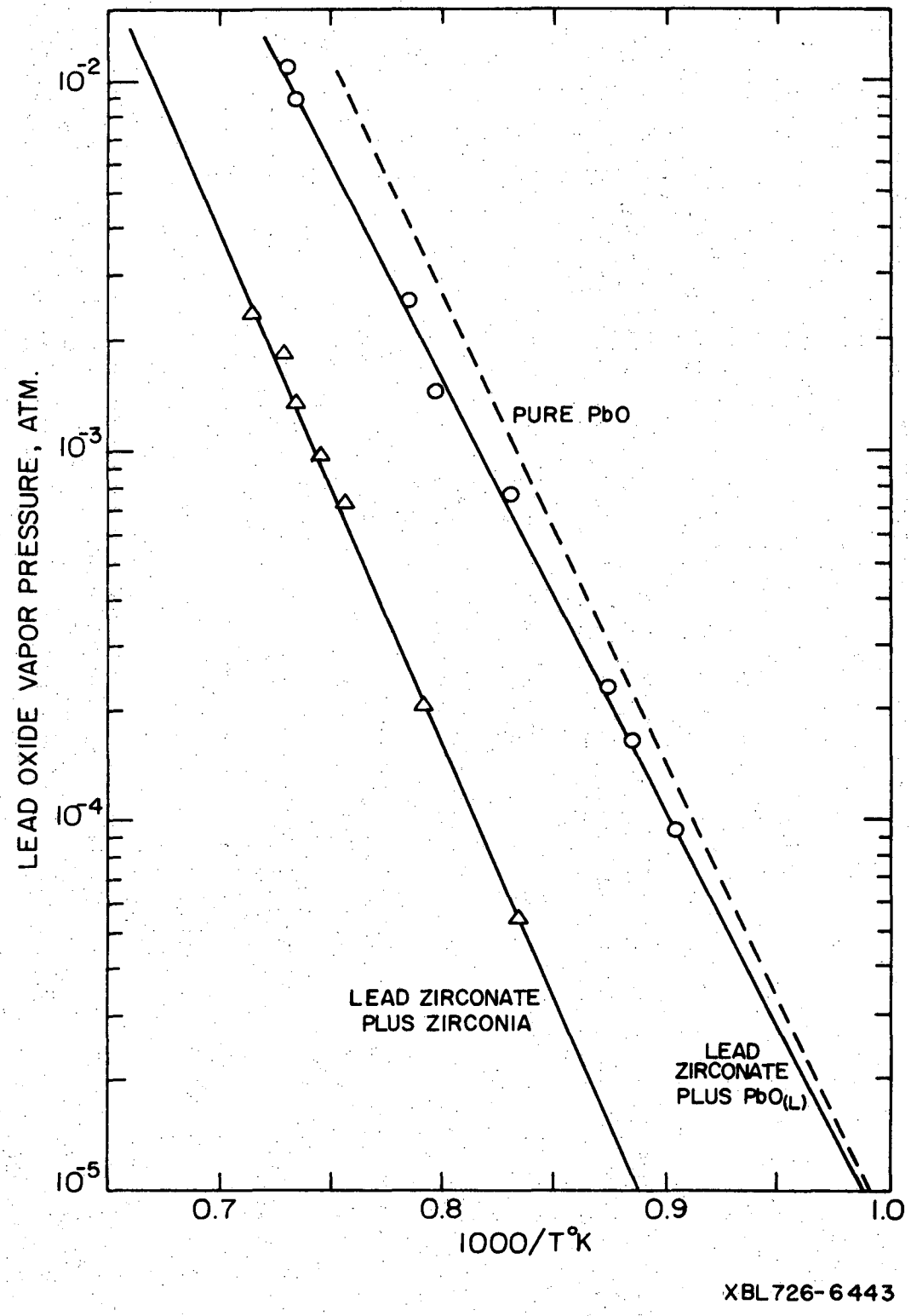


Fig. 24. $\text{Log}_e$(lead oxide vapor pressure) vs. 1000/T°K for lead zirconate in equilibrium with a lead rich liquid and with zirconia. The results are compared to those for pure lead oxide.

Table III. Tabulation of linear least squares fit to the Knudsen Effusion experiments (see Appendix C).

| KNUDSEN SAMPLE COMPOSITION | LINEAR LEAST SQUARES FIT A | LINEAR LEAST SQUARES FIT B | SECOND LAW ANALYSIS ENTHALPY | SECOND LAW ANALYSIS ENTROPY |
|---|---|---|---|---|
| $PbO$ | $-2.916\times10^{4}$ $\sigma=9.07\times10^{2}$ | $17.405$ $\sigma=0.788$ | $-5.795\times10^{4}$ $\sigma=1.8\times10^{3}$ | $34.59$ $\sigma=1.56$ |
| * $PbZrO_3 + PbO_{(\ell)}$ | $-2.64\times10^{4}$ $\sigma=4.47\times10^{2}$ | $14.70$ $\sigma=0.359$ | $-5.255\times10^{4}$ $\sigma=8.89\times10^{2}$ | $29.21$ $\sigma=0.714$ |
| * $PbTiO_3 + PbO_{(\ell)}$ | $-2.25\times10^{4}$ $\sigma=5.13\times10^{2}$ | $10.75$ $\sigma=0.424$ | $-4.471\times10^{4}$ $\sigma=1.02\times10^{3}$ | $21.36$ $\sigma=0.843$ |
| $PbZrO_3 + ZrO_{2\,ss}$ | $-31.86\times10^{4}$ $\sigma=9.75\times10^{2}$ | $16.75$ $\sigma=0.734$ | $-6.33\times10^{4}$ $\sigma=1.94\times10^{3}$ | $33.29$ $\sigma=1.45$ |
| $PbTiO_3 + TiO_{2\,ss}$ | $-3.64\times10^{4}$ $\sigma=9.18\times10^{2}$ | $17.89$ $\sigma=0.648$ | $-7.23\times10^{4}$ $\sigma=1.82\times10^{3}$ | $35.55$ $\sigma=1.289$ |

LEAST SQUARES FIT TO KNUDSEN CELL DATA OF FORM:

$$\ln P_{PbO} = A\,(1/T) + B \qquad A = \Delta H/R \qquad B = \Delta S/R$$

$\sigma$ = STANDARD DEVIATION

XBL 726 6456

* Second Law constants are not true enthalpy or entropy.

constants reported in Table III for these cases do not correspond to true entropies or enthalpies.

The composition of the vapor is assumed to be essentially monomer. Small amounts of dimer and trimer lead oxide in the vapor above pure condensed lead oxide[30] introduce small errors, but these are not believed to be important. The raw experimental data are summarized in Appendix C.

It is informative to plot the lead oxide activity of PZT in equilibrium with lead rich liquid as a function of temperature (Fig. 25) and the $Pb(Ti_xZr_{1-x})O_3$ composition, as shown in Fig. 26. While the results for PZT in equilibrium with titania and/or zirconia are in good agreement with those reported by Hardtl and Rau,[29] Atkin and Fulrath's[7] approximation of PbO activity of PZT plus lead rich liquid compositions which assumed the applicability of Raoult's law for the liquid based on the phase equilibria information reported by Fushimi and Ikeda,[5] is found to be in error. The actual activity coefficients as calculated from the present experimental data, deviate substantially from Raoult's law. They are plotted as a function of composition in Fig. 27.

Finally, by evaporation of all the lead oxide from the Knudsen cell, and by carefully weighing and analyzing the sample residue that is left in the cell, it was possible to locate the stoichiometric PZT composition relative to the boundaries of its single-phase region.

This is accomplished as follows:

$w_r$ = the amount of titania and/or zirconia residue that is left in the cell at the end of the experiment in grams

$w_{PbO}$ = the total amount of PbO that vaporizes from the cell during the experiment in grams

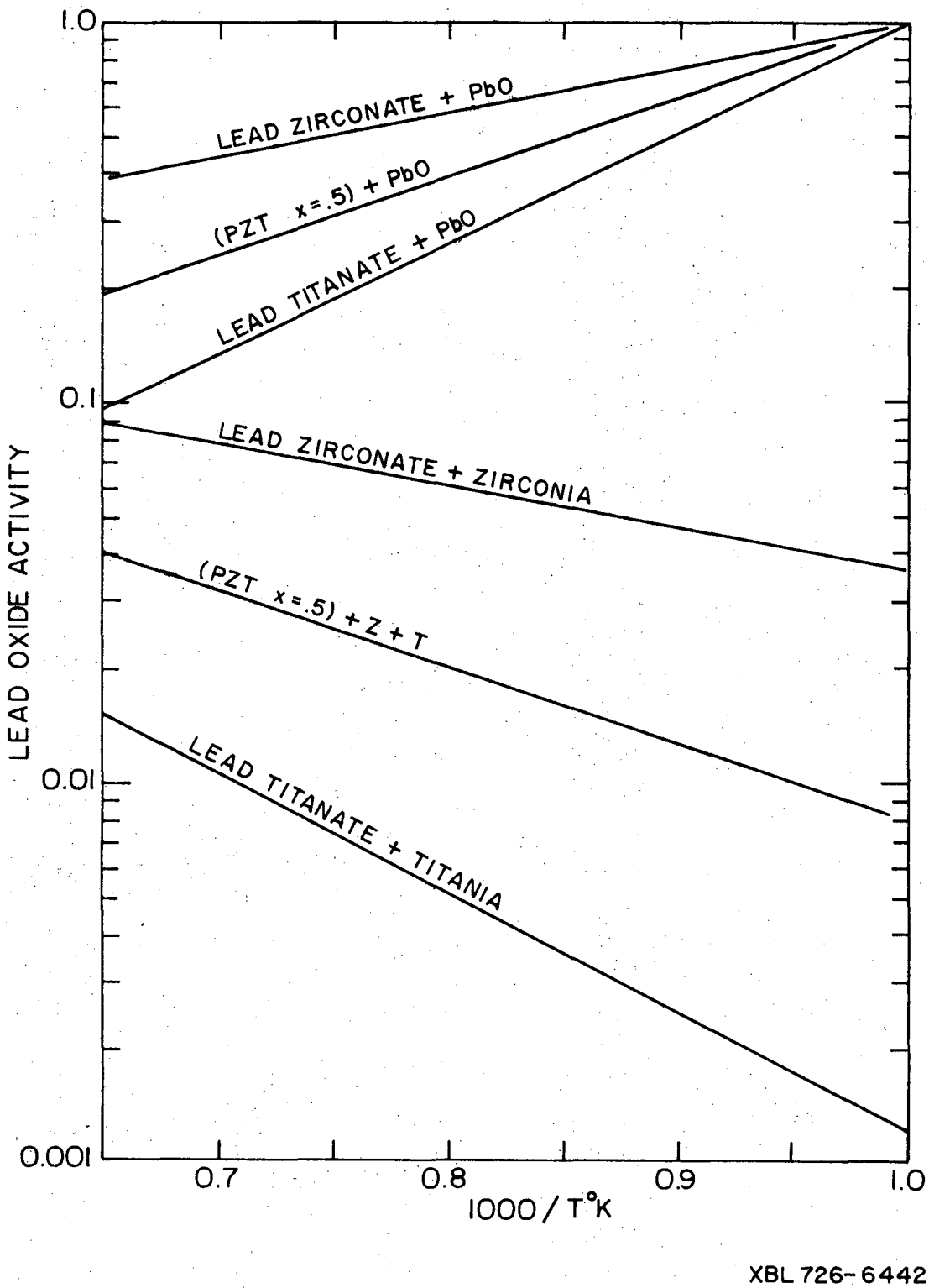


Fig. 25. Lead oxide activity as a function of reciprocal temperature (1000/T°K) for all experimental Knudsen effusion vapor pressure data:

$$a_{PbO}(PZT) = P_{PbO}\ (PZT)/P_{PbO}(pure).$$

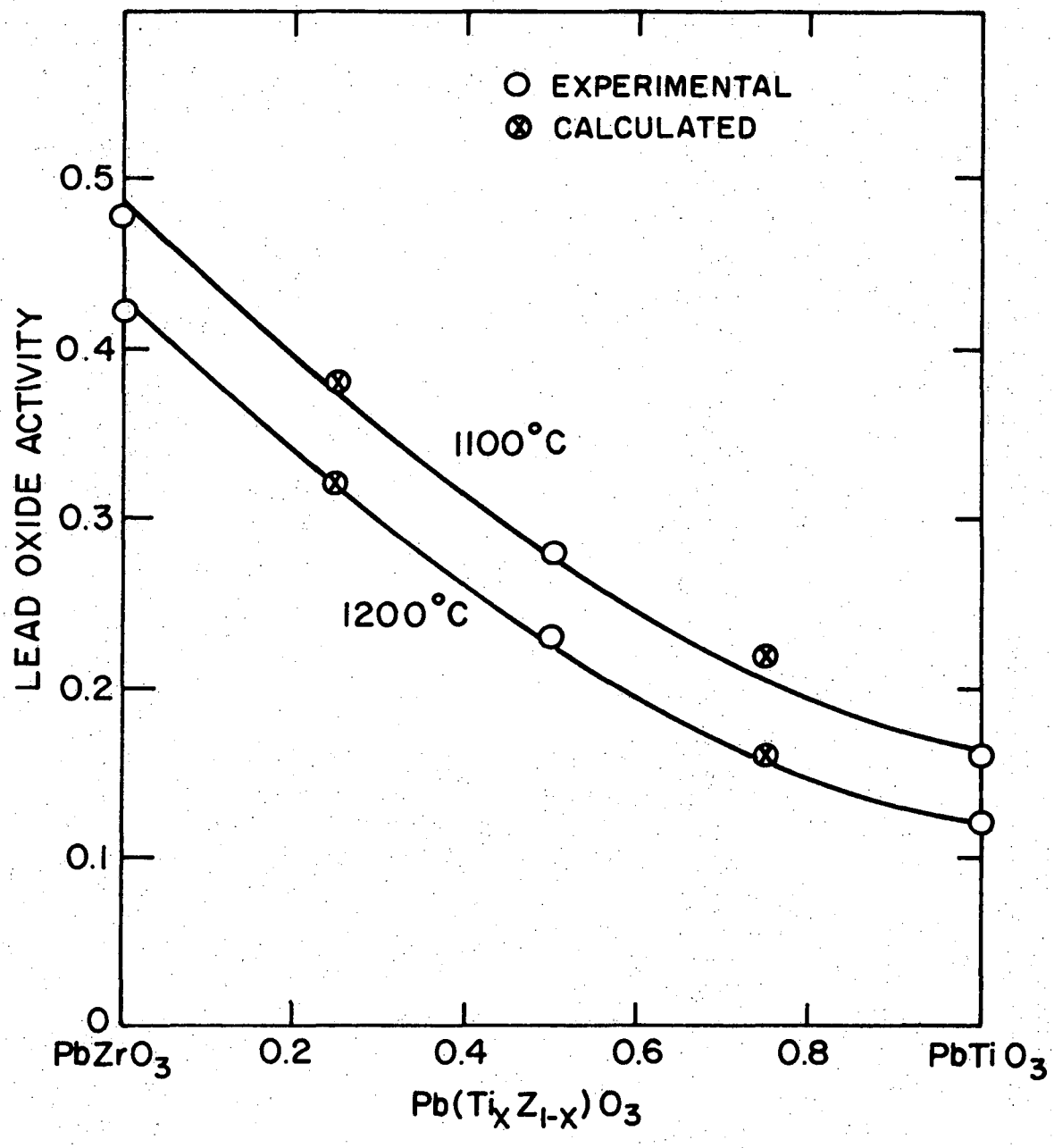


XBL726-6437

Fig. 26. Lead oxide activity as a function of $Pb(Ti_xZr_{1-x})O_3$ when the PZT compound is in equilibrium with a lead rich liquid: 0 - refer to experimentally determined points, X - refers to extrapolated points.

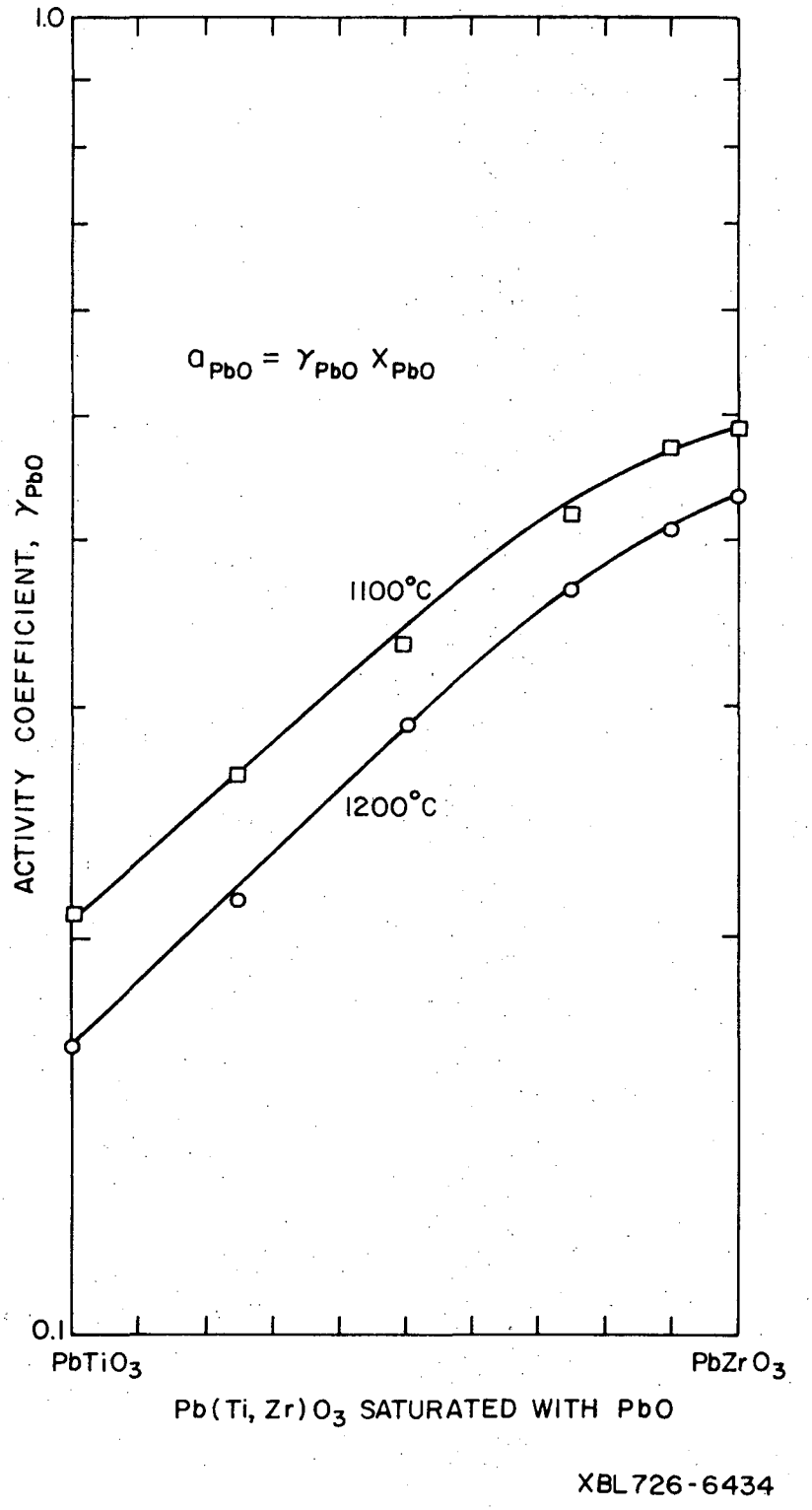


Fig. 27. The activity coefficient of lead oxide as a function of $PbTi_xZr_{1-x}O_3$ composition at 1100°C and 1200°C, calculated from the experimental Knudsen data showing a deviation from Raoults law.

x = the wt % PbO in the perfectly stoichiometric $PbTi_zZr_{1-z}O_3$ sample

y = the wt % $(Ti_zZr_{1-z})O_2$ in the perfectly stoichiometric $Pb(Ti_zZr_{1-z})O_3$ sample

$\Delta w$ = the width of the single-phase region (milligrams) as determined from the non-linear portion of the weight loss vs. time curve

w' = the amount of PbO (milligrams) that vaporized from the cell between the end of the single-phase region and the completion of the experiment

T = the weight of perfectly stoichiometric $Pb(Ti_zZr_{1-z})O_3$ that is formed by reacting PbO with the titania and/or zirconia residue

P = the weight of PbO (grams) that is required to react with the $w_r$(mgs) of $(Ti_zZr_{1-z})O_2$ to form the perfectly stoichiometric compound.

$(y)(T) = w_r$; so $T = (w_r)/(y)$; therefore $P = (x)(t) = (x)(w_r)/(y)$.

Hence, if the experiment was done carefully, $(w'+\Delta w) \geq P \geq w'$, and P grams locates where the stoichiometric composition should be relative to the boundaries of the single-phase region, as illustrated in Fig. 28.

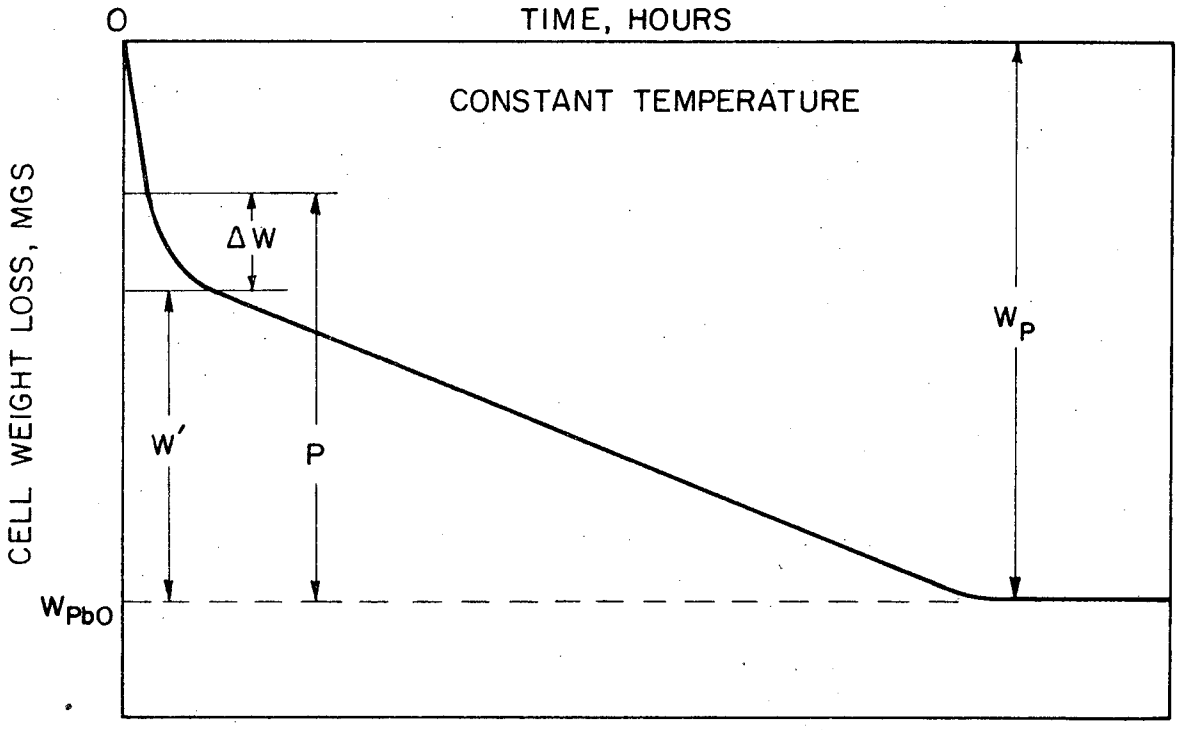


Fig. 28. The entire Knudsen Effusion Experiment conducted at a constant temperature illustrating the calculation of the location of the perfectly stoichiometric $Pb(Ti_xZr_{1-x})O_3$ compound relative to the determined boundaries of its single-phase region.

## III. EXTRINSIC NON-STOICHIOMETRY

### 1. Introduction

Small additions of other oxides to lead zirconate-titanate have been reported to affect the electrical properties, sintering kinetics, and grain growth. Bismuth and niobium have been shown to act as sintering aids, and to improve the ferroelectric behavior. Lanthanum has markedly enhanced the sinterability of PZT ceramics. Haertling and Land[13], incorporating lanthanum in the presence of a lead oxide liquid phase, have produced optically transparent material by hot pressing, while Snow[9] has achieved similar results by sintering. Very interesting optical switching devices have been produced from this material. In addition, Lee[43] has demonstrated that scandium can convert the ferroelectric characteristics of PZT to an anti-ferroelectric-like behavior.

To generate commercially useful devices, reproducibility of results must be assured, which implies that the processing kinetics must be controlled. It appears that to explain the reported results correctly, one must understand the kinetics of the incorporation of the Bi, Nb, La, and Sc ions into the perovskite lattice, their location in the lattice, and the defect structure that is generated. Consequently, an experiment was developed that provided direct observation of the mechanisms.

By maintaining proper atmosphere control, thermogravimetry may be used to study the continuous weight changes caused by the reaction between any second phase oxide addition with lead zirconate-titanate. In this analysis, the number of titanium and/or zirconium ions distributed on the B-site of the perovskite lattice is constant due to the extremely low vapor pressure of these species. However, the lead ion

concentration is free to adjust itself by means of equilibration with a surrounding lead oxide atmosphere. Hence, should a cation diffuse into the A-sublattice, some lead ions would be released, keeping the ratio of A-sites to B-sites at unity. If a cation diffused into the B-sublattice, the total number of B-sites would be increased, and additional lead ions would be obtained from the atmosphere, again holding the A/B site ratio at unity. This type of reaction weight-change analysis was first demonstrated by Weston et al.,[11] who determined the substitutional lattice site of $Fe^{3+}$ in lead zirconate-titanate by weighing a sample containing iron oxide before and after a long high temperature firing.

However, this method may be further refined to reveal the valency of the substituted cation and the active charge compensation mechanism. Also, thermogravimetry has the advantage of continuously recording both the weight-changes caused by the ionic substitution, including the development of any dominant, though transient, second phases, at the temperature of interest.

Thus, divalent ion substitutions on the A-sublattice and quatravalent ion substitutions on the B-sublattice of the perovskite require only equivalent amounts of PbO lost or gained from the original composition. However, trivalent ion substitutions on the A-sublattice and pentavalent substitutions on the B-sublattice require an additional mechanism to neutralize the charge imbalance created. This neutralization may be accomplished in several ways. Excess positive charge may be neutralized by:

(a) creation of lead vacancies (reduction in the number of lead ions on lead sites)

(b) reduction of Ti and/or Zr to trivalent species

(c) distribution of the substituting ions on both A and B lattice sites

(d) creation of B-site vacancies--theoretical number of B sites are increased with no change in the number of Ti and/or Zr ions.

The reduction of titania and/or zirconia may be dropped from further consideration as it has been shown that reduced lead titanate turns black and becomes a good semi-conductor; no color or conductivity change was observed under present experimental conditions. If the ions to be investigated are selected such that their ionic radii closely match either the A or the B site radius, it should be unlikely that a distribution would result without grossly perturbing the perovskite crystal structure. Useful data of Shannon and Prewit[44] are presented in Table IV.

Table IV. Ionic Radii

| Perovskite $A^{2+}B^{4+}O_3^{2-}$ | | | |
|---|---|---|---|
| Ion | C.N. | Effective Radius (Å) | Probable PZT Lattice Site |
| $Pb^{2+}$ | 12 | 1.49 | A |
| $Ti^{4+}$ | 6 | 0.605 | B |
| $Zr^{4+}$ | 6 | 0.72 | B |
| $Bi^{3+}$ | 8* | 1.11 | A |
| $Bi^{5+}$ | 6 | 0.74 | B |
| $Nb^{3+}$ | 6 | 0.70 | B |
| $Nb^{5+}$ | 6 | 0.64 | B |
| $La^{3+}$ | 12 | 1.32 | A |
| $Sc^{3+}$ | 6 | 0.73 | B |

* Highest C.N. tabulated.

Therefore, it is expected that either (a), the creation of lead vacancies, or (d), the creation of B-site vacancies, or some combination of these serve to neutralize the charge. These possibilities are analytically stated by equations (1) and (2).

(1) The complete substitution of $M^{3+}$ ions on the lead sublattice

$$[Pb(Ti,Zr)O_3 + xMO_{1.5}] \longrightarrow \begin{cases} \text{(a)} \\ \text{(b)} \end{cases}$$

(a) $[(Pb_{1-1.5x}\square_{.5x}M_x)(Ti,Zr)O_3] + 1.5x\ PbO_v$

lead vacancy charge compensation

(b) $[(Pb_{1-.75x}M_x)(Ti,Zr\ \square_{.25x})O_{3+.75x}] + .75x\ PbO_v$

(Ti,Zr) vacancy charge compensation

(2) The complete substitution of $M^{5+}$ ions on the (Ti,Zr) sublattice

$$Pb(Ti,Zr)O_3 + xMO_{2.5} + \longrightarrow \begin{cases} \text{(a)} \\ \text{(b)} \end{cases}$$

(a) $.5xPbO_v \rightarrow Pb_{1+.5x}\square_{.5x}(Ti,Zr\ M_x)O_{3+3x}$

lead vacancy charge compensation

(b) $1.25xPbO \rightarrow Pb_{1+1.25x}(Ti,Zr,M_x\ \square_{.25x})O_{3+3.75x}$

(Ti,Zr) vacancy charge compensation

Hence the final weight change observed will suggest which model is more appropriate. The stoichiometric sample containing the trivalent substituent compatible with the lead sublattice will either show a weight

loss corresponding to .75x moles of lead oxide or 1.5x moles of lead oxide. If a weight loss between these values is obtained, it is possible that both charge compensating mechanisms are operable. Similarly, samples containing the pentavalent B-site substituent should exhibit a weight gain of lead oxide of either .5x moles or 1.25x moles of lead oxide.

Another situation is created by the substitution of a trivalent ion on the (Ti,Zr) B-sublattice. In this case there is a deficiency of positive charge which must be neutralized. Neutralization may be accomplished by the removal of oxygen ions (i.e. the creation of oxygen vacancies), or by an increase in the lead ion concentration, reduction of lead vacancies. If an increase in lead ions is required to make up for the charge deficiency, a weight gain should be observed equal to 0.5 moles of PbO in addition to the x moles of PbO required by the direct substitution. When oxygen vacancies form, the sample weight gain of x moles PbO is the only change that will be detected. These situations are illustrated by Eqs. (3a) and (3b).

(3) The complete substitution of $M^{3+}$ on the (Ti,Zr) sublattice

$$Pb(Ti,Zr)O_3 + xMO_{1.5} + \longrightarrow \begin{cases} (a) \\ (b) \end{cases}$$

(a) $xPbO_v \rightarrow Pb_{1+x}(Ti,Zr,M_x)O_{3+3x-.5x}\emptyset_{.5x}$

oxygen vacancy charge compensation

(b) $1.5xPbO_v \rightarrow Pb_{1+x+.5x}\square_{I-.5x}(Ti,Zr,M_x)O_3$

reduction of lead vacancies

I = the intrinsic vacancy concentration.

The sample weight changes that might be expected are summarized in Table V.

Table V. Possible Ionic Substitution Reactions

| [PZT+y/2 (metal oxide)] sample | | |
|---|---|---|
| Ion | Weight Change | Mechanisms |
| $M^{2+}$ | $\ominus$ y PbO (loss) | A-site substitution |
| $M^{3+}$ | $\ominus \frac{3}{2}$y PbO (loss) | A-site substitution<br>lead vacancy charge comp. |
| $M^{3+}$ | $\ominus$ y PbO (loss)<br>( $\ominus$ .75y PbO vacancies) | A-site substitution<br>$B^{4+}$ reduction or $B^{4+}$ vacancies |
| $M^{3+}$ | $\oplus$ y PbO (gain) | B-site substitution<br>oxygen vacancy charge comp. |
| $M^{4+}$ | $\oplus$ y PbO (gain) | B-site substitution |
| $M^{5+}$ | $\oplus$ y/2 PbO (gain)<br>( $\oplus$ 1.25y PbO vacancies) | B-site substitution<br>lead vacancy charge comp. |
| $M^{5+}$ | $\oplus$ y PbO (gain) | B-site substitution<br>$B^{4+}$ reduction or B-vacancies |
| $M^{5+}$ | $\ominus \frac{5}{4}$y PbO (loss) | A-site substitution<br>lead vacancy charge comp. |

Gravimetric analysis in a controlled PbO atmosphere was made possible by the fabrication of multi-phase lead zirconate-titanate crucibles that establish a constant equilibrium lead oxide atmosphere and effectively isolate the sample being weighed. The crucible composition established the lead oxide activity of the sample's atmospheric environment. It is important that the weight changes measured are associated

only with the reaction with the second phase addition. The intrinsic stoichiometry must not change during the experiment. This could be assured by fixing the stoichiometry of the lead zirconate-titanate sample prior to the addition of the dopant.

If a crucible was fabricated of a (PZT + Z + T) composition, and a "stoichiometric" mixture of PbO, $TiO_2$ and $ZrO_2$ was placed in it, the high-temperature calcination established the equilibrium composition for the powder. This is implied in Fig. 2(b). If any further heat treatment of this powder was done within this same crucible, no PbO exchange would be expected for the powder with the atmosphere provided by the crucible.

Alternately, this experiment could be conducted with a crucible, or burial powder, which has the identical single-phase composition as the sample. However, as the crucible loses PbO and its composition changes, the weight change data would vary in an unpredictable manner.

2. Experimental

High purity PbO, $TiO_2$, and Hf-free $ZrO_2$ were homogeneously mixed in their stoichiometric proportions in the manner discussed in the previous section. This powder was then divided into two portions: (a) to be fabricated into crucibles, and (b) to be fabricated into samples. The crucible fabrication and calcination techniques were identical to those discussed in the previous section, and are summarized in Fig. 29. The sample powder was poured into the crucible, covered, enclosed within an outer platinum crucible, and calcined for 20 hours at 850°C in air, followed by a 3 hour soak at 1100°C, to achieve vapor phase equilibration with the atmosphere provided by the crucible. Then the sample powder of

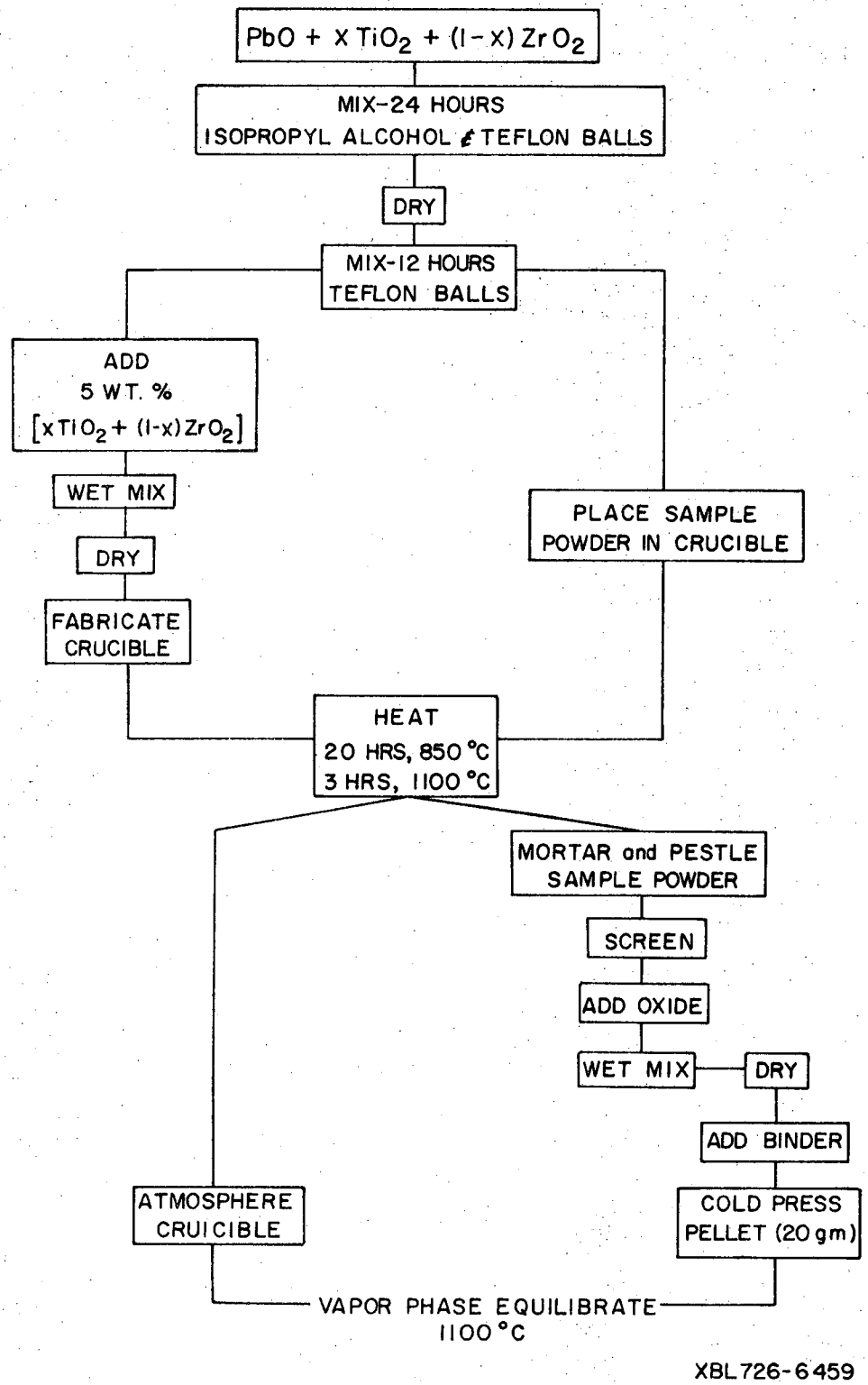


Fig. 29. Processing diagram for the study of the ionic substitutions in lead zirconate-titanate by gravimetry and vapor phase equilibration.

fixed stoichiometry was suitably modified with the second phase oxide additions of interest. In this study, 0.5, 1.0, and 2.0 mole % quantities of $BiO_{1.5}$, $NbO_{2.5}$, $ScO_{1.5}$ and $LaO_{1.5}$ were chosen. In addition, samples containing excess PbO or $(Ti,ZrO)O_2$ were included.

It is critical that the samples contain as much open porosity as possible to assure rapid equilibration with the atmosphere. To achieve this result, approximately 7 wt % napthalene crystals were mixed into the sample. Pellets were cold-pressed in a 3/4" steel die. A 30 mil hole was drilled through each pellet to allow the suspension of the sample by a platinum wire. Alternatively, some samples were isostatically pressed about a platinum coil, as is shown in Fig. 3.

The pellets were then raised at 10°/min in air to 450°C, held there for 24 hours, and furnace cooled to burn out all the napthalene.

The sample suspended from a gravimetric balance was then positioned within the same PZT crucible that was first used to calcine the powder, and heated to the desired temperature (1100°C).

The crucible cap was designed in such a way that cavities were created to enclose samples identical to the sample being weighed. Thus, at any time during the experimental run the furnace could be opened, and the extra sample removed for destructive analysis (X-ray diffraction, chemical analysis, microscopy, D.T.A. etc.) without interrupting the gravimetric experiment.

The experimental arrangement was identical to the one discussed for the measurement of the single-phase width (Fig. 5).

3. Results and Discussion

a. Bismuth and Niobium. The samples containing bismuth and niobium were selected as experimental controls. Crystal chemistry considerations present a strong case for assuming that trivalent bismuth will substitute for lead and pentavalent niobium will substitute for titanium/zirconium. Preliminary experiments[27] conducted using a burial powder of the same composition as the sample, confirm this hypothesis (these results are summarized in the Appendix A).

The present results are shown in Fig. 30(b) and 31(b) for 1.0 mole % additions of $MO_x$ to samples of approximately the same weight. The equilibrium results clearly indicate total $Bi^{3+}$ substitution for $Pb^{2+}$ and $Nb^{5+}$ substitution for $(Ti,Zr)^{4+}$ with both requiring lead vacancy charge compensation. However, in both cases, weight gains are observed which are significantly larger than reported in earlier data referred to in Appendix A. This is particularly interesting for the case of $Nb_2O_5$ substitution. It is suggested that the refractory niobia particles (initially at $a_{PbO}=0$) reacts with the lead oxide obtained from the atmosphere (constant $a_{PbO}=0.280$), forming layers of complex lead niobates as equilibrium conditions are approached. The PbO-$Nb_2O_5$ phase diagram[45] is reproduced in Fig. 32(a). No sample weight losses were observed until the sample had shown a 1.4 wt %* gain of PbO. At this point the $Nb_2O_5$-PbO composition is 83 mole % PbO, 17 mole % $Nb_2O_5$ which creates about 1.5 vol. % second phase. From the phase diagram it may be seen

---

* wt % = $\frac{\text{PbO gain (grams)}}{\text{sample wt. (grams)}}$

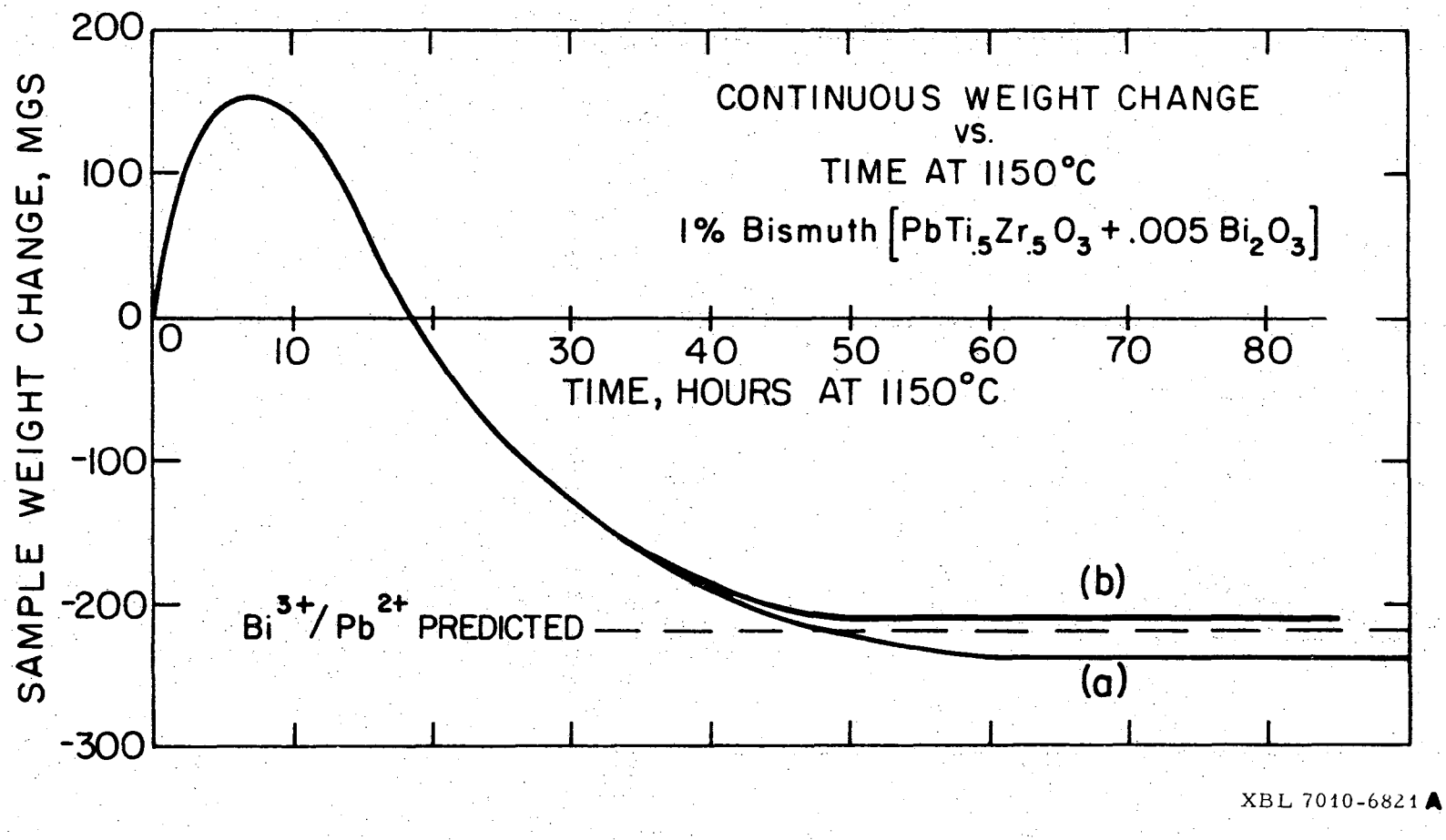


Fig. 30. Continuous weight change vs. time at 1150°C of a $PbTi_{.5}Zr_{.5}O_3$ sample containing 1 mol.% bismuth oxide ($BiO_{1.5}$): (a) lead oxide atmosphere provided by a stoichiometric $PbTi_{.5}Zr_{.5}O_3$ crucible (b) lead oxide atmosphere provided by a low-CAMP crucible.

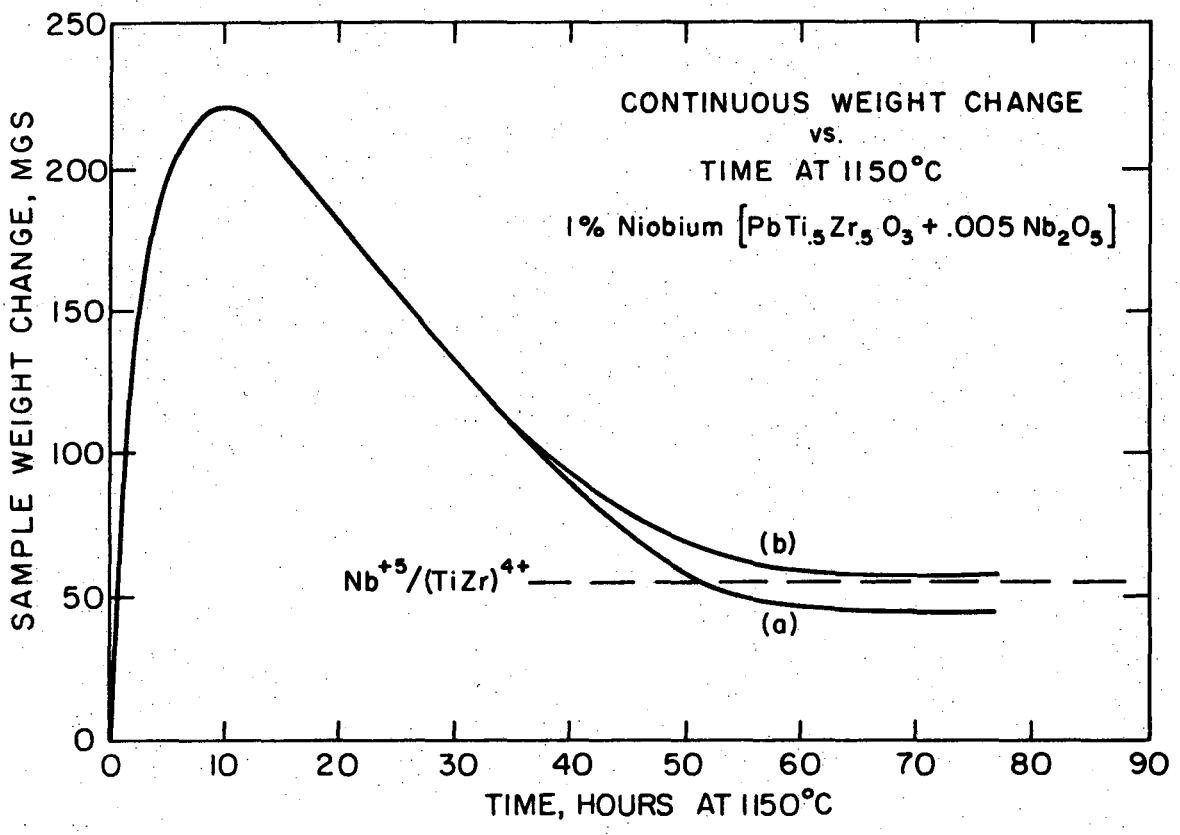


XBL 7010-6825 A

Fig. 31. Continuous weight change vs. time at 1150°C of a $PbTi_{.5}Zr_{.5}O_3$ sample containing 1 mol.% niobium oxide ($NbO_{2.5}$): (a) lead oxide atmosphere provided by a stoichiometric $PbTi_{.5}Zr_{.5}O_3$ crucible (b) lead oxide atmosphere provided by a low-CAMPF crucible.

(a)

—System $PbO-Nb_2O_5$. $P_Y$—yellow PbO, orthorhombic; $P_3N$—$3PbO \cdot Nb_2O_5$; $P_5N_2$—$5PbO \cdot 2Nb_2O_5$; $P_2N$—$2PbO \cdot Nb_2O_5$; $P_3N_2$—$3PbO \cdot 2Nb_2O_5$; T-PN—tetragonal $PbO \cdot Nb_2O_5$; R-PN—rhombohedral $PbO \cdot Nb_2O_5$; $PN_2$—$PbO \cdot 2Nb_2O_5$; N—$Nb_2O_5$; ss—solid solution; L—liquid.

R. S. Roth, *J. Research Natl. Bur. Standards*, **62**, [1] 34 (1959).

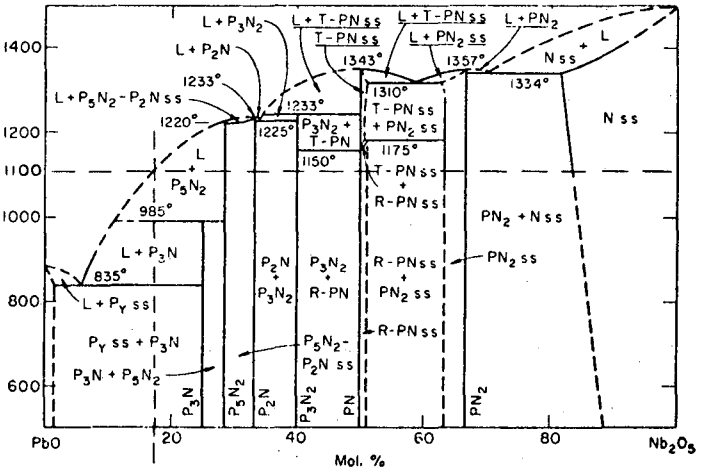


(b)

—System $Bi_2O_3$–RO near $Bi_2O_3$ component. bcc = body centered cubic phase, C = cubic $Bi_2O_3$, Mon = monoclinic $Bi_2O_3$, Rh = phase of rhombohedral symmetry, ss = solid solution, ? = unknown.

E. M. Levin and R. S. Roth, *J. Research Natl. Bur. Standards*, **68A** [2] 198 (1964).

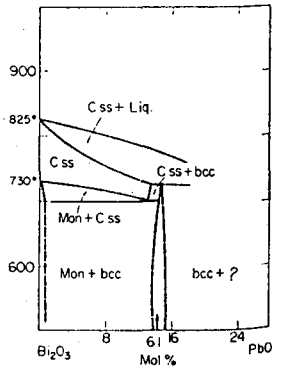


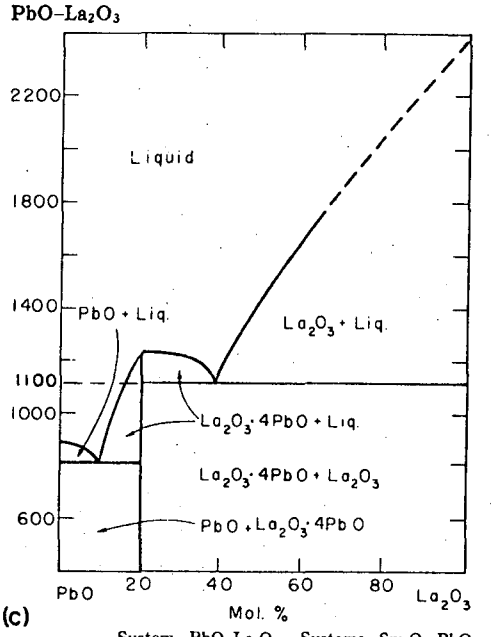


(c)

—System $PbO-La_2O_3$. Systems $Sm_2O_3$–PbO and $Gd_2O_3$–PbO are similar.

M. H. Warzee, Marcel Maurice, Franz Halla, and W. R. Ruston, *J. Am. Ceram. Soc.*, **48** [1] 16 (1965).

XBL726-6438

Fig. 32. Equilibrium phase diagrams of PbO and the second phase oxide additions: (a) $PbO-Nb_2O_5$, (b) $PbO-Bi_2O_3$, and (c) $PbO-La_2O_3$.

that at this composition (located by the dotted line) a liquid phase may have formed.

Mechanistically, liquid formation is possible since the amount of $Nb^{5+}$ ions that diffuses into the PZT lattice is at least partially controlled by the area of solid-liquid contact. Initially, the homogeneously dispersed refractory particulates have a very small contact area with the PZT particles. As these particulates gain PbO from the atmosphere, they increase in volume, but still exist primarily as solid particles. The surface contact area is still insufficient to observe signs of diffusion. When the liquid phase forms, it spreads out, covering large areas of PZT surface, and $Nb^{5+}$ diffusion is enhanced. As $Nb^{5+}$ leaves the liquid, its lead oxide activity is momentarily greater than that of the atmosphere. Hence, additional PbO leaves the liquid, and the partially open system. It should be re-emphasized that because the PZT sample powder particles are in equilibrium with the atmosphere as a result of the pretreatment described, no non-stoichiometry weight changes are expected. Therefore, only the niobia contributes to the observed weight changes.

A similar situation is observed in the bismuth modified system, except that the liquid phase forms from the outset ($Bi_2O_3$ melts at 825°C). However, as the PbO dissolves, increasing the lead oxide activity of the liquid, the liquid volume increases while liquid viscosity may be decreasing. When about .615 vol. % or .735 wt % liquid is attained, $Bi^{3+}$ diffusion becomes apparent.

b. Lanthanum and Scandium. This work was primarily undertaken to investigate the kinetics of solution of the lanthanum and scandium oxides. The reaction weight-change data is presented in Fig. 33(b) and

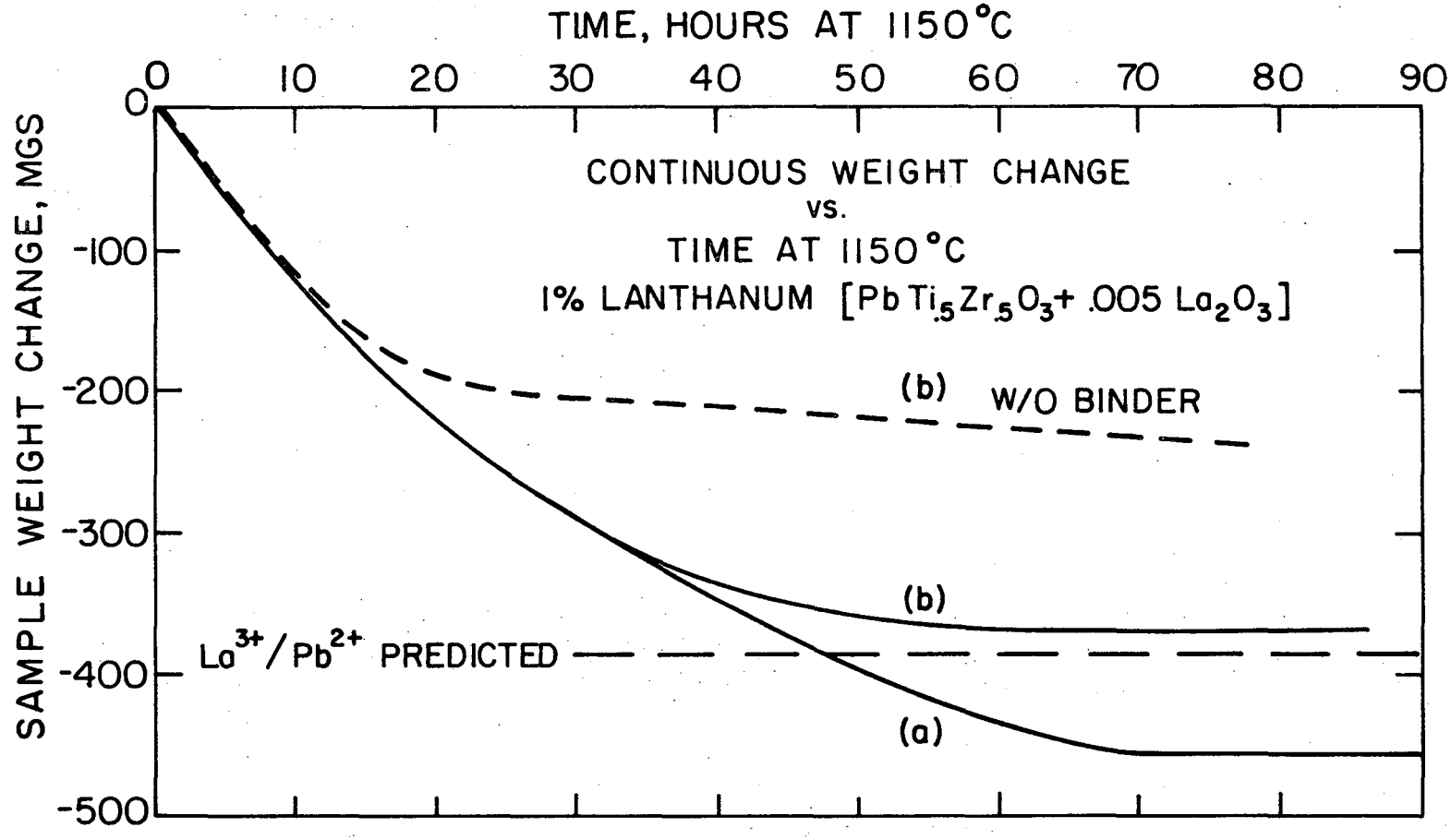


XBL 7010-6820A

Fig. 33. Continuous weight-change vs. time (hours) at 1150°C of a pre-treated $PbTi_{.5}Zr_{.5}O_3$ sample containing 1 mol. % lanthanum oxide ($LaO_{1.5}$): (a) lead oxide atmosphere provided by a stoichiometric $PbTi_{.5}Zr_{.5}O_3$ crucible, (b) lead oxide atmosphere provided by a low CAMP crucible (b-dotted). Sample contains no binder.

Fig. 34(b) for data representative of 1.0 mole % $LaO_{1.5}$ and 1.0 mole % $ScO_{1.5}$ respectively.

For the lanthanum substitution, no initial weight gains are observed. However, the rate of equilibration is seen to be quite dependent upon the incorporation of a maximum amount of binder to control porosity. Fig. 33(b) demonstrates this effect, where (b-dotted) describes the data of a sample which was sintered simultaneously without binder, and (b-solid) describes the data of an identical sample containing approximately 7 wt % napthalene. In addition, it was observed that the smaller the sample in volume, the more rapid the equilibration.

It is possible that the $PbO-La_2O_3$ liquid phase that forms (see the phase diagram reproduced in Fig. 32(c))[46] is not as viscous as either the pure $Bi_2O_3$ liquid or its dilute solution with PbO. Hence, the lanthana liquid may be able initially to cover a much larger surface area, such that the diffusion of the $La^{3+}$ ions into PZT can proceed at a greater rate. In addition, it is possible that the lead oxide activity in the $(La_2O_3+PbO)_{liq.}$ could be high enough so that it is initially nearly in equilibrium with the atmosphere. In either event, the diffusion of $La^{3+}$ proceeds gradually until an equilibrium is reached corresponding to a total $La^{3+}$ substitution for $Pb^{2+}$ via a total lead vacancy charge compensation mechanism such as was detailed by equation 1(a), for all doping levels studied.

As a result of study by a different technique, it has recently been reported,[47,48] that for low doping levels, lanthanum ions substitute on the lead sublattice of lead titante, and that charge compensation is accomplished by A-site vacancies. In addition, it was determined that

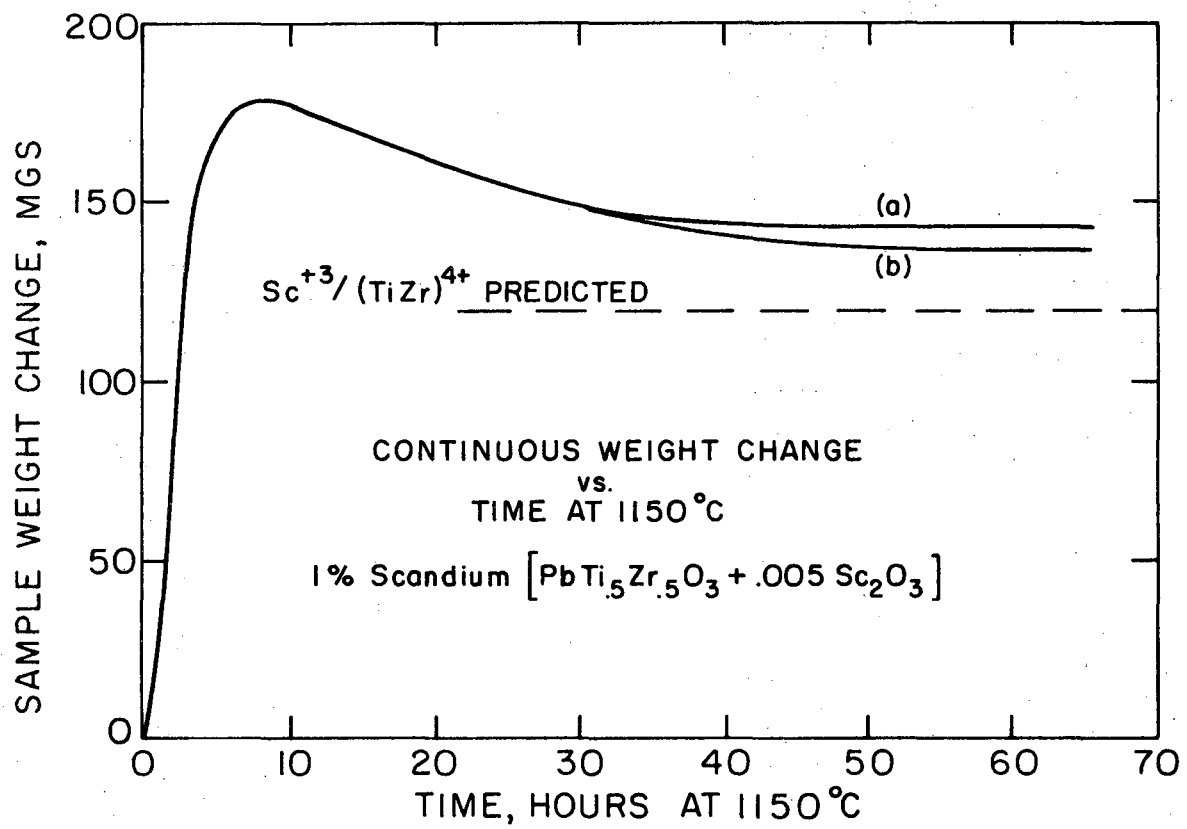


Fig. 34. Continuous weight-change vs. time (hours) at 1150°C of a pre-treated $PbTi_{.5}Zr_{.5}O_3$ sample containing 1 mol. % scandium oxide ($Sc_{1.5}O_3$). (a) lead oxide atmosphere provided by a stoichiometric $PbTi_{.5}Zr_{.5}O_3$ crucible, (b) lead oxide atmosphere provided by allow CAMP crucible (b-dotted) sample contains no binder.

for the higher doping levels[47] (greater than 5 mole %), while $La^{3+}$ substitutes for $Pb^{2+}$, charge compensation is best explained by a distribution of A-site and B-site vacancies. The same workers have recently extended this analysis to $PbTi_{.5}Zr_{.5}O_3$ for the high doping levels.[12]

Finally, experiments were conducted to characterize the addition of $Sc_2O_3$. From crystal chemistry considerations it is deduced that scandium illustrates a trivalent substitution on the $(Ti,Zr)^{4+}$ sublattice, but that the substitution occurs with either decreased lead vacancy or increased oxygen vacancy charge compensation, as described in equation 3(a). The data obtained supports this conclusion and indicate clearly that oxygen vacancies (3(a)) are formed to neutralize the charge. This is illustrated in Fig. 34.

In this case the initial weight gain is believed to occur in the manner described for niobia.

c. Lead Oxide and $(Ti,Zr)O_2$. As an additional control, samples containing known excesses of either PbO or $(Ti,Zr)O_2$ were equilibrated with the atmosphere crucible at 1100°C. The results were as expected: a sample containing excess lead oxide did not show any weight change when equilibrated in a crucible composition of PZT + PbO. A sample containing excess titania + zirconia also remained the same weight when equilibrated with a crucible composition of PZT + Z + T. However, when the excess quantities were below 1.0 mole % and were added to PZT powder slightly off stoichiometry and the crucibles were fabricated of a composition identical to the PZT sample powder, the samples lost the excess PbO or gained an amount of PbO equal to the excess $(Ti,Zr)O_2$.

d. The Atmosphere. The method of equilibrium atmosphere control used in these studies is far more accurate and reproducible than the "disc" technique used by Weston et al.[11] after the earlier work of Jaffe et al.[8] Weston's samples were sintered in the presence of lead zirconate discs. It has been shown in Part II.B. that stoichiometric lead zirconate (PZ) maintains the highest lead oxide vapor pressure in the PZT system. Thus, a positive pressure is established between the surrounding atmosphere, determined by pure PZ, and the PZT sample, which results in misleading weight gains.

If large quantities of lead zirconate are provided, it is clear that there is no $PbTi_xZr_{1-x}O_3$ sample that can equilibrate with the atmosphere, unless a liquid is formed. This conclusion can be deduced from the isothermal (1100°C) ternary phase diagram drawn to include the experimentally determined lines of constant activity (see Fig. 35). A $PbTi_{0.5}Zr_{0.5}O_3$ sample, for instance, is constrained to alter its overall composition only along the lines of constant Zr/Ti=1 composition. Therefore, the sample will not achieve an activity balance with the atmosphere until the lead rich liquid phase is formed. While the kinetics of the system may not allow this result in practice, sizable weight gains are possible.

Additionally, it was established in Part II.B. that lead zirconate has a very wide range of non-stoichiometry with large variation in lead oxide activity (0.5 to 0.07). This was illustrated in Fig. 19. As the composition of a lead zirconate disc is altered by the evaporation of PbO from the system, the lead oxide activity of the atmosphere falls, creating additional weight changes that are not related to the ionic

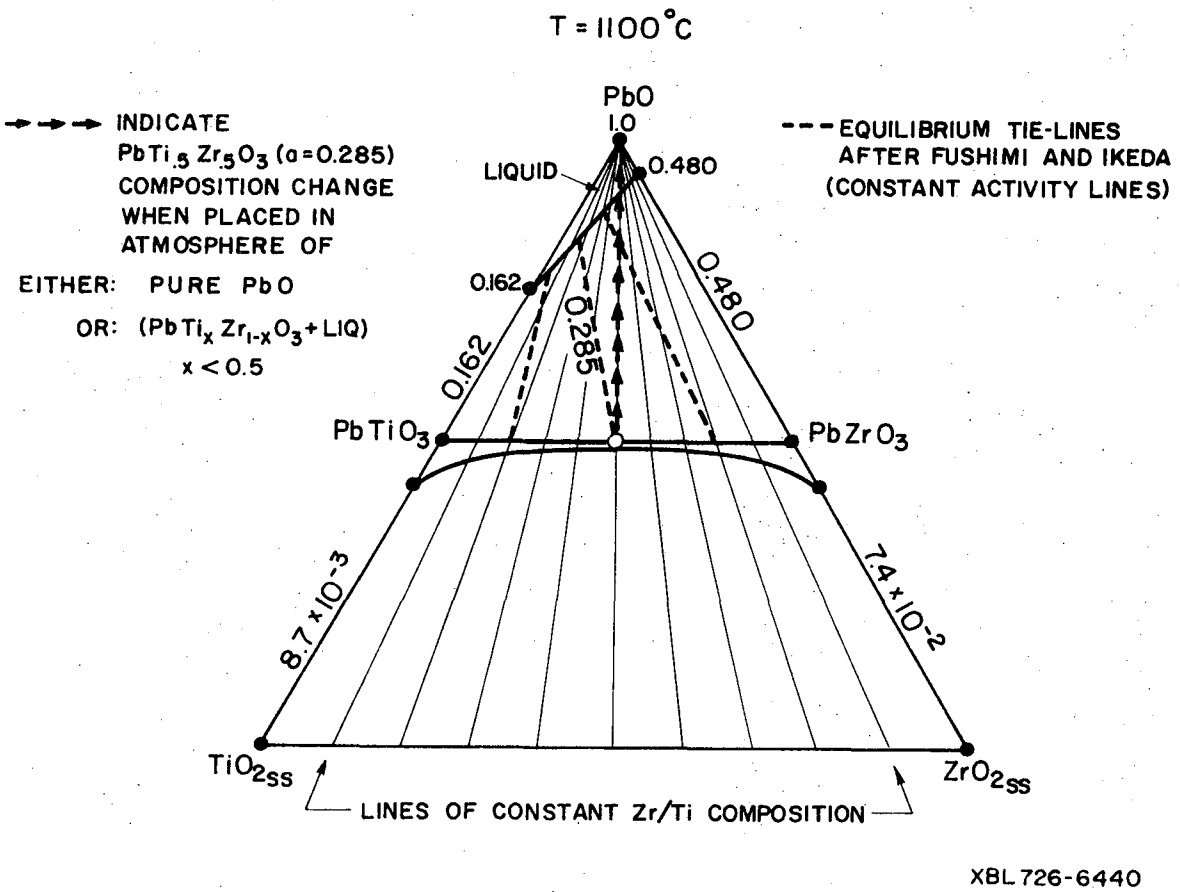


Fig. 35. The $PbO-TiO_2-ZrO_2$ isothermal (1100°C) ternary phase diagram sketched to include the experimentally determined lead oxide isoactivity lines after the phase equilibria of Fushimi. The arrows indicate the compositional changes occurring to a $PbTi_{.5}Zr_{.5}O_3$ sample equilibrating with any $PbTi_xZr_{1-x}O_3$ + PbO mixture with x less than 0.5, or with pure lead oxide. The sample must transform totally to a liquid phase to achieve an activity balance with the atmosphere.

substitution mechanisms.

The actual magnitude of both of these unwanted weight changes is a function of time at temperature, the PbO loss character of the particular system, and the amount of lead zirconate used.

In the earlier studies of bismuth and niobium ionic substitutions in PZT, as summarized in Appendix A, the basic technique of Dungan et al.[10] incorporating a burial powder of the same composition as the sample was used. This technique was modified, however, by replacing the burial powder with a solid PZT crucible, either single-phase or multi-phase, as discussed in Part II.A. There are several distinct advantages to this approach. First, experiments involving gravimetry may be performed. Second, PZT may be preprocessed as a powder in its own container, to firmly establish its exact stoichiometry and its homogeneity. In addition, the crucibles may be fabricated of most desired compositions facilitating experimentation, even when the crucible contains a reasonable amount of liquid phase. In a burial powder the liquid phase encourages sintering, making for difficult sample removal.

While reasonable data was obtained using single-phase PZT crucibles, even this approach is subject to small inconsistencies which result from the changes in the composition of the crucible. However, it was found that smaller errors are observed with the crucible technique than with the burial powder, when precautions were taken to maximize the reproducibility. Specifically, the sample powder and crucible powder must come from the same batch, and the sample must be placed within the companion crucible during a common calcination. In addition, the atmosphere crucible may be used for only the single experiment.

While the results obtained employing either crucible technique were within sufficient range of the predictions of the proposed models, the deviation from theory were greater with use of single-phase crucibles than with the use of the low constant activity multi-phase (CAMP) crucibles. The incremental weight losses observed were in the direction expected to result from a decrease in lead oxide activity of the "stoichiometric" crucible, as a result of the evaporation of PbO. This loss is unrelated to the ionic substitution mechanisms. The differences are illustrated in Figs. 30, 31, 33, 34, where the (a) curves describe results obtained in the "stoichiometric" crucibles and the (b) curves correspond to results obtained in low CAMP crucibles.

# IV. SUMMARY AND CONCLUSIONS

The range of intrinsic and the nature of extrinsic non-stoichiometry in lead zirconate-titanate has been characterized. A simple method has been developed to obtain precise and reproducible control of the defect structure.

Two different gravimetric experiments led to similar values for the $Pb(Ti_xZr_{1-x})O_3$ single-phase region width. First, the development of high and low constant activity multi-phase (CAMP) crucibles made possible the gravimetric vapor phase equilibration of a PZT sample and a PbO atmosphere. Weight changes produced in obtaining equilibrium indicated the extent of the stoichiometric variations. Second, a modified Knudsen effusion experiment yielded the same width of the PZT single-phase region, the relative location of the stoichiometric compound within the region, and complete thermodynamic vapor pressure data.

By modifying the vapor phase equilibration technique, gravimetric analysis could be used to study the kinetics of solution of Bi, Nb, La, and Sc ions in PZT. Results indicated a lead vacancy defect structure created by the substitution of Bi, Nb, and La in the PZT lattice, and an oxygen vacancy defect structure for Sc, obeying electroneutrality rules, and following simple predictions of crystal chemistry (Bi and La substitution for Pb, Nb and Sc substitution for (Ti,Zr)).

The production of multi-phase crucibles, in addition to allowing gravimetric experiments, afforded atmosphere control and a simple processing technique. Thus, it is possible to fabricate PZT materials with precise, reproducible and homogeneous intrinsic or extrinsic stoichiometry.

These experimental techniques should be applicable to any A-B-O compound, provided several requirements are satisfied at the desired temperature:

1. The oxide vapor pressure of one cation must be high enough to allow vapor transport.

2. The oxide vapor pressure of the other cations must be low enough to prevent any significant vaporization loss.

3. The "vapor phase equilibration" experiments require the presence of an equilibrium atmosphere of the high vapor pressure oxide, and an activity gradient sufficiently large to motivate the equilibration.

4. The high vapor pressure oxide must have sufficient molecular weight to produce measurable sample weight changes.

In addition, it would be useful if the composition of the vapor above the A-B-O compound was specified by mass spectrometric analysis. This information is necessary to calculate the exact vapor pressures and activities from the Knudsen effusion data.

ACKNOWLEDGMENTS

I would like to express my sincere appreciation to Professor R. M. Fulrath for his guidance and support during this work. I am also grateful to Professors A. Searcy and L. Brewer for their helpful comments, suggestions, and editing of the manuscript.

The author reserves special thanks to a good friend and colleague, Dr. Alton Lacy, for his editorial assistance, for his many useful suggestions (including the need for the acronym), and for his invaluable encouragement and counsel, particularly during the early stages of this work.

Other friends have been of great help during this thesis. Innumerable discussions with Dave Feather and John Sherohman were always useful and enjoyable. Conversations and other experiences with Bob Powell, Craig Shumaker, Bill Snowden, Wolfgang Stannek, Gautam Bandyopadhyay, Jim Holzgraf, Chris Young, Ilhan Aksay, Joe Masaryk and Jim Shackelford have contributed in a variety of tangible and intangible ways.

Further thanks are extended to Don Whittaker and Jack Wodei for their outstanding technical advice, assistance and contributions.

The author would also like to thank Gloria Pelatowski for her superb and speedy drawings; K. Radmilovic for her typing; and the Control Data 6600 computer for its excellent memory.

And finally, I am especially thankful to my wife Wendie, who has supported and encouraged me in so many ways.

This work was carried out under the auspices of the U.S. Atomic Energy Commission.

REFERENCES

1. P. D. Levett, "Factors Affecting Lead Zirconate-Lead Titanate Ceramics," Am. Ceram. Soc. Bull. 42 [6] 348-52 (1963).

2. A. H. Webster, T. B. Weston and N. F. H. Bright, "Effect of PbO Deficiency on the Piezoelectric Properties of Lead Zirconate-Titanate Ceramics," J. Am. Ceram. Soc. 50 [9] 490-1 (1967).

3. D. A. Northrop, "Vaporization of Lead Zirconate-Titanate Materials," J. Am. Ceram. Soc. I 50 [9] 441-45 (1967); II 51 [7] 357-61 (1968).

4. R. L. Moon, "High Temperature Phase Equilibria in the Lead Titanate-Lead Zirconate System," Ph.D. Thesis, Univ. of Calif. Berkeley, 1967 (UCRL 17545).

5. S. Fushimi and T. Ikeda, "Phase Equilibrium in the System PbO-$TiO_2$-$ZrO_2$," J. Am. Ceram. Soc., 50 [3] 129-32 (1967).

6. T. Ikeda, T. Oakno, M. Watanabe, "A Ternary System PbO-$TiO_2$-$ZrO_2$," Japan Journ. Appl. Phys. 1 [4] 218 (1962).

7. R. B. Atkin and R. M. Fulrath, "Point Defects and Sintering of Lead Zirconate-Titanate," J. Am. Ceram. Soc., 54 [5] 265-70 (1971).

8. B. Jaffe, R. S. Roth and S. Marzullo, "Properties of Piezoelectric Ceramics in the Solid-Solution Series Lead Titanate-Lead Zirconate-Lead Oxide: Tin Oxide and Lead Titanate-Lead Hafnate," J. of Research of the National Bureau of Standards, 55 [5] 239-53 (1955).

9. B. S. Snow, Fabrication of Electro-optic PLZT by Atmosphere Sintering, presented at the Spring meeting of the American Ceramic Society, Washington, D.C., May 9, 1972.

10. R. H. Dungan, H. M. Barnett and A. H. Stark, "Phase Relations and Electrical Parameters in the Ferroelectric-Antiferroelectric Region of the System $PbZrO_3$-$PbTiO_3$-$PbNb_2O_6$," J. Am. Ceram. Soc. 45 [8] 382-8 (1962).

11. T. B. Weston, A. H. Webster and V. M. McNamara, "Lead Zirconate-Lead Titanate Piezoelectric Ceramics with Iron Oxide Additions," J. Am. Ceram. Soc., 52 [5] 253-57 (1969).

12. K. H. Hardtl and D. Hennings, "Distribution of A-Site and B-Site Vacancies in $(Pb,La)(Ti,Zr)O_3$ Ceramics," J. Am. Ceram. Soc. 55 [5] 230-1 (1972).

13. G. H. Haertling and C. E. Land, "Hot-Pressed $(Pb,La)(Zr,Ti)O_3$ Ferroelectric Ceramics for Electro-optic Applications," 54 [1] 1-11 (1971).

14. G. H. Haertling, "Hot-Pressed Ferroelectric Lead Zirconate Titanate for Electro-Optical Applications," Am. Ceram. Soc. Bull., 49 [6] 264-7 (1970).

15. C. E. Land and P. D. Thacher, "Ferroelectric Ceramic Electro-optic Materials and Devices," Proc. IEEE, 57 [5] (1969). Also see IEEE Trans on Elect. Devices, Vol. ED-16 No. 6 (1969).

16. A. J. Parisi, "Ceramic 'Solid-State' Imaging Leaps into Development State," Product Engineering, 13-15, May 25, 1970.

17. D. W. Chapman, "Some Thin-film Properties of a New Ferroelectric Composition," J. Appl. Phys., 40 [6] 2381-85 (1969).

18. G. W. Taylor, "Electrical Properties of Niobium-Doped Ferroelectric $Pb(Zr,Sn,Ti)O_3$ Ceramics," J. Appl. Phys., 38 [12] 4697-704 (1967).

19. E. C. Subbarao, "Studies on Lead Titanate Ceramics Containing Niobium or Tantalum," J. Am. Ceram. Soc. 43 [3] 119-22 (1960).

20. R. Gerson, "Variation in Ferroelectric Characteristics of Lead Zirconate Titanate Ceramics Due to Minor Chemical Modifications," J. Appl. Phys. 31 [1] 188-94 (1960).

21. T. Ikeda and T. Okano, "Piezoelectric Ceramics of Lead Zirconate-Titanate Modified by Bismuth Ferrite," Japan J. Appl. Phys. 2, 63-4 (1963).

22. T. Ikeda and T. Okano, "Piezoelectric Ceramics of $Pb(Zr-Ti)O_3$ Modified by $A^{1+}B^{5+}O_3$ or $A^{3+}B^{3+}O_3$," Japan J. Appl. Phys., 3 [2] 63-71 (1964).

23. I. Veda and S. Ikegami, "Piezoelectric Properties of Modified $PbTiO_3$ Ceramics," Japan J. Appl. Phys. 7 [3] 236-42 (1968).

24. F. Kulcsar, "Electromechanical Properties of Lead Titanate Zirconate Ceramics Modified with Certain Three or Five-Valent Additions," J. Am. Ceram. Soc., 42 [7] 343-49 (1959).

25. R. B. Atkin and R. M. Fulrath, "Solubility of Aluminum in Lead Zirconate Titanate," J. Am. Ceram. Soc., 53 [1] 51-2 (1970).

26. G. H. Haertling, "Hot-Pressed Lead Zirconate-Lead Titanate Ceramics Containing Bismuth," J. Am. Ceram. Soc., 43 [12] 875-9 (1964).

27. R. B. Atkin, R. L. Holman, and R. M. Fulrath, "Substitution of Bi and Nb Ions in Lead Zirconate-titanate," J. Am. Ceram. Soc. 54 [2] 113-115 (1971).

28. R. A. Swalin, Thermodynamics of Solids, Chapt. 11, John Wiley & Sons, Inc., New York, 1962.

29. K. H. Hardtl and H. Rau, "PbO Vapour Pressure in the $Pb(Ti_{1-x}Zr_x)O_3$ System," Solid State Communications, 7 41-5 (1969).

30. K. Nagase and T. Nitta, Evaporation from $Pb(Ti_{1-x}Zr_x)O_3$ Compositions on Firing, Matsushita Elec. Ind. Co. National Tech. Report 10, 2 162-169 (1964).

31. J. Drowart, R. Colin, and G. Exsteen, "Mass-Spectrometric Study of the Vaporization of Lead Monoxide," Trans. Faraday Soc., 61 1376-83 (1965).

32. J. L. Margrave (Ed.), The Characterization of High Temperature Vapors, Chapter 5, K. D. Carlson, "The Knudsen Effusion Method," p. 115-128, John Wiley & Sons, Inc., New York (1967).

33. C. L. Hoenig and A. W. Searcy, "Knudsen and Langmuir Evaporation Studies of Stannic Oxide," J. Am. Ceram. Soc., 49 [3] 128-134 (1966).

34. C. L. Hoenig, "Phase Equilibria, Vapor Pressure, and Kinetic Studies in the Uranium-Nitrogen System," J. Am. Ceram. Soc., 54 [8] 391-398 (1971).

35. A. H. Webster, R. C. MacDonald and W. S. Bowman, "The System $PbO-ZrO_2-TiO_2$ at 1100°C," J. Can. Ceram. Soc. 34, 97-102 (1965).

36. P. Clausing, Annln. Phys. 12, 961 (1932).

37. J. L. Margrave (Ed.), The Characterization of High Temperature Vapors, Appendix C, p. 508-29, John Wiley & Sons, Inc., New York (1967).

38. A. W. Searcy and D. J. Meschi, "Calculation of Integral and Partial Thermodynamic Functions for Solids from Dissociation-Pressure Data," Reprint from "Thermodynamics of Nuclear Materials."

39. A. W. Searcy, Condensed State Reactions, Dept. of Min. Tech., Univ. of Calif., Berkeley.

40. Lewis and Randall, revised by Pitzer and Brewer, Thermodynamics, Chapt. 20, p. 242-79, McGraw Hill, New York (1961).

41. O. Kubaschewski and E. L. L. Evans, Metallurgical Thermochemistry, Pergamon Press (1958).

42. JANF Thermodynamic Tables

43. D. Lee, "Sintering Sc and Nb Modified Lead Zirconate Titanate," M.S. Thesis, Univ. of Calif. Berkeley, 1970 (UCRL-19188).

44. R. D. Shannon and C. T. Prewitt, "Effective Ionic Radii in Oxides and Fluorides," Acta Crystallogr., SECT. B, 25 [Pt. 5] 925-46 (1969).

45. R. S. Roth, J. Res. Natl. Bur.Standards, 62 [1] 34 (1959).

46. M. H. Warzee, M. Maurice, F. Halla, and W. R. Ruston, J. Am. Ceram. Soc. 48 [1] 16 (1965).

47. D. Hennings and K. H. Hardtl, "The Distribution of Vacancies in Lanthana-Doped Lead Titanate," Phys. Stat. Sol., 3 465-474 (1970).

48. D. Hennings, "The Range of Perovskite Phases in the System PbO-$TiO_2$-$La_2O_3$," Mat. Res. Bull., 6 329-340 (1971).

## APPENDIX A: Bi and Nb Substitution in $PbTi_{.5}Zr_{.5}O_3$ [27]

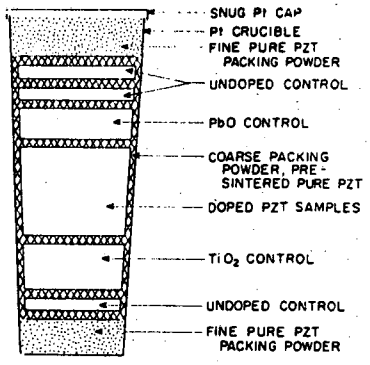


**Fig. 1. Weight change cell.**

**Table II. Observed Weight Changes in Doped Lead Zirconate-Titanate**

| Sample doping (mol%) | Sample wt (g) | Time (h) at 1150°C | Wt change observed (wt%)† | Wt change predicted (wt%)†‡ |
|---|---|---|---|---|
| 0.5 PbO | 34.813 | 11 | −0.33 (−115) | −0.345 (−120) |
| 1.0 PbO | 35.783 | 19 | −0.703 (−251) | −0.685 (−245) |
| 1.5 PbO | 12.879 | 20 | −1.065 (−137) | −1.025 (−132) |
| 0.5 $TiO_2$ | 35.273 | 10 | +0.397 (+140) | +0.343 (+121) |
| 1.0 $TiO_2$ | 38.356 | 7 | +0.637 (+244) | +0.680 (+260) |
| 0.5 $BiO_{1.5}$ | 35.413 | 24 | −0.50 (−177) | −0.515 [1] (−182) |
| 1.0 $BiO_{1.5}$ | 42.010 | 32 | −1.02 (−430) | −1.03 [1] (−432) |
| 2.0 $BiO_{1.5}$ | 39.214 | 41 | −1.63 (−640) | −2.05 [1] (−805) |
| | | 60–70* | −2.04 (−800) | |
| 0.5 $NbO_{2.5}$ | 16.705 | 20 | +0.120 (+20) | +0.175 [2] (+29.3) |
| | | 29 | +0.167 (+28) | |
| 1.0 $NbO_{2.5}$ | 20.231 | 28 | +0.376 (+76) | +0.344 [2] (+69.5) |

*Extrapolated.
†Number in parentheses is actual weight change (mg).
‡Number in brackets designates equation used for calculation.

These experiments indicate the substitution of Bi as $Bi^{3+}$ on the $Pb^{2+}$ A lattice site of lead zirconate-titanate, in agreement with the proposed model. Niobium dissolves as $Nb^{5+}$ on the $(Ti,Zr)^{4+}$ sublattice of lead zirconate-titanate, as would be expected. The data for both Bi and Nb doping support a Pb vacancy charge compensation mechanism, and the solid solubility of each is >2 mol%.

Although the high vapor pressure of PbO during the reactions allowed Pb to be lost or gained readily by the lead zirconate-titanate samples, the reaction mechanism was complex and probably involved the sluggish disappearance of a nonequilibrium second phase.

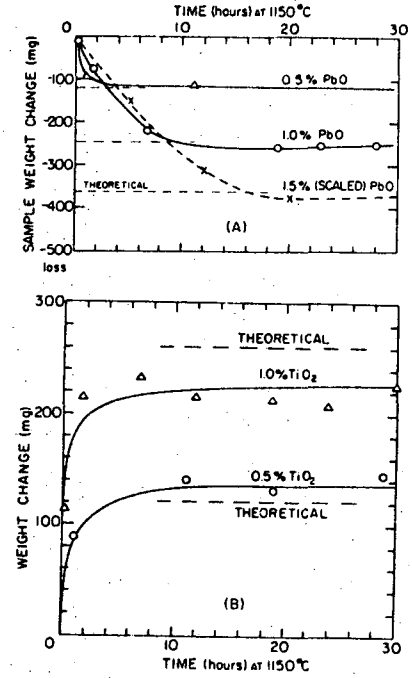


**Fig. 2. Weight change vs time at 1150°C for lead zirconate-titanate specimens with additions of *(A)* PbO and *(B)* $TiO_2$.**

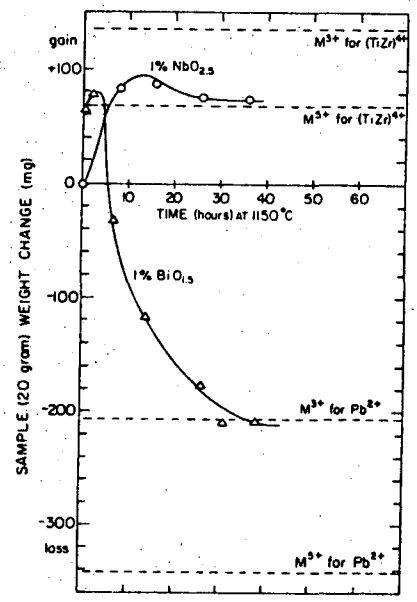


**Fig. 3. Weight change results for lead zirconate-titanate specimens with Bi and Nb additions compared to predictions of proposed model. Constancy of specimen weights after 30 h believed to indicate equilibrium; data normalized to 20-g samples.**

XBL 726-1206

The solid state substitution of Bi and Nb ions in the perovskite crystal structure of $PbTi_{.5}Zr_{.5}O_3$ was investigated by sample weight change at 1150°C after the technique described by Weston et al.[11] An equilibrium PbO atmosphere was provided for the samples by a $PbTi_{.5}Zr_{.5}O_3$ burial powder after Dungan et al.[10] (1962). The same sample was weighed, heated and held, cooled, re-weighed, and re-heated repetitively.

APPENDIX B: Integration of the Gibbs-Duhem Equation in the Lead Titanate and Lead Zirconate Single-phase Regions

Lead titanate and lead zirconate may be considered as two component systems. If the activity of one component A (PbO) is a known function of composition, then the Gibbs-Duhem[38-40] Equation (4) may be solved for the activity of the other component B ($TiO_2$ or $ZfO_2$), provided at least one additional boundary condition is known.

$$X_A d\ln a_A + X_B d\ln a_B = 0 \tag{4}$$

$$\int_{X_B^o}^{X_B} d\ln a_B = - \int_{X_B^o}^{X_B} (X_A/X_B) d\ln a_A \tag{5}$$

It is expected that only a negligible amount of PbO can dissolve in either $TiO_2$ or $ZrO_2$, and those solid solution regions may be reasonably neglected. Thus, if Raoult's Law is applicable, it is clear that the unit activity of pure component B is negligibly lowered, and the activity of component B at the compound/compound plus solid phase boundary may be assumed to be 1.0 ($a_B^o$ at $X_B^o = 1.0$), see Fig. 1(b).

Equation (5) may be partially integrated:

$$\ln a_B = 1 \int_{X_B^o}^{X_B} (X_A/X_B) d\ln a_A \tag{6}$$

This remaining integral may be solved graphically within the single-phase region ($PbTiO_3$ or $PbZrO_3$) that extends from $X_B^o$ to $X_B = 0.5$, where $X_B^o$ defines the maximum extent of non-stoichiometry

(as determined by the modified Knudsen Effusion experiment discussed in Part I-B). Since the activity of component A has been determined as a function of composition in this region, the integral (6), is solved by itteritively calculating the area under the curve of $(X_A/X_B)$ as a function of $\ln a_A$.

This itteritive integration may be performed with the assistance of a computer; the fortran statements appear below. If delta ($\Delta$) = the maximum width of the $Pb(B)O_3$ single-phase region, the most non-stoichiometric perovskite may be written as $Pb_{1-\Delta}\square_{\Delta}(B)O_{3-\Delta}\emptyset_{\Delta}$. Thus, the mole fractions are defined as follows:

$$X_B^o \equiv \frac{1-\Delta}{2-\Delta}, \quad X_A^o = 1-X_B^o \tag{7}$$

$$X_A \equiv \frac{1-GOD}{2-GOD} \quad X_B = 1-X_A \tag{8}$$

An incremental width of the single phase region GOD = WL/(mol. wt. PbO) (grams of compound in the sample) is associated with the deviation in milligrams from perfect stoichiometry (WL), as reduced from the effusion data. This allows the calculation of the appropriate mole fractions, such that the activity of component A is specified as a function of the mole fraction of both components A and B through the single phase region. (Fig. 18, 19)

These calculations tabulated for lead titanate and lead zirconate. See Part I-B for the experimental details.

The free energy of mixing of PbO and $TiO_2$ is calculated:

$$\Delta G^{Mix} = RT(\ln a_{PbO} + \ln a_{TiO_2}).$$

Computer program:

```
      PROGRAM HOL(INPUT,OUTPUT)
      DIMENSION R(50),XA(50),XB(50),Z(50),AA(50),AB(50),GA(50),GB(50),
     * WL(50),F(50),XAGA(50),XBGB(50)
      DIMENSION GOD(50)
      DIMENSION WORD(12)
   11 READ 2, N,T,WW,WS
    2 FORMAT (I5,F10.3,F10.3,F10.5)
      IF(N)   99,99,1
    1 READ 16, (WORD(I),I=1,12)
   16 FORMAT (12A6)
    8 PRINT 20, (WORD(I),I=1,12)
   20 FORMAT (1H1,12A6)
C     WL IS EQUAL TO THE POSITION WITHIN THE SINGLE PHASE REGION
C    WL(N) BEING THE WIDTH OF THE REGION IN MGS
C  WS IS THE WT. OF THE SAMPLE IN GRAMS  -  STOICHIOMETRIC COMP.
      READ 3, (R(I),WL(I),I=1,N)
    3 FORMAT (F10.4,F10.4)
      TEMP=T+273.15
C     DELTA IS EQUAL TO THE WIDTH OF THE SINGLE PHASE REGION
      DELTA=(WL(N)*WW)/(223.1894*WS)
      DO 25 I=1,N
      XB(1)=.5
      XA(1)=.5
      XA(N)=(1.-DELTA)/(2.-DELTA)
      GOD(I)=(WL(I)*WW)/(223.1894*WS)
      XA(I)=(1.-GOD(I))/(2.-GOD(I))
      XB(I)=1.-XA(I)
      Z(I)=XA(I)/XB(I)
      AA(I)=(4.675E-7*R(I)*SQRT(TEMP)/.485)/(EXP(-28750/TEMP+17.0435))
      GA(I)=ALOG(AA(I))
   25 CONTINUE
      PRINT 4
    4 FORMAT(3X,1H ,*N*,6X,*TEMP(C)*,6X,*MOL.WT.*,6X,*STOIC.WT.*,11X,
     * *DELTA W*)
      PRINT 5, N,T,WW,WS,DELTA
    5 FORMAT (1H ,I4,3X,F10.3,3X,F10.3,3X,F8.5,3X,E22.7)
      PRINT 6
    6 FORMAT (1H0,6X,1HR,9X,2HXB,9X,2HXA,10X,1HZ,10X,1HA,10X,1HGA)
      PRINT 7, (R(I),XB(I),XA(I),Z(I),AA(I),GA(I),I=1,N)
    7 FORMAT (1X,6E11.3)
C   GB IS THE ANSWER OF THE GIBBS-DUHEM INTEGRATION
C   GB IS ALSO THE NATURAL LOG OF THE ACTIVITY OF COMPONENT B
      GB(N)=0
      AB(N)=1
C  AB IS THE ACTIVITY OF COMPONENT B
      N1=N-1
      DO 28 I=1,N1
      J=N-I
      GB(J)=GB(J+1)+(GA(J+1)-GA(J))*(Z(J+1)+Z(J))/2
      AB(J)=EXP(GB(J))
   28 CONTINUE
      DO 31  I=1,N
      XAGA(I)=XA(I)*GA(I)
      XBGB(I)=XB(I)*GB(I)
      F(I)=1.9872*TEMP*(XAGA(I)+XBGB(I))
   31 CONTINUE
      PRINT 9
    9 FORMAT(4X,1H ,*XB*,12X,*ACTIVITY A*,4X,*LOG ACT. A*,4X,*ACTIVITY
     * B*,4X,*LOG ACT. B*,4X,*FREE ENERGY OF MIXING*)
      PRINT 10, (XB(I),AA(I),GA(I),AB(I),GB(I),F(I),I=1,N)
   10 FORMAT(1H ,E11.3,3X,E11.3,3X,E11.3,3X,E11.3,3X,E11.3,3X,E11.3)
      GO TO 11
   99 STOP
      END
```

Tabulated data:

GIBBS-DUHEM INTEGRATION — LEAD ZIRCONATE (T = 1091 °C)

| dw/dt (mg/hr) | $X_{ZrO_2}$ | $X_{PbO}$ | $\frac{X_{PbO}}{X_{ZrO_2}}$ | $a_{PbO}$ | $a_{ZrO_2}$ | $\Delta G_{PZ}^{MIX}$ |
|---|---|---|---|---|---|---|
| 2.600E+02 | 5.000E-01 | 5.000E-01 | 1.000E+00 | 5.266E-01 | 1.618E-01 | -3.338E+03 |
| 2.340E+02 | 5.036E-01 | 4.965E-01 | 9.863E-01 | 4.739E-01 | 1.796E-01 | -3.348E+03 |
| 2.280E+02 | 5.044E-01 | 4.956E-01 | 9.826E-01 | 4.618E-01 | 1.843E-01 | -3.351E+03 |
| 2.202E+02 | 5.052E-01 | 4.948E-01 | 9.794E-01 | 4.460E-01 | 1.907E-01 | -3.353E+03 |
| 2.184E+02 | 5.103E-01 | 4.897E-01 | 9.596E-01 | 4.423E-01 | 1.922E-01 | -3.364E+03 |
| 2.184E+02 | 5.129E-01 | 4.871E-01 | 9.497E-01 | 4.423E-01 | 1.922E-01 | -3.370E+03 |
| 2.184E+02 | 5.146E-01 | 4.854E-01 | 9.432E-01 | 4.423E-01 | 1.922E-01 | -3.374E+03 |
| 2.085E+02 | 5.159E-01 | 4.841E-01 | 9.385E-01 | 4.223E-01 | 2.008E-01 | -3.377E+03 |
| 1.933E+02 | 5.175E-01 | 4.825E-01 | 9.323E-01 | 3.915E-01 | 2.155E-01 | -3.380E+03 |
| 1.809E+02 | 5.183E-01 | 4.817E-01 | 9.295E-01 | 3.664E-01 | 2.292E-01 | -3.381E+03 |
| 1.771E+02 | 5.190E-01 | 4.810E-01 | 9.269E-01 | 3.588E-01 | 2.337E-01 | -3.382E+03 |
| 1.677E+02 | 5.197E-01 | 4.803E-01 | 9.240E-01 | 3.396E-01 | 2.459E-01 | -3.383E+03 |
| 1.623E+02 | 5.203E-01 | 4.797E-01 | 9.219E-01 | 3.287E-01 | 2.534E-01 | -3.383E+03 |
| 1.560E+02 | 5.213E-01 | 4.787E-01 | 9.182E-01 | 3.159E-01 | 2.628E-01 | -3.384E+03 |
| 1.327E+02 | 5.225E-01 | 4.775E-01 | 9.139E-01 | 2.688E-01 | 3.047E-01 | -3.384E+03 |
| 1.207E+02 | 5.233E-01 | 4.767E-01 | 9.110E-01 | 2.445E-01 | 3.322E-01 | -3.383E+03 |
| 9.990E+01 | 5.240E-01 | 4.760E-01 | 9.085E-01 | 2.023E-01 | 3.947E-01 | -3.382E+03 |
| 9.060E+01 | 5.248E-01 | 4.752E-01 | 9.056E-01 | 1.835E-01 | 4.313E-01 | -3.381E+03 |
| 7.650E+01 | 5.253E-01 | 4.747E-01 | 9.036E-01 | 1.549E-01 | 5.026E-01 | -3.379E+03 |
| 5.250E+01 | 5.256E-01 | 4.744E-01 | 9.027E-01 | 1.063E-01 | 7.062E-01 | -3.378E+03 |
| 3.600E+01 | 5.259E-01 | 4.741E-01 | 9.016E-01 | 7.291E-02 | 9.925E-01 | -3.376E+03 |
| 3.570E+01 | 5.261E-01 | 4.739E-01 | 9.009E-01 | 7.230E-02 | 1.000E+00 | -3.375E+03 |

GIBBS-DUHEM INTEGRATION — LEAD TITANATE (T = 1091 °C)

| dw/dt (mg/hr) | $X_{TiO_2}$ | $X_{PbO}$ | $\frac{X_{PbO}}{X_{TiO_2}}$ | $a_{PbO}$ | $a_{TiO_2}$ | $\Delta G_{PT}^{MIX}$ |
|---|---|---|---|---|---|---|
| 1.140E+02 | 5.000E-01 | 5.000E-01 | 1.000E+00 | 2.309E-01 | 4.796E-02 | -6.104E+03 |
| 1.020E+02 | 5.048E-01 | 4.952E-01 | 9.812E-01 | 2.066E-01 | 5.355E-02 | -6.123E+03 |
| 1.010E+02 | 5.075E-01 | 4.925E-01 | 9.705E-01 | 2.045E-01 | 5.406E-02 | -6.133E+03 |
| 9.800E+01 | 5.089E-01 | 4.911E-01 | 9.652E-01 | 1.985E-01 | 5.567E-02 | -6.137E+03 |
| 9.620E+01 | 5.095E-01 | 4.905E-01 | 9.627E-01 | 1.948E-01 | 5.667E-02 | -6.140E+03 |
| 9.400E+01 | 5.102E-01 | 4.898E-01 | 9.602E-01 | 1.904E-01 | 5.794E-02 | -6.142E+03 |
| 9.300E+01 | 5.121E-01 | 4.879E-01 | 9.526E-01 | 1.883E-01 | 5.854E-02 | -6.148E+03 |
| 9.200E+01 | 5.147E-01 | 4.853E-01 | 9.429E-01 | 1.863E-01 | 5.914E-02 | -6.156E+03 |
| 9.100E+01 | 5.155E-01 | 4.845E-01 | 9.398E-01 | 1.843E-01 | 5.975E-02 | -6.159E+03 |
| 8.620E+01 | 5.165E-01 | 4.835E-01 | 9.360E-01 | 1.746E-01 | 6.287E-02 | -6.162E+03 |
| 8.350E+01 | 5.178E-01 | 4.822E-01 | 9.313E-01 | 1.691E-01 | 6.477E-02 | -6.165E+03 |
| 8.110E+01 | 5.190E-01 | 4.810E-01 | 9.269E-01 | 1.642E-01 | 6.654E-02 | -6.168E+03 |
| 7.750E+01 | 5.206E-01 | 4.794E-01 | 9.209E-01 | 1.570E-01 | 6.940E-02 | -6.172E+03 |
| 7.450E+01 | 5.217E-01 | 4.783E-01 | 9.169E-01 | 1.509E-01 | 7.196E-02 | -6.174E+03 |
| 6.830E+01 | 5.227E-01 | 4.773E-01 | 9.131E-01 | 1.383E-01 | 7.791E-02 | -6.176E+03 |
| 6.650E+01 | 5.231E-01 | 4.769E-01 | 9.115E-01 | 1.347E-01 | 7.984E-02 | -6.176E+03 |
| 6.050E+01 | 5.241E-01 | 4.759E-01 | 9.081E-01 | 1.225E-01 | 8.701E-02 | -6.178E+03 |
| 4.840E+01 | 5.252E-01 | 4.748E-01 | 9.040E-01 | 9.802E-02 | 1.065E-01 | -6.178E+03 |
| 3.075E+01 | 5.261E-01 | 4.739E-01 | 9.007E-01 | 6.228E-02 | 1.604E-01 | -6.177E+03 |
| 2.400E+01 | 5.265E-01 | 4.735E-01 | 8.993E-01 | 4.861E-02 | 2.004E-01 | -6.175E+03 |
| 1.925E+01 | 5.268E-01 | 4.732E-01 | 8.982E-01 | 3.899E-02 | 2.444E-01 | -6.174E+03 |
| 1.235E+01 | 5.270E-01 | 4.730E-01 | 8.974E-01 | 2.501E-02 | 3.640E-01 | -6.173E+03 |
| 1.050E+01 | 5.272E-01 | 4.728E-01 | 8.969E-01 | 2.126E-02 | 4.211E-01 | -6.171E+03 |
| 6.500E+00 | 5.273E-01 | 4.727E-01 | 8.963E-01 | 1.316E-02 | 6.473E-01 | -6.170E+03 |
| 5.700E+00 | 5.274E-01 | 4.726E-01 | 8.960E-01 | 1.154E-02 | 7.281E-01 | -6.169E+03 |
| 4.000E+00 | 5.275E-01 | 4.725E-01 | 8.958E-01 | 8.101E-03 | 1.000E+00 | -6.169E+03 |

XBL726-6436

APPENDIX C: A Tabulation of the Knudsen Effusion Experimental Data

R = the Knudsen cell weight loss rate (dw/dt) in milligrams/hour
T = the Knudsen cell temperature in degrees Centigrade

## I. PbO

| | R | T |
|---|---|---|
| (a) | | |
| | 1.333300 | 794.10 |
| | 1.625000 | 794.10 |
| | 2.333300 | 819.00 |
| | 2.437500 | 823.80 |
| | 9.136400 | 868.00 |
| | 9.300000 | 866.10 |
| | 9.000000 | 866.10 |
| | 13.875000 | 882.40 |
| | 5.937500 | 856.50 |
| | 8.000000 | 869.90 |
| | 73.000000 | 966.90 |
| | 75.500000 | 966.90 |
| | 74.500000 | 966.90 |
| | 37.500000 | 918.90 |
| | 97.500000 | 1006.20 |
| | 97.000000 | 1006.20 |
| (b) | 1.500000 | 787.00 |
| | 6.750000 | 849.00 |
| | 12.500000 | 877.00 |
| | 1.333300 | 794.10 |
| | 1.625000 | 794.10 |
| | 2.333300 | 819.00 |
| | 2.437500 | 823.80 |
| | 9.136400 | 868.00 |
| | 9.300000 | 866.10 |
| | 9.000000 | 866.10 |
| | 13.875000 | 882.40 |
| | 5.937500 | 856.50 |
| | 8.000000 | 869.90 |
| | 73.000000 | 966.90 |
| | 75.500000 | 966.90 |
| | 74.500000 | 966.90 |
| | 37.500000 | 918.90 |
| | 97.500000 | 1006.20 |
| | 97.000000 | 1006.20 |

## II. $PbTiO_3 + TiO_2$

| | R | T |
|---|---|---|
| (a) | | |
| | 4.050000 | 1091.00 |
| | 13.500000 | 1158.00 |
| | 23.000000 | 1188.00 |
| | 44.000000 | 1225.00 |
| | 43.000000 | 1225.00 |
| (b) | | |
| | 6.500000 | 1119.50 |
| | 43.750000 | 1219.40 |
| | 15.300000 | 1156.00 |
| | 5.400000 | 1103.00 |
| | 2.085000 | 1057.00 |
| (c) | | |
| | 6.000000 | 1102.00 |
| | 5.800000 | 1102.00 |
| | 18.000000 | 1166.00 |
| | 10.000000 | 1128.00 |

## III. $PbZrO_3 + PbO$

| | R | T |
|---|---|---|
| (a) | 2.950000 | 834.40 |
| | 7.120000 | 870.90 |
| | 23.400000 | 929.40 |
| | 75.000000 | 1001.00 |
| | 313.500000 | 1101.00 |
| (b) | 5.080000 | 857.00 |
| | 42.000000 | 980.00 |
| | 250.000000 | 1091.00 |
| | 240.000000 | 1091.00 |
| | 260.000000 | 1091.00 |

## IV. $PbTiO_3 + TiO_2$

| | R | T |
|---|---|---|
| (a) | | |
| | .187500 | 710.00 |
| | .467200 | 764.00 |
| | 1.205800 | 803.00 |
| (b) | 108.000000 | 1100.00 |
| | 11.700000 | 940.00 |
| | 106.500000 | 1119.50 |
| (c) | 93.000000 | 1119.50 |
| | 3.353000 | 843.00 |
| | 112.000000 | 1091.00 |
| | 117.000000 | 1091.00 |
| | .129400 | 640.00 |
| | .187500 | 710.00 |
| | .467200 | 764.00 |
| | 1.205800 | 803.00 |
| (d) | | |
| | 45.000000 | 1016.00 |
| | 19.350000 | 960.00 |
| | 18.500000 | 960.00 |
| | 109.000000 | 1102.00 |

## V. $PbZrO_3 + ZrO_2$

| | R | T |
|---|---|---|
| (a) | 1.625000 | 927.50 |
| | 6.000000 | 991.00 |
| | 21.000000 | 1048.50 |
| | 27.400000 | 1068.60 |
| | 51.000000 | 1101.00 |
| (b) | 38.000000 | 1091.00 |
| | 57.500000 | 1126.00 |
| | 65.000000 | 1126.00 |

XBL726-6435

Computer program:

```
      PROGRAM NUDE(INPUT,OUTPUT)
      DIMENSION R(300)
      DIMENSION T(300),G(300),S(300),CS(300),CXI(300),CXH(300),Q(2,3)
      DIMENSION DS(300),DXI(300),DXH(300),DSQS(300),DSQXI(300),
     *DSQXH(300),RT(300),TEMP(300)
      DIMENSION TC(300),TMV(300), SCA(300) , TINV(300)
      DIMENSION WORD(12)
4128  READ 39, N
   39 FORMAT (I12)
      IF(N) 4130,4130,1
    1 READ 16, (WORD(I),I=1,12)
   16 FORMAT (12A6)
4129  PRINT 26, (WORD (I), I= 1,12)
   26 FORMAT (1H1,12A6)
      READ 48, WW
   48 FORMAT (E20.5)
      PRINT 21
   21 FORMAT    (/ *WEIGHTING FACTOR*)
      PRINT 22, WW
   22 FORMAT (E20.5)
      READ 59,(R(I),TC(I),I=1,N)
   59 FORMAT(F10.4,F10.3)
      DO 9 I= 1,N
      T(I) = TC(I) + 273.15
      TINV(I) = 1.0/T(I)
      G(I)=SQRT(T(I))
      S(I)=R(I)*G(I)*4.675E-7/WW
    9 CONTINUE
      PRINT 20
   20 FORMAT(1H *RATE*,11X,*TEMP(C)*,6X,*SQUARE TEMP*,6X,*TEMP(K)*)
      PRINT 86,(R(I),TC(I),G(I),T(I),I=1,N)
   86 FORMAT(1H ,F12.6,3X,F10.2,3X,F14.6,3X,F10.2)
      PRINT 28
   28 FORMAT(1H ,*PRESSURE IN ATM.*,6X,*1/TEMP(K)*,15X,*TEMP(K)*,6X,
     **TEMP(C)*)
C     S(I)  IS THE KNUDSEN VAPOR PRESSURE IN ATM.
      PRINT 431,(S(I),TINV(I),T(I),TC(I),I = 1,N)
  431 FORMAT(1H ,E20.5,2X,E22.7,2X,F11.3,2X,F12.3)
      DO 2601  I= 1,N
      S(I)=ALOG(S(I))
2601  CONTINUE
 2500 Z1T = 0.
      Z1TT = 0.
      ZS = 0.
      ZS1T = 0.
      DO 3000 I=1,N
      Z1T = Z1T+1./T(I)
      Z1TT = Z1TT+1./T(I)/T(I)
      ZS = ZS+S(I)
      ZS1T = ZS1T+S(I)/T(I)
 3000 CONTINUE
      Q(1,1) = N
      Q(1,2) = Z1T
      Q(1,3) = ZS
      Q(2,1) = Z1T
      Q(2,2) = Z1TT
      Q(2,3) = ZS1T
      D =  Q(1,1)*Q(2,2)-Q(1,2)*Q(2,1)
```

```
      A = (Q(1,3)*Q(2,2)-Q(2,3)*Q(1,2))/D
      B = (Q(2,3)*Q(1,1)-Q(1,3)*Q(2,1))/D
      XI = A
      XH = B
      HH=XH*1.9872
      SS=XI*1.9872
      PR=EXP(XH*7E-4 + XI)
      GR=EXP(XH*8E-4 + XI)
      PRINT 100
  100 FORMAT(1H ,*P(AT 1000/T=.7)*,10X,*P(AT 1000/T=.8)*)
      PRINT 101,PR,GR
  101 FORMAT(1H ,E20.5,5X,E20.5)
      PRINT 49
   49 FORMAT(10X,1H ,*A*,20X,*B*,22X,*ENTHALPY*,14X,*ENTROPY*)
      PRINT 51,  XH,XI,HH,SS
   51 FORMAT(1H ,E19.8,3X,E20.8,3X,E19.8,3X,E15.8)
      PRINT 37
   37 FORMAT(5X,1H ,*T(I)*,11X,*1/T(I)*,9X,*ALOG(S(I))*,5X,*DS(I)*,
     * 10X,*DEV.A(I)*,7X,*DEV.B(I)*)
      DO 4000 I=1,N
      CS(I)=XI+XH*1.0/1.0/T(I)
      CXI(I)=S(I)-XH*1.0/1.0/T(I)
      CXH(I)=(S(I)-XI)*1.0*T(I)
      CXH(I)=(S(I)-XI)*T(I)
      RT(I) = 1./T(I)
      DS(I) = CS(I)-S(I)
      DXI(I) = CXI(I)-XI
      DXH(I) = CXH(I)-XH
      DSQS(I) = (CS(I)-S(I))**2
      DSQXI(I) = (CXI(I)-XI)**2
      DSQXH(I) = (CXH(I)-XH)**2
      PRINT 18, T(I),RT(I),S(I),DS(I),DXH(I),DXI(I)
   18 FORMAT(1H ,E12.4,3X,E12.4,3X,E12.4,3X,E12.4,3X,E12.4,3X,E12.4)
 4000 CONTINUE
      ZS = 0.
      ZSS = 0.
      ZI = 0.
      ZII = 0.
      ZH = 0.
      ZHH = 0.
      ZRT = 0.
      ZRTRT = 0.
      ZDSQS = 0.
      ZDSQI = 0.
      ZDSQH = 0.
      DO 5000 I=1,N
      ZS = ZS+CS(I)
      ZSS = ZSS+CS(I)**2
      ZI = ZI+CXI(I)
      ZII = ZII+CXI(I)**2
      ZH = ZH+CXH(I)
      ZHH = ZHH+CXH(I)**2
      ZRT = ZRT+RT(I)
      ZRTRT = ZRTRT+RT(I)**2
      ZDSQS = ZDSQS+DSQS(I)
      ZDSQI = ZDSQI+DSQXI(I)
      ZDSQH = ZDSQH+DSQXH(I)
 5000 CONTINUE
```

```
      XN = N
      DXI = XN*ZRTRT-ZRT**2
      RXI = SQRT(ZSQS/(XN-2.))
      PXI = RXI*SQRT(ZRTRT/DXI)
      SXI = PXI
      DXH = DXI
      RXH = RXI
      PXH = RXH*SQRT(XN/DXH)
      SXH=PXH
      SSH=SXH*1.9872
      SSS=SXI*1.9872
      PRINT 99
   99 FORMAT(1H ,*STAND.DEV.A*,5X,*STAND.DEV.B*,5X,*STAND.DEV.ENTHALPY*,
     *2X,*STAND.DEV.ENTROPY*)
      PRINT 38, SXH,SXI,SSH,SSS
   38 FORMAT(E13.4,3X,E13.4,3X,E13.4,7X,E13.4)
C     AO EQUALS THE A-CONSTANT FOR PURE PBO
      AO=-2.91634E+04
C     BO EQUALS THE B-CONSTANT FOR PURE PBO
      BO=1.74057E+01
C     ACT IS THE ACTIVITY OF PBO AT 1000/T = .7
      ACT=EXP((XH-AO)*(7E-4)+(XI-BO))
C     ACTA IS THE ACTIVITY OF PBO AT 1000/T =.8
      ACTA=EXP((XH-AO)*(8E-4)+(XI-BO))
      PRINT 1000
 1000 FORMAT(1H ,*A(AT 1000/T=.7)*,10X,*A(AT 1000/T=.8)*)
      PRINT 1001,ACT,ACTA
 1001 FORMAT(1H ,E20.5,5X,E20.5)
      GO TO 4128
 4130 STOP
      END
```

APPENDIX D: Thermodynamics of PbO

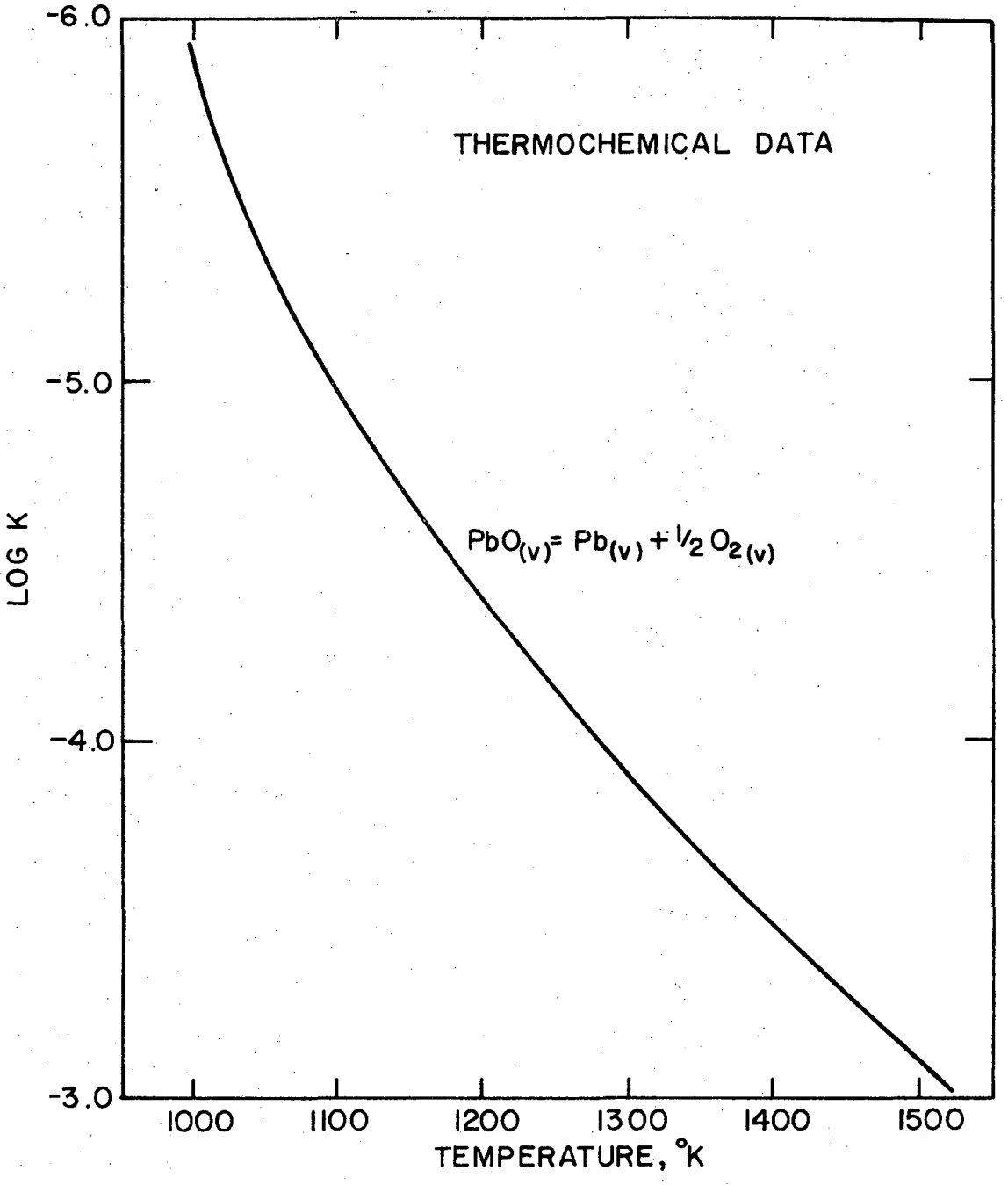


XBL 726-6449

Summary of the thermochemical data from the JANF Tables[42] for the equilibria between PbO vapor, Pb vapor, and $O_2$ vapor, as a function of temperature.

If the system oxygen pressure becomes low enough, an undesirable lead vapor pressure may be established by the reduction of PbO vapor.

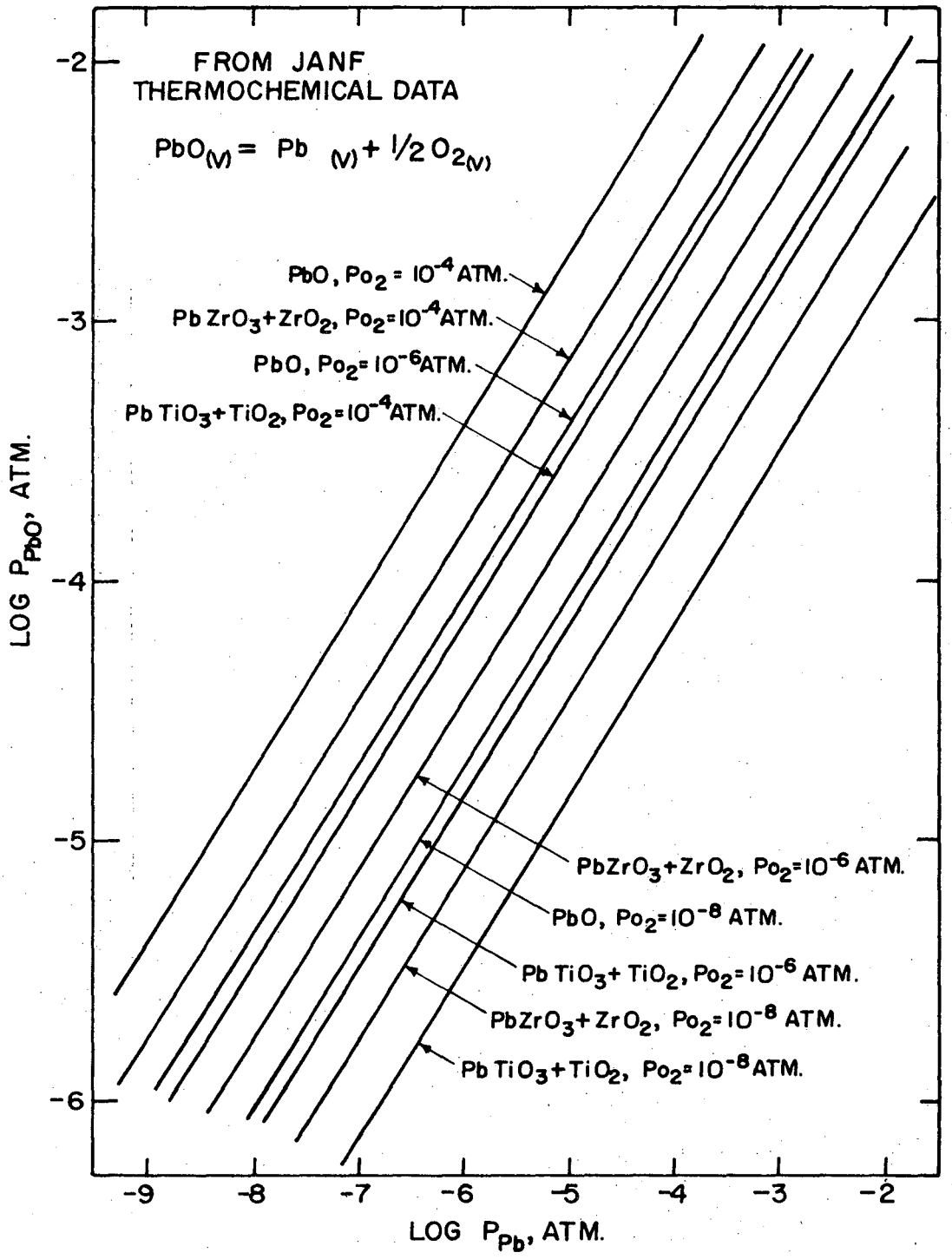


XBL 726-6458

PbO liquid is taken as the standard state. The PbO vapor pressure is set by the temperature of the condensed phase or phases as determined by Hardtl and Rau[29] or Part I(b) of this study. Typical system values are assumed for the oxygen pressure. Thus the lead vapor pressure is calculated for any $p_{PbO}(T)$, K(T), and $p_{O_2}$:

$$K = \frac{[a_{Pb}][a_{O_2}]^{1/2}}{[a_{PbO}]} = \frac{[p_{Pb}][p_{O_2}]}{[p_{PbO}]}$$

This type of display is useful for determining the minimum system oxygen pressure allowed without appreciably reducing the lead oxide vapor. Suppose non-stoichiometric $PbTiO_3$ is to be heated at 1200°C in a vacuum of $10^{-8}$ atm. It is shown in Fig. 23 that at this temperature the PbO vapor pressure is about $6.5 \times 10^{-4}$ atm. It can be seen from the preceeding graph that these conditions would establish a lead vapor pressure of about $10^{-3}$ atm., hardly negligible.

The same analysis may be applied to the equilibria between PbO liquid, Pb liquid and $P_{O_2}$.

*TECHNICAL INFORMATION DIVISION*
*LAWRENCE BERKELEY LABORATORY*
*UNIVERSITY OF CALIFORNIA*
*BERKELEY, CALIFORNIA 94720*